Investigations of non-enzymatic glycation with new bioanalytical methods

Ph. D. Thesis

Katalin Böddi

Doctoral School of Pharmaceutical Science

Supervisor: Prof. Dr. Róbert Ohmacht
Co-supervisor: Dr. Zoltán Szabó

Program leader: Prof. Dr. József Deli

Head of Doctoral School: Prof. Dr. Lóránd Barthó

University of Pécs
Medical School
Department of Biochemistry and Medical Chemistry

Pécs
2011.

Content

Abbreviations

AC	Amadori compound
ACN	acetonitrile
AGE	advanced glycation endproduct
CE	capillary electrophoresis
CHCA	α-cyano-4-hydroxycinnamic acid
DHB	2,5-dihydroxybenzoic acid
DTT	dithiotreitol
ESI	electrospray ionization
FAB	fast atom bombardment
FIA	flow injection analysis
FL	fructosyl lysine
FL-18	fructosyl lysine after loss of water
HbA1c	hemoglobin A1c
HPLC	high performance liquid chromatography
HSA	human serum albumin
ISD	in-source decay
LC	liquid chromatography
LC-MS	liquid chromatography coupled with mass spectrometry
LDI	laser desorption ionization
MALDI	matrix assisted laser desorption/ionization
MALDI-TOF/MS	matrix assisted laser desorption/ionization time of flight mass spectrometry
MS	mass spectrometry
ODS	octadecil silane
PBS	phosphate buffers saline
PMF	peptide mass fingerprint
PSD	post source decay
PTM	post translational modification
RNAse	ribonuclease A
RP	reversed phase
RSD	relative standard deviation
SA	sinapic acid
SPE	solid phase extraction
TFA	trifluoroacetic acid
THAP	2,4,6-trihydroxyacetophenone
THF	tetrahydrofurane
TOF	time of flight
TRIS	tris(hydroxymethyl)aminomethane

1. Introduction

1.1 Identification of peptides and proteins by MALDI-TOF mass spectrometry technique

Matrix assisted laser desorption/ionization (MALDI) was first described by Karas and Hillenkamp in 1988 [1]. MALDI is an improvement of the laser desorption ionization (LDI). In LDI the ionization is performed by irradiating with an ultraviolet laser. The disadvantage of LDI is that it has low sensitivity, the ionization causes ion fragmentation, and the signal is very dependent on the ultraviolet-adsorbing characteristics of the analyte [2]. As a result, this method is unsuitable for larger molecules like proteins, DNA, RNA etc.. To eliminate these problems, the analyte is mixed with a compound, the matrix that adsorbs the energy of the laser. Irradiation with the short-pulsed laser causes mainly ionization of the matrix and supports the ionization of the analyte [3]. That is why the MALDI technique can be used for the examination of peptides and proteins.

1.1.1. General set up of MALDI-TOF instrument

Ionsource - N_2 laser

Formation of ions and transition into the gas phase are required before the molecular masses of a component can be measured with the mass analyser. The generation of intact gas phase ions in general, is more difficult for higher molecular mass molecules. The advantage of recently discovered soft ionization techniques: MALDI and the electrospray ionization (ESI) is that intact gas phase ions are effectively formed from large biomolecules with minimal fragmentation [4].

In MALDI the sample molecules are co-crystallized with an excess amount of matrix. Ionization takes place through protonation in the acidic environments produced by the acidity of matrix and also through the addition of dilute acid solution to the samples. Pulses of 337 nm N_2 laser light are used to vaporize small amounts of the matrix and the ions included in the sample are carried into the gas phase in the process (Figure A in Appendix).

Mass analyzer – Time of flight (TOF) mass analyser

In Time of flight mass spectrometers the application of the high voltage, typically +20kV to +30kV (for positive ions, such as peptides) generates electric field that gives fixed amount of kinetic energy to the small pack of the ions. Following the acceleration, the ions enter the field-free region, where they travel at a velocity that is inversely proportional to their *m/z*. Because of this inverse relationship, ions with low *m/z* travel more rapidly than ions with high *m/z*. At the end of the field-free region a detector measures the time of flight (TOF). The resolution in a time of flight mass analyser is affected by the instrument and the operating conditions. The most remarkable limit on *m/z* resolution is the range of initial velocities of the ions as they are accelerated [4].

Instead of minimising the effects of the initial kinetic energy of the ions, Wiley and McLaren used first the time–lag focusing method, equipped with electron ionization source [5]. The delayed extraction (between ~100 nsec to ~500 nsec after the laser pulse) corrects the effect of the initial kinetic energy spread by the modification of the ion optics of the time of flight *m/z* mass analyser. Higher-energy ions move farther into the field-free region than lower-energy ions with the same mass. When the accelerating voltage is applied, it is applied with a potential gradient across the source region. The initial energy spread causes a small difference in the effective accelerating voltage. This compensates for the initial kinetic energy distribution so that ions with the same *m/z* arrive at the detector at the same time [6].

The ion mirror or ion reflector also corrects the effect of the initial kinetic energy spreads on mass resolution, created by an electric field that reverses the flight path of the ion. The most significant effect of the reflectron is focusing on ions with the same *m/z* but different velocities. Higher-velocity ions penetrate farther, and thereby spend a longer time in the reflectron than lower velocity ions.

When using the combination of delayed extraction and reflectron ion optics, the resolution of a time of flight mass spectrometer will increase to >100000. The practical effect of this increase in resolution is that monoisotopic peptide molecular weights can be determined as < 20 ppm (± 0.2 Da for a 1000 Da ion) in commercially available matrix assisted laser desorption time of flight mass spectrometers. This type of mass accuracy can have a significant effect on the database searches [4, 6].

1.1.2. In-source and post source fragmentation and tandem mass spectrometry

Proteins from complex biological samples are often identified by mass spectrometry (MS) with

"top-down" strategy, (the investigation of the proteins is carried out without enzymatic digestion), the in-source decay (ISD) mass spectrometry is an example

or

"bottom-up" approaches: peptide bonds in the protein are cleaved enzimatically and the identification of the unknown protein is implemented according to its peptide pool/peptide mass fingerprint (PMF) generated by the digestion [7].

In-source decay (ISD)

Although MALDI is a soft ionization technique, a significant degree of metastable decay can occur along the peptide or protein backbone. The in-source decay (ISD), one of the metastable fragmentations is directly observed after the desorption/ionization step in the source region [8]. Brown and Lemmon were the first to show the advantages of this procedure for analyzing the proteins.

First, the sample preparation is very simple: the analysis is accomplished without enzymatic digestion; the protein is mixed with matrix and directly deposited on the target.

Second, proteins fragment in three major series ions (c_n-, z_n-, y_n-ions (Figure B in Appendix) according to the Roepstoff's nomenclature) that greatly simplifies the mass spectrum interpretation [9, 10]. An N-terminus (and /or C-terminus) sequence tag are rapidly determined and used for protein identification in the database. The observed c_n, y_n produced from the fast metastable ion decay process is much different than the fragmentation produced from the more widely used post-source decay (PSD) MALDI technique [11]. Formation of b_n-, y_n-, a_n- and x_n-ions may occur by increasing the laser power [7].

Third, post translational modifications (PTMs) can be studied without loss of the modified group as it is often the case in conventional MS/MS.

Post-source decay (PSD)

MALDI was initially described as a “soft” ionization process. In the PSD technique, some fractions of the MALDI-generated ions undergo metastable decay during flight by either unimolecular or bimolecular (collisions) pathways producing smaller *m/z* ions and neutral molecules. Metastable ion decay occurs after ion acceleration and prior to detection (in the first field-free region of TOF analyser). PSD-MALDI fragmentation is typically most effective for small and moderate-sized peptides. (In contrast to larger peptides (>5000 Da) and even small proteins exhibit sequence-specific ISD fragmentation [12]). The ion fragments produced from the metastable ion decay of peptides and proteins typically include both neutral molecule losses (such as water, ammonia and portions of the amino acid side chains) and random cleavage at peptide bonds [11]. Typical fragmentation observed in PSD-MALDI corresponds to a_n, b_n ion series [13] and y_n type fragment ions with very small side chain specific cleavages (Figure 1). Another common phenomenon in PSD mass spectra is the predominance of fragment ions less than 17 Da (a_n-17, b_n-17 series) which is usually thought to be due to the loss of ammonia from the N-terminal residue [11]. Mass spectrum in PSD mode gives different informative data such as sequence and posttranslational modification (PTMs) identification [14-19].

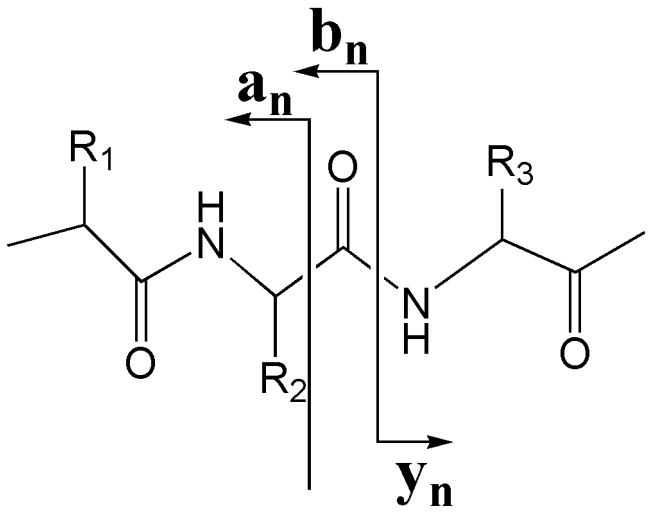

Figure 1: Nomenclature of fragment ions observed in post-source decay (PSD) [7]

Tandem Mass Spectrometry

Mass analysis is essentially a separation of ions according to their *m/z*. Tandem mass spectrometers use this separation as a preparative tool to isolate an ion with a specific *m/z* for further analysis. It is carried out by fragmentation of the mass-selected ion and by the determination the *m/z* of the fragment ions in a second stage mass analysis. The term "tandem mass spectrometry" reflects the fact that two stages of mass analysis are used in a single experiment. The result is that a specific ion in a complex mixture can be selectively studied in an experiment that gives structural information about that ion. In the case of peptide ions, the structural information is the amino acid sequence of the peptide [4].

Tandem-in-time instruments:

Instruments used for performing tandem mass spectrometry experiments in time have only one mass analyser (ion trap mass spectrometer) [4].

Tandem-in-space instruments:

Instruments in the tandem-in-space category have more than one mass analyser, and each mass analyser performs separately to accomplish the different stages of the experiments.

-"*triple quadrupole" mass spectrometer*: This type of mass spectrometer contains an octapole collision cell between two quadrupole mass filters (mass analyser).

-*quadrupole-time of flight mass spectrometer*: This instrument used for protein sequencing has a quadrupole mass filter for the first mass analyser and a time of flight mass analyser for the second one.

-*reflectron-time of flight mass spectrometer*:

In the reflectron time of flight instrument there is an electrostatic gate used for a precursor ion selection. This gate uses voltage pulses to deflect non-selected *m/z* ions away from the entrance to the flight tube. The PSD reactions are fragmentation reactions of metastable ions formed by matrix assisted laser desorption, which occur in the field-free region of the TOF instrument [19]. In a reflectron instrument that operates in a mass analysis mode, product ions from fragmentation are not detected because they are improperly focused by reflectron. Measuring the *m/z* of product ions requires a change of the potentials applied to the reflectron to compensate their lower kinetic energies [4, 5].

1.1.3. Peptides mass fingerprinting (PMF) and post-translational modification (PTM)

The sequence of the amino acid is unique to each protein and sequence analysis of whole proteins by sequential Edman degradation followed by BLAST (database) searching is a basic technique for monitoring proteins on proteomic investigation. A sequence of 12-15 amino acids is often sufficient for an unambiguous identification. However, Edman sequencing (specifically remove the N-terminal amino acid from the protein) is too slow (and expensive) for routine proteomic analysis and frequently the proteins N-terminally blocked. Edman degradation has now been almost entirely substituted by mass spectrometry.

The determination of the molecular weight of peptides, generated from photolytic or chemical digestion of a protein is a so called “mixture analysis” of peptides by mass spectrometry. The “MAPPING” of protein structures by soft ionization methods such as MALDI and Electrospray have become an important strategy for protein identification and post-translational modification analysis. New methods have been recently developed using a combination of protease digestion, MALDI MS and screening of peptide–mass database that offer significant increase in the speed at which proteins can be identified [20].

The method involves the generation of peptides from known or unknown proteins using residue-specific endoproteinases. All peptides are detected as singly charged ions, and no doubly charged peptide ions are observed. All mass values are measured for the monoisotopic $(M+H)^+$ ion. The peptide mass profile or fingerprint (PMF) of the query protein can be compared with theoretical peptide libraries generated from protein sequence databases to produce a list of likely matches. Practical sensitivity extends into the low-femtomole range, and three or four masses are often enough to get a significant match in the databases derived from more than 100 000 proteins [20].

The mass tolerance of the experimental peptides should reflect the accuracy of the mass spectrometer being used: typically this is 0.2 Da or 200 ppm or better. Search discrimination can be improved by combining results obtained using more than one photolytic enzyme or simple chemical cleavage. Increasing the size of the error window the number of the false positives will also rise [21].

A more important consideration in the use of MALDI analysis is the accuracy of the molecular weight measurement. The mass calibration can be implemented with internal standard ions (matrix ions and/or trypsin autolysis peptide ions) or external calibration.

Good external calibration requires placing the standard sample in close proximity to the analyte sample on the sample stage and acquiring the standard spectrum either immediately prior to or immediately after the acquisition of the spectrum [4, 6].

Post-translational modification (PTM)

The ability of mass spectrometry to characterize post-translational modifications is also unique among the protein and peptide sequencing methods and this use has been described as a vital contribution of mass spectrometry to polypeptide characterization.

By definition, a post-translational modification of a protein is any modification of the protein structure that occurs after the synthesis by translation of the messenger RNA. Post-translational modification of a protein, however, is most often envisaged as a change made to the structure of the side groups of specific amino acid residues contained in the protein. Mostly, no such modifications are expected for the aliphatic amino acids (glycine, alanine, valine, leucine and isoleucine) or the aromatic amino acid (phenylalanine). For the other amino acids, however, the presence of amine, carboxylic acid, hydroxyl, thiol, and thioether functional groups creates reactive sites that are vulnerable to a wide variety of chemical and biochemical reactions that can occur in the active milieu of the biological system. A common characteristic of these modifications is that the change made in the amino acid structure, produces a corresponding change in the amino acid residue. This change of formula weight constitutes the basis of the detection and characterisation by mass spectrometry [22].

1.1.4. Different on target sample preparation approaches

The function of the matrix is to dilute the sample, absorb the laser energy and ionise the sample. Each pulse from the laser vaporises both sample and matrix from the surface of the target and catalyses a chemical reaction which, in the positive ion mode, results in a proton $[M+H]^+$ or alkali metal atom being attached to the sample molecules. In the negative ion mode, the ionic species produced is usually $[M- H]^-$ [23].

Matrices:

The matrix is important in MALDI analysis because it serves both as laser energy absorbent and for energy transport. The matrix also separates the analyte molecules from each other, anticipating cluster formation and obviating direct laser "hit" that would effect intense peptide fragmentation [24]. Matrices can be small aromatic acids. The aromatic groups absorb at the wavelength of the laser light, while the acid helps the ionization of the sample molecules [4, 6]. A great variety of matrices are available.

A "good" matrix should meet several requirements: strong absorption at the laser wavelength, being a good solvent for the analytes, resulting in homogenous co-crystallisation.

Frequently used MALDI matrices:

sinapinic acid (**SA)**

A large number of matrices have been investigated by Beavis and Chait and sinapinic acid [21] has been found to be the best for larger ions giving better signals accordingly. This compound is preferred for the ionization of larger proteins and glycoproteins [25].

2,4,6-trihydroxyacetophenone (THAP)

Trihydroxyacetophenone has been thought to be the best matrix for analysing glycoproteins and glycopeptides, because it provides low limit of detection and gives less prompt fragmentation. THAP offers improved sensitivity for detection of acidic glycopeptides over alpha-cyano-4-hydroxycinnamic acid (Figure 2/d) [26].

α-cyano-4-hydroxycinnamic acid (CHCA)

For smaller proteins, α-cyano-4-hydroxy-cinnamic acid [27] is preferred [23], although CHCA forms small crystals that are unevenly distributed over the sample surface, i.e.; areas with lower crystal densities at the centre of the preparation (Figure 2/a) [25, 28].

2,5-dihydroxybenzoic acid (DHB)

DHB is better suited for analysing glycopeptides in combination with dried droplet technique than any other matrices [26]. Typically DHB tends to crystallise from the periphery of the target spot in the form of long needles that point towards the centre of the target (Figure 2/b) [23, 28, 29].

Various sample preparation methods are available:

dried-droplet method:

0.5–2 µL of sample and 0.5–1 µL of matrix solution (8 mg×mL^{-1}-saturated solution) (CHCA, SA, DHB, THAP) are mixed on the target and allowed to dry in the ambient air (slow crystallization technique), or optionally, in a gentle stream of forced air or argon (rapid crystallization method) (Figure 2) [25].

Thin layer method:

A thin layer of small, homogeneous matrix crystals is made on the target by placing either 0.5–1 µL of CHCA or 0.5–1 µL of THAP (2 mg×mL^{-1}) onto the target and the droplet is allowed to spread and dry, after that 1 µL of sample is added to the thin layer of crystalized matrix [25].

Mixed matrix:

In practice, one matrix may not meet the requirements mentioned above at the same time for the diversity of analytes in a sample, so co-matrices formed by the use of a suitable additive in the matrix solution are often used.

The combination of two common matrices (CHCA and DHB) mixed in dried droplet preparation was written as an excelent co-matrix. Combination of the matrices showed better crystal distribution with DHB-like crystals forming short needles at the rim and evenly distributed CHCA-like crystals inside the rim [28]. Combination of CHCA and DHB results in increased surface homogeneity and spot-to-spot reproducibility, increased signal-to-noise ratio and tolerance to impurities [28].

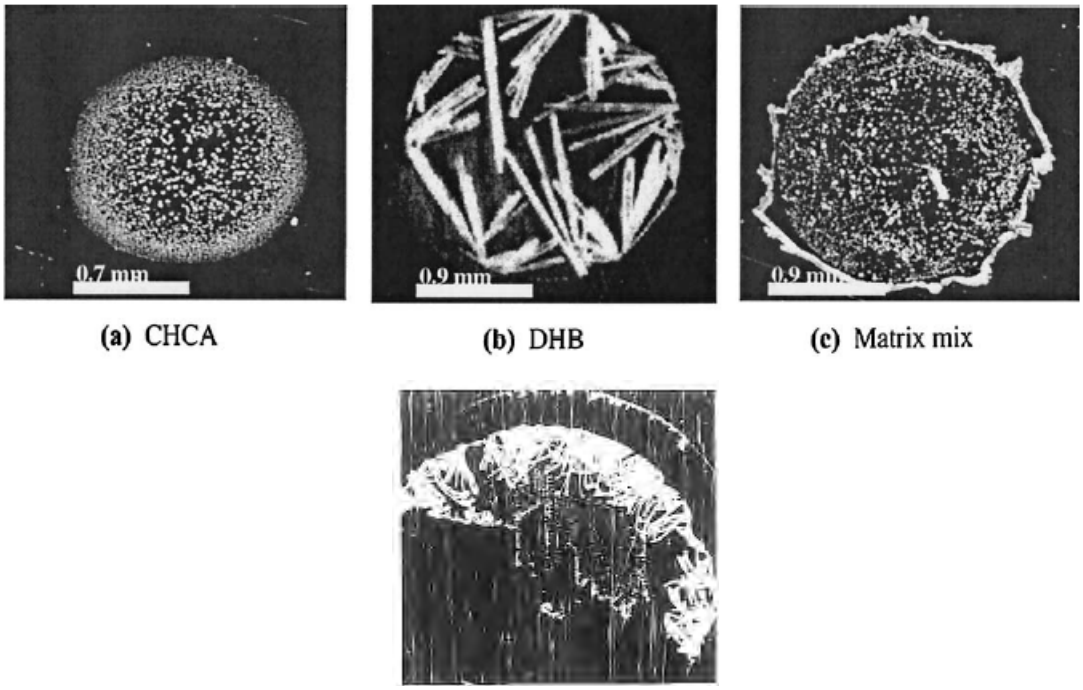

Figure 2: a) CHCA b) DHB c) Matrix mixture [28] d) THAP [26]
Microphotographs obtained with a) CHCA b) DHB d) THAP and c) mixed matrix preparations in the dried-droplet method.

1.2. Desalting of proteins and peptides by solid phase extraction (SPE)

An important prerequisite of the MALDI-TOF/MS measurements is the removal of disturbing compounds; e.g. salts from the buffer or urea, guanidine hydrochloride after proteolysis [29].

SPE is an easily applicable method most frequently used for desalting, purification, preconcentration and fractionation of a complex mixture of peptides [30-32]. Fractionation prior to analyses can have a significant effect on sequence coverage of proteins particularly implemented for those peptides obtained from the proteolysis of larger proteins [24]. Further advantages of the SPE method include relatively high recovery rate, short extraction time, high enrichment factor and low consumption of organic solvents [33, 34].

1.2.1. SPE packings often used in bioanalytical investigations

The classical commonly used sorbents are porous silica-based particles surface-modified with C18 or other hydrophobic alkyl groups such as C4, C14, C30. The Oasis from Waters and the Abselut from Varian are available from polymer monolithic columns.

1.2.1.1 Silica based phases

The most widely used SPE materials in the field of bioanalytical research are silica-based C18 reversed phase sorbents, since the introduction of Sep-Pak cartridges in 1978 [34], despite some drawbacks of using alkylated silica (low recovery for basic analytes, relatively low capacity and poor wettability, etc.) [35].

1.2.1.2 Polymer based resins

The new generation of polymers (Oasis from Waters, Abselut from Varian) are developed to extract widespread spectrum of analytes, i.e., lipophilic, hydrophobic, acidic, basic and neutral with a single cartridge with a simplified procedure (no conditioning is required) [36]. The polymer beads in the extraction cartridge can be used from pH 1 to 14 (in contrast to classical reversed phase silica extraction columns) and with many different polar and apolar organic solvents (methanol, chloroform, diethyl ether, etc.). Therefore, when using polymer sorbents, it is easier to find an appropriate extraction condition for specific compounds and especially for mixture of analytes with different chemical properties [37].
By the introduction of Oasis HLB sorbent prepared by the copolymerization of lipophilic divinylbenzene and hydrophilic N-vinylpyrrolidone the flowthrough of some polar compounds, the undesirable effect of silanol groups and the poor wettability in water were eliminated [38]. Another important SPE medium is the Abselut™, which is a blend of methacrylic ester-based polymeric and polystyrene resin mixed in a particular ratio [37].

1.2.1.3 Novel stationary phases for SPE

Fullerene

Fullerenes, allotropic forms of carbon were discovered in 1985 [39] and they can be considered as a well-characterized nanostructure [40]. The use of C60 or a mixture of C60 and C70 fullerene has increased. Many different applications of fullerenes have been reported in analytical chemistry for preconcentration purposes due to its good stability, wide pH range for working conditions, and high surface area [41].

Fullerene derivatized silica - C60 silica

Hydrophilic peptides like phosphopeptides and glycopeptides can be retained and purified on neither RP silica particles nor polymeric SPE resins mentioned above. For the purification and enrichment of such molecules the preparation and application of fullerene(C60)-silica (Figure 3) have been recently described [42]. Fullerene(C60)-silica can be prominent SPE sorbent material, showing reversible interactions with analytes with low masses such as flavonoids and peptides. These newly developed fullerene-derivatized silica materials are compared with some already obtainable SPE materials on the market. C60-silica has proven to have excellent features toward SPE applications with different molecules [42].

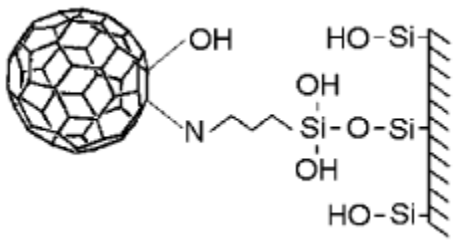

Figure 3: structure of the fullerene silica [42]

1.2.2. On-line and off-line solid phase extraction

The principles of HPLC and SPE are similar: adsorption and distribution of analytes between the mobile and stationary phases. The surface chemistry of the particles is mostly based on C18 modified silica and the design of SPE cartridges is similar to chromatographic columns.

On-line solid phase extraction:

Two approaches (to improve throughput and reliability of the analytical method) have been developed to automate solid phase extraction. It is required to employ a robotic system to automate the sample preparation using traditional desalting devices or extraction plates.
The sample is loaded and concentrated onto a modified SPE device (capable of high-pressure operation) which is located at the injection sample loop. The undesired components are washed off the SPE cartridge to waste by the mobile phase. Afterwards a valve is switched and the required components of the SPE device is eluted on to the analytical column and the sample can be analysed by a mass spectrometric instrument [30].

Off-line solid phase extraction:

Modern solid phase extraction is most often based on alkyl surface modified silica. The instrumental design of SPE is similar to a small chromatographic column, although off-line SPE devices vary from chromatographic columns in such features:

(i) off-line SPE devices are disposable, made for a single use only
(ii) SPE devices are packed with larger particle size sorbents (30-100µm), while HPLC columns are filled with 3-5µm particles.
(iii) the length of SPE devices are smaller than that of the HPLC columns
(iv) SPE devices can easily be loaded and can elute the sample into diverse collection devices
(v) there is significant dead volume of the SPE devices
(vi) SPE devices ensure considerably lower chromatographic efficiency than HPLC columns [30].

The two most popular applications for SPE:

One is when the analyte is derived from biological liquids and drugs of interest are retained on the sorbent, as long as most of the protein components are eliminated to the waste by the washing solution (aqueous buffer).

The other common use of the SPE is desalting peptides or DNA oligonucleotides. While these required sample molecules are retained on the sorbents, non-volatile salts are washed off the sorbent with pure water [30].

The choice of the pH and the mobile phase strength is crucial for the best SPE selectivity because of the strength of the possible washing solvent to eliminate the interfering components without loss of desired analyte. The convenient pH is selected for suppressing in analyte ionization, because the non-ionized form of the analytes are much more strongly retained on reversed phase sorbents.

Microextraction methods:

Miniaturization of sample pre-treatment was a current trend in the last years. This derived from several factors:

- The available sample amount is limited (proteins isolated from gel slabs, single cell analysis).
- Some samples may be expensive
- Miniaturized techniques (capillary electrophoresis (CE) and capillary HPLC) require less than a few microliters for analysis
- Miniaturization of sample clean-up apparatus allows for parallel processing of samples for high throughput.

This trend of biological sample processing leads to smaller sample volumes and higher sample enrichment efficiency [30].

Miniaturized solid phase extraction tips are packed with a small amount (0.1mg) of reversed phase material or other sorbent, which allows eluting the desired components in small volume of mobile phase [30]. Microscale SPE has been developed for MALDI-TOF/MS [43] and off-line nano-electrospray (ESI) MS [44].

To fulfil the requirement, pipette-like tips were manufactured using small amounts of sorbent trapped in plastic tips [45]. Prior to analysis, the peptides/proteins can be preconcentrated or selectively captured employing tips packed with particles with different affinities (normal phase, RP silica, ion exchanger or resins provided with affinity chromatography, molecular

imprinted stationary phases, restricted access sorbents or mixed mode sorbents). The extensively used ZipTips (C18-silica) (Millipore, Bedford, USA) is similar to a 10µl micropipette tip with a bed volume of 0.55 µl. Sample volumes of 2-4 µl can be processed with a capacity of up to 15µg for peptides [46].

1.3. Boronate affinity chromatography

Boric acid and boronic acid are well known to form stable esters with polyols and saccharides containing *cis*-diol groups [47]. Increased attention has been paid to these compounds because of their prospective applicability to recognize sugars [48].

Boronate affinity columns were first used for the separation of sugars, polysaccharides and nucleic acid components by Weith et al in 1970 [49]. Up till now this method has been adopted ubiquitously for the separation of *cis*-diol compounds such as nucleosides, nucleotides, nucleic acids, carbohydrates, enzymes, glycated proteins, glycated peptides. This method is described as a useful separation technique for the measurement of glycohemoglobin, the study of the glycation pattern of hemoglobin, the determination of hemoglobin HbA1c in diabetic patients, the purification of arginine containing peptides and the separation of glycoproteins and glycopeptides [50].

1.3.1. Interactions between immobilized boronate and analytes

Primary interactions:

The most important interaction in boronate affinity chromatography is the esterification that exfoliates between a boronate ligand and a *cis*-diol containing compound. Ideally, this ester bound requires that the two hydroxyl groups of the diol be adjacent carbon atoms and in an approximately coplanar configuration. If the interactions between boronates and 1,3-*cis*-diols or trident interactions between boronates and *cis*-inositol or trietanolamine occur, they give weaker ester bonds than those between the 1,2-*cis*-diols and the boronates.

The interaction occurs in aqueous solution under basic conditions, the boronate is hydroxylated and then it can form cyclic diesters with *cis*-diols. The formed esters can be hydrolysed under acidic conditions. This reaction is reversible in aqueous solution (Figure 4) [51].

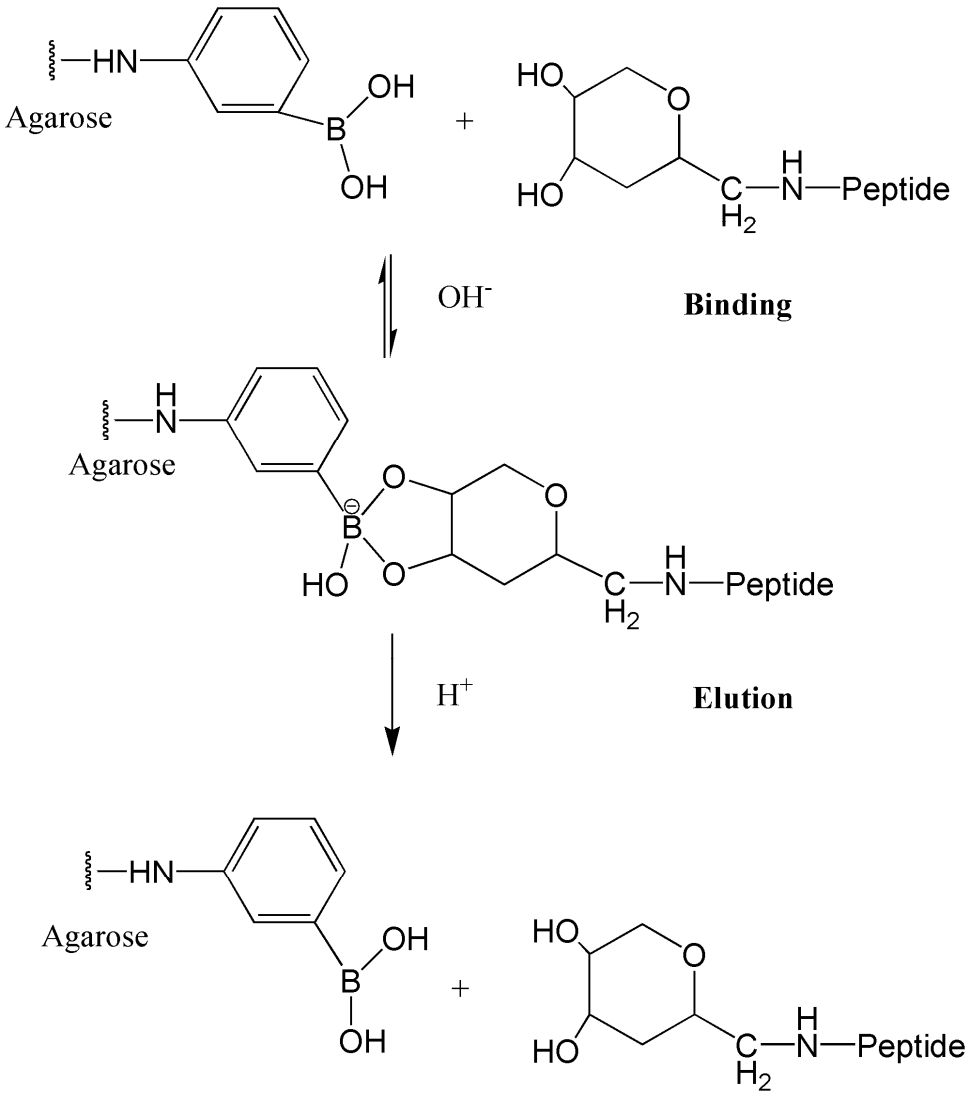

Figure 4: Mechanism of binding and elution processes between *cis*–diol-containing compounds, for example Amadori peptides and boronic acid [51].

While using boronate affinity chromatography, secondary interactions (especially hydrophobic and ionic interactions) must be considered.

Secondary interactions:

Four types of secondary interactions can occur on boronate affinity material: hydrophobic interactions, ionic interactions, hydrogen bonding and coordination interactions.

Hydrophobic interactions:

Most of the used boronate affinity ligands are aromatic boronates. These include a phenyl ring that could give rise to hydrophobic interactions or aromatic π-π interactions. Hydrophobic interactions could give an additional selectivity to the column. Hydrophobic interactions are sometimes responsible for the nonspecific binding of undesired proteins or peptides. This phenomenon can entirely be avoided by adding detergents to the mobile phase/binding buffer [50, 52]. To reduce hydrophobic influences in the boronate affinity chromatography is to keep the ionic strength of the mobile phase low.

Ionic interactions:

The active tetrahedral boronate is negatively charged therefore boronate ligands can create coulumbic attraction or repulsion for ionic analytes. Generally, this effect is weaker than boronate/*cis*-diol ester formation. Ionic interactions between the negatively-charged boronate and anionic proteins can hinder the necessary binding; this is why Mg^{2+} ions at low concentrations are to be added to the mobile phase/binding buffer in order to eliminate the undesirable ionic effects [50, 52]. As in hydrophobic interaction, ionic interactions can cause additional selectivity for boronate affinity separation. To decrease ionic effects, the ionic strength of the mobile phase should be kept high, although this will also effect stronger hydrophobic interactions.

Hydrogen bonding:

Since boronic acid has three hydroxyls in the active tetrahedral form (or two in the non-active form) it has several possibilities for form hydrogen bonds. Although the effect of this possible interaction is usually small, under special condition hydrogen bond bonding could be strong enough to be the main mechanism for retention on a boronate column.

Coordination interactions:

In the non-activated trigonal uncharged boronate molecule the boron atom has an empty orbital; this could attend as an electron pair acceptor for a coordination interaction. In the sample the unprotonated amines are perfect electron pair donors and when an amine donates a pair of electrons to the boron atom, the boronate molecule becomes tetrahedral. This explains why amines may attend to promote boronate/*cis*-diol esterification. However, if there is a hydroxyl group adjacent to the amine, this hydroxyl group could interact with the tetrahedral boronate. This interaction could prevent the esterification between the boronate ligand and the analyte. For this reason it is required that TRIS (tris(hydroxymethyl)aminomethane) and ethanolamine derivatives be avoided in buffers used for boronate affinity chromatography [50].

1.3.2. Types of stationary phases of boronate affinity chromatography

Boronate can be employed as a matrix which can selectively bind the glycol moieties through covalent binding with a 1,2-*cis*-diol of glycostructure. Zhou et al. [48] prepared aminophenylboronic acid-functionalized magnetic nanoparticles and successfully applied them to selective separation in proteomics; in addition, Xu et al. [50] have successfully utilized boronic acid-functionalized mesoporous silica to enrich glycopeptides. Potter et al. [53] and Ren et al. [54] reported using boronate monoliths for affinity separation and capturing of *cis*-diol containing compounds, respectively.

Carboxylic acid terminated magnetic beads

Recently, magnetic beads have been used for immobilization of aminophenilboronic acid and applied for the specific binding of *cis*-diol containing compounds. Since these magnetic beads can be washed and separated easily with an external magnetic field, the use of phenilboronic acid immobilized magnetic beads is a very efficient method for the sample preparation of glycoproteins, glycopeptides and glycated peptides for mass spectrometry, especially for MALDI measurement [55].

Agarose beads

The application of the immobilized phenylboronic acid on agarose and sepharose hydrogel microparticles, which are deposited on an aluminium chip, enabled the high throughput analysis of AGEs from serum sample by MALDI–MS. One of the most advantageous features of the microchip is that no elution of the bound molecules is required [56].

Silica based boronate affinity chromatography

Boronic acid functionalized mesoporous silica, which preserves the attractive features of high surface area and large accessible porosity, was developed to enrich *cis*-diol compounds, e.g. glycopeptides. Boronic acid functionalized mesoporous silica has a comparatively large specific surface area, so it could adsorb glycopeptides fast and efficiently. Its other great advantage that is easy to recover by centrifuge in order to extract glycopeptides from the peptide pool effectively. [57]

polymer monolith as a stationery phase in boronate affinity chromatography

Recently the boronic affinity chromatography was combined with monolithic stationary phase by Potter et al. in 2006 [53]. Monolithic beds can be described as an integrated continuous porous separation media without interparticular voids [58]. This combination of boronate affinity chromatography with monolithic column format offers better performance and more functions for the analysis of *cis*-diol-containing compounds. Besides, it avoids non-specific interactions, especially reversed phase interaction. The optimization of these new-generation columns has not been executed, and unfortunately, the literature of boronate functionalized monolithic columns is still in progress [58, 59, 60].

1.3.3. Application of boronate affinity in the field of proteomics

Boronate affinity columns were first used for the separation of sugars, polysaccharides and nucleic acid components by Weith et al in 1970 [49]. The application of the boronate affinity column in proteomics for the separation and quantification of glycohemoglobin was published by Mallia et al. in 1981. A low–performance agarose gel was applied as the support and absorbance detection at 414 nm was used to quantify the retained and non-retained

hemoglobins in human hemolysate samples. Elution was carried out by a soluble diol-containing agent (sorbitol solution) that eluted the retained glycohemoglobin from the column.

Up till now this method has been adopted ubiquitously for the separation of *cis*-diol compounds such as nucleosides, nucleotides, nucleic acids, carbohydrates, enzymes. This method is described as a useful separation technique for the quantitative measurement of glycohemoglobin [61], the study of the glycation pattern of hemoglobin, the determination of hemoglobin HbA1c in diabetic patients, the purification of arginine containing peptides, the separation of enzymes [47, 48] glycoproteins and glycopeptides glycosylated proteins [24, 62-66] and glycosylated peptides [50, 59, 67, 68].

1.4. Non-enzymatic glycation

Non-enzymatic glycation is the covalent binding of single reducing sugars to amino groups in proteins. The initial product is a labile Schiff base intermediate, which slowly isomerises to form a stable ketoamine, called Amadori compound (AC). The AC can undergo further oxidation rearrangement reactions to form a series of more reactive, coloured, fluorescent compounds, termed advanced glycation end-products (AGEs), which play a pathogenic role in the development of diabetic complications [69].

1.4.1 Non-enzymatic glycation of proteins

Formation of Schiff base and Amadori compounds

The non-enzymatic reaction of the amino groups of amino acids, peptides and proteins with reducing sugars was first studied under defined conditions in the early 1900s by L. C. Maillard [70]. Non-enzymatic glycation is the covalent binding of single reducing sugars (glucose, fructose, ribose, etc.) to primary amino groups in proteins, such as the ε-amino group of the protein lysine residue (Figure 5) [71, 72, 73]. The initial product of Maillard reaction is a labile Schiff base intermediate [64, 74]. In the 1920s Amadori showed that the Schiff bases could be converted to isomeric products via an intermediate, an open-chain enol form (Figure 5) by the Amadori rearrangement [75]. In the reaction the labile adduct slowly

isomerizes and therefore forms a stable ketoamine, called the Amadori compound (AC) [74, 76] (83). To simplify the discussions of the Maillard reactions, the adducts are frequently depicted as the more reactive open-chain forms. Formation of the Schiff base is relatively fast and highly reversible and the formation of the Amadori product from the Schiff base is slower, but much faster than the reverse reaction, so that the glycation product tends to accumulate on proteins [64, 72].

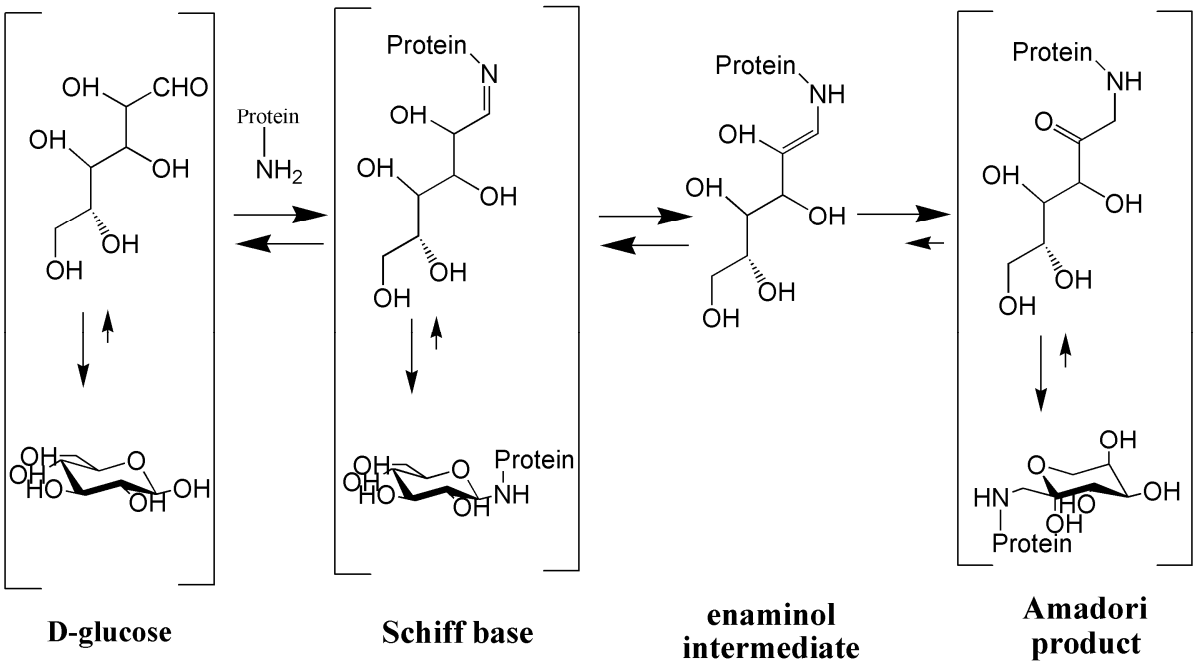

Figure 5: Formation of the glucose-protein Schiff base and the Amadori rearrangement [64]

Advanced Glycation End products (AGEs)

The AC can undergo additional oxidation and rearrangement reactions and eventually dehydration, condensation, fragmentation, oxidation and cyclization reactions to form a series of biologically considerably more reactive constituents, termed advanced glycation end-products (AGEs) [74, 77].

Different types of AGEs are known, depending on the compound they originate from. Six distinct classes of AGEs were recognized deriving from glucose (AGE-1), from other carbohydrates, such as glyceraldehydes (AGE-2), and from α-dicarbonyls, such as glycoaldehyde (AGE-3), methylglyoxal (AGE-4), glyoxal (AGE-5), 3-deoxyglucosone (AGE-6) by Takeuchi et al. in 2004 [78]. All these compounds can react with the amino group

of lysine of the terminal amino group of proteins and with the guanidine group of arginine and also with cystein. Moreover, AGEs can generate crosslinks in proteins [79], free radical reactions that might catalyze further damaged proteins, lipids or DNA [72].

1.4.2. Physiological importance of non-enzymatic glycation

As a result of the non-enzymatic glycation the above mentioned types of AGEs can be formed because of the increased blood glucose level in hyperglycaemia, diabetes mellitus types I and II. However, the total biochemical pathway between chronic hyperglycaemia and functional alterations and tissue damage are still incompletely understood. There are several candidate mechanisms for explanation: such as, the increase in non-enzymatic glycation of proteins, with irreversible formation and deposition of AGEs and the increased oxidative stress (possibly caused by the presence of the increased level of the AGEs) [79].
Three core reactions of AGE damage were described as follows: interactions with specific receptors, intracellular accumulation and abnormal crosslink formation.

Until now, crosslink formation, especially at collagen level was thought to be the most important mechanisms of the AGE damage, as well as the physical and chemical modifications of collagen causing abnormal vascular rigidity, arterial stiffness, basement membrane thickness [74, 80]. On the other hand long-lived proteins, such as lens crystalline, collagen of the extracellular matrix, serum albumin and haemoglobin accumulate AGEs *in vivo* [72].

Diabetes is an extensive disease, affecting 4% of the whole world population. For this reason, great efforts have been made to optimize the control of the acute complications of the disease (hypoglycaemic coma, ketoacidosis, and infections), but the long-term complications of the diabetes such as macroangyopathy, vasculopaty, immunodeficiency, nephropathy, retinopathy and neuropathy, which still remain widely spread [81, 82].

1.4.3. Clinical methods used for the detection of non-enzymatic glycation

Since the 1970s, the measurement of glycated hemoglobin A1c (HbA1c) has been used routinely as a clinical diagnostic marker for relatively long term (4-6 weeks) glucose control in diabetic patients [63]. In order to find more specific and informative protein biomarkers for monitoring the glycemic state and to get a deeper insight in the role of

glycation in the development of diabetic complications comprehensive proteomic studies are required.

The level of the glycated albumin in serum is thought to represent the condition of the blood glucose over the last 2 to 4 weeks, while HbA1c indicates glycaemia state over the last 1 or 2 months [65]. Glycated human serum albumin (HSA) is an important midterm indicator of diabetes that is more sensitive to changes in blood glucose level than HbA1c [64]. The glycated albumin level also provides useful information on glycaemic control when monitoring the efficiency of therapy [65].

Recently, the main techniques investigating the glycation of proteins have been based on a variety of on- and off-line mass spectrometric methods (LC coupled to MS, CE or LC separation/fractionation-MALDI MS, etc) [24, 66, 67, 68]. Although a great number of studies deal with the examination of glycation as well as with the methodological development concerning the investigation of glycated constituents, there is a need to improve the existing methods or to develop novel, more sufficient and less time consuming techniques.

2. Aims

2.1 Development in the application of Solid Phase Extraction:

I. ***Determination of the binding capacity of C30 and C60(30) fullerene silica with Leu-enkephalin***

II. ***Identification of C18, C30, C60(10), C60(30) and C60(100) on the sequence coverage of the tryptic digests***

III. ***Determination of glycated sites of Human Serum Albumin (HSA) and fibrinogen with C30 and C60(30)-silica***

2.2 Experiments of boronate affinity chromatography for the separation of glycated peptides:

IV. ***Optimization of different approaches of elution in the case of boronate affinity tips***.

V. ***Desalting of glycated peptides using different sorbents***

VI. ***Application of the new method for the detection of glycated peptides obtained from digested human serum albumin, collected from patients suffering from type 2 diabetes– compared to that of healthy volunteers***

3. Materials and methods

3.1 Materials and methods in the case of solid phase (SPE) experiments

The first part of this chapter of the thesis includes the instrumentation and the documentation of the research on the optimization of the solid phase extraction method for glycated peptides.

3.1.1 Materials

C60-fullerene (≥99.5 %) was bought from MER Corp. (Tucson, AZ, USA). Acetonitrile, methanol (both gradient grade), human serum albumin (HSA, 97-99%), fibrinogen (fraction I, type I: from human plasma, 67 % protein), Leu-enkephalin acetate hydrate (≥97 %), [Arg^8]-Vasopressin acetate salt (≥99 %), angiotensin I human acetate hydrate (≥90 %), trifluoroacetic acid (≥99%), α-cyano-4-hydroxycinnamic acid (CHCA, ≥99 %), 2,5-dihydroxybenzoic acid (DHB, ≥99%), 2',4',6'-trihydroxyacetophenone monohydrate (THA ≥99.5 %), sinapinic acid (SA, ≥99%), D/L-dithiothreitol (DTT, >99 %), iodoacetamide (≥98 %), 2-mercaptoethanol (≥98 %), ammonium bicarbonate (>99 %), 3-chloroperoxybenzoic acid (70-75 %) and (aminopropyl)trimethoxysilane (>97 %) were purchased from Sigma-Aldrich (Budapest, Hungary). D-glucose monohydrate (puriss), urea, toluene (>99 %) and tetrahydrofuran (>99.8 %) were from Reanal Finechemical Co. (Budapest, Hungary). Formic acid (98-100%) was bought from Scharlau Chemie S.A. (Barcelona, Spain). Peptide calibration standard (consisting of bradykinin, angiotensin II, angiotensin I, substance P, renin substrate, ACTH clip (1-17), ACTH clip (18-39) and somatostatin) and protein calibration standard (consisting of trypsinogen, protein A, BSA, BSA-dimer) were obtained from Bruker Daltonics (Bremen, Germany). Trypsin (sequencing grade, modified) was provided by Promega Corporation (Madison WI, USA). Bidistilled water was prepared in our laboratory.

3.1.2 Instrumentation

Autoflex II MALDI instrument from Bruker Daltonics was used for the mass spectrometric measurements.

The HPLC instrument consists of a Dionex P680 gradient pump, Rheodyne 8125 injection valve, a Dionex UVD 340U UV–Vis detector (Dionex, Germany). Data acquisition was carried out using the Chromeleon software (version: 6.60 SP3 Build 1485).

A Jasco V-550 UV–Vis spectrophotometer (Tokyo, Japan) was employed for measuring the adsorption spectra of SPE materials.

Pore size and pore volume of the phases were measured employing mercury intrusion porosimetry method (Porosimeter 2000, Thermo Finnigan, San Jose, USA).

Elemental analysis of all the investigated phases was implemented by a Carlo Erba EA 1110 CHNS instrument (Rodano, Italy).

The specific surface area of the phases was determined by BET method using a homebuilt device [42].

3.1.3 Preparation of the SPE phases

For the SPE experiments C18 and C30 RP materials were synthetised from Kovasil silica gel according to the method described by Szabó et al. [83]. The C60(fullerene)-derivatised silica particles, (prepared, described and characterised by Vallant et al.) [42] were made from three different silica gels with distinctive characteristics in order to study the effects of porosity. The amino groups remained on C60-derivatives after the first derivatisation considerably shielded by the bulky C60 balls (Figure 3); therefore the phase behaves RP rather than normal phase. Moreover, the protonated NH_3^+ groups repulse the protonated, positively charged peptides. So they are not supposed to be well accessible to the peptides.

3.1.4 In-vitro glycation of HSA and fibrinogen

HSA (Sigma-Aldrich) (5 mg) was dissolved in D-glucose solution (0.167 M in phosphate buffered saline (PBS), pH 7.4) [81]. Fibrinogen (Sigma-Aldrich) does not dissolve in water; therefore 2 mg of protein was layered on top of warm (37°C) saline solution (0.9% m/v) consisting of D-glucose at a concentration of 0.167 M [84]. This solution was gently agitated till the material was dissolved and then it was further diluted with PBS buffer (containing D-glucose at a concentration of 0.167 M) in 1:1 ratio. Solutions of both proteins were incubated under aseptic conditions for 28 days at 37°C. Before further modifications and tryptic digestion the glycated HSA and glycated fibrinogen were purified by centrifugation through a membrane (Millipore, cut-off: 3000 Da).

3.1.5 Tryptic digestion of nonglycated and glycated HSA and fibrinogen

HSA (1 mg) or fibrinogen (1 mg) was dissolved in 500 µL of denaturing buffer consisting of 8 M urea and 0.5 M ammonium bicarbonate, and was shaken for 30 min, at 37°C to denature the proteins. DTT (50 µL, 30 mM) solution was added to break the disulphide bonds (37°C, 4 h). After the solution was cooled down, 25 µL 100 mM iodoacetamide solution was added for 15 min in darkness to alkylate the cysteines. The reaction was stopped by the addition of 50 µL 100 mM 2-mercaptoethanol and the mixture was kept at ambient temperature for 15 min. Then the solutions of both proteins were put into a Microcon-YM3 centrifugal filter tube (Millipore) and centrifuged at 13000 × g for 4 h. This assured the removal of excess chemicals through the membrane (cut-off: 3000 Da). The residues of the modified proteins were digested with trypsin to a protein ratio of 1:100 in 50 mM ammonium bicarbonate solution overnight at 37 °C. The digestion was stopped by evaporation under vacuum and the resulting digest was redissolved in 5 µL water. The same protocol was used for the glycated proteins. Figure 6 shows the photolytic digestion by trypsin [85].

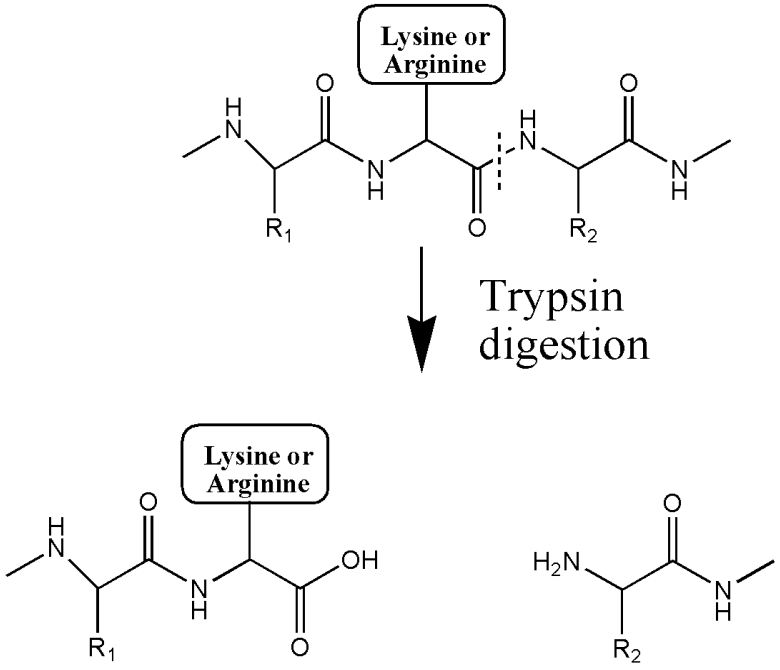

Figure 6: cleavage by trypsin

Trypsin is known to cleave proteins at the carboxyl side of the arginine and lysine residues except those that have a proline at their C-terminal end [67].

3.1.6 Recovery study of the phases

Into five 1.5 mL volume SPE cartridges (Alltech Extract-CleanTM SPE 1.5 mL Reservoir, Alltech Associates, Deerfield, USA) 5 mg from each SPE material was placed and sealed with Teflon frits. All materials were washed with 2 mL tetrahydrofurane (THF), and then with 1 mL methanol to eliminate the contaminants that might have ensued from the derivatization. This was followed by an activation step; using 2 mL acetonitrile (ACN) containing 0.1% trifluoroacetic acide (TFA). Then the particles were rinsed with 2 mL of a 0.1% TFA in 50% ACN and the cartridges were equilibrated with 2 mL 0.1% TFA in water. Solutions (200 µL) consisting of three peptides (Leu-enkephalin, [Arg^8]-vasopressin and angiotensin I) in different concentrations (10, 30, and 50 µg from each) were loaded onto the equilibrated cartridges. The permeate was collected and the cartridge was washed with 0.1% TFA in water. The bound peptides were eluted with 300 µL 50% ACN containing 0.1% TFA. To ensure the complete and quantitative removal of peptides the elution step was repeated and the two fractions were combined. The solvent from the breakthrough and the eluates were evaporated under vacuum, the remaining peptides were redissolved in 1 mL 0.1% TFA in water and the solution of the peptides was analysed with HPLC. The separation of the three peptides was carried out on a Kovasil ODS (C18) column using gradient elution. Eluent "A" was 0.1% v/v TFA containing 5% v/v ACN, while eluent "B" 0.1% TFA in 95% v/v ACN. The gradient profile was: 0–6 min: 0% "B" → 20% "B", 6–20 min: 20% "B" → 38% "B", 20– 22 min: 38% "B" → 60% "B", 22–24 min: 60% "B". The flow rate was: 1.2 $mL \times min^{-1}$. Chromatograms were monitored at 214 nm [85].

3.1.7 Adsorption of peptides on C30 and C60 silica

After the activation and equilibration, 3 mg of both C30-silica and C60(30) were incubated overnight with a solution of Leu-enkephalin (0.1% TFA in water) at different concentrations ranging from 60 to 210 µg/mL under vigorous shaking at 20°C. Then the particles were centrifuged and the supernatants were analysed.

3.1.8 SPE of the digests

The tryptic digest (20 pmol) from HSA and fibrinogen in 200 µL 0.1% TFA/water were loaded onto the equilibrated particles, and the SPE tubes were washed three times with 1 mL 0.1% TFA/water to remove the non-bound peptides. The peptide pool was fractionated

gradually with 5–70% v/v of ACN/water with 0.1% TFA, increasing the ACN concentration of the eluents with 5% in each step. From each eluent 300 µL was used. Fractions were collected, evaporated, redissolved in 5 µL water and analysed by MALDI-TOF/MS. For the fractionations of the glycated protein digests the same procedure was done.

3.1.9 Enrichment of the glycated peptides using boronate affinity tips

Pipette tips containing 5 µL gel of immobilized m-aminophenylboronic acid with a total volume of 200 µL (PhyTip 1000+ columns, PhyNexus, San Jose, USA) were used for the enrichment of the glycated peptides. After rehydration the tips were equilibrated with binding buffer (150 mM NH_4Cl and 50 mM $MgSO_4$ at pH 8.2). Glycated peptides were diluted with the binding buffer and the solution was aspirated through the affinity gel. Then the tips were washed with 1 mL of binding buffer to remove unselectively bound peptides, and with bidistilled water to get rid of the residues of buffer constituents. Glycated peptides were eluted with 4x50 µL formic acid solution at pH 2.

3.1.10 Preparation of different MALDI matrices

Three different matrices were compared for the ionisation of peptides. 2,5-dihydroxybenzoic acid (DHB) was prepared in 20% v/v ACN /0.1% TFA/ water at a concentration of 25 $mg \times mL^{-1}$.

Saturated solution of α-cyano-4-hydroxycinnamic acid (CHCA) was prepared in a mixture of water and ACN 2:1 ratio containing 0.1% TFA.

2',4',6'-trihydroxyacetophenone monohydrate (THAP) was dissolved at a concentration of 15 $mg \times mL^{-1}$ in 50% v/v ACN / 0.1% TFA/water.

The saturated solution of sinapinic acid (SA) was prepared in 50% v/v ACN and 0.1% TFA in water for the ionization of proteins.

3.1.11 MALDI-TOF/MS analysis

All mass spectra were acquired in positive mode with pulsed ionisation (k = 337 nm; nitrogen laser, maximum pulse rate: 50 Hz; maximal intensity 20–30% of the laser for peptides). Tryptic peptides were measured in reflectron mode using a delayed extraction of 120 ns and were monoisotopically resolved.

Proteins were measured in linear mode at a delayed extraction of 550 ns. The accelerating voltage was set to +19 kV, the reflectron voltage was set to +20 kV. Spectra of peptides and proteins were the sum of 1000 shots on the same sample spot, external calibration was used. Data processing was executed with Flex Analysis software packages (version: 2.4.). For the in-silico digestion Sequence Editor software (Bruker Daltonics) was used with the following criteria:

(i) all cysteines (C) were supposed to be treated with iodoacetamide,

(ii) monoisotopic masses were allowed and

(iii) the maximum number of missed cleavage sites was two.

3.2 Material and methods for experiments of the boronate affinity chromatography

The second part consists of the description of the instrumentation and methods of the optimization and application of boronate affinity enrichment of the glycated peptides.

3.2.1 Materials

Acetonitrile (ACN), methanol (both gradient grade), human serum albumin (HSA, 97-99%), ribonuclease A (RNase, from bovine pancrease, >90 %), trifluoroacetic acid (TFA, ≥99%), α-cyano-4-hydroxycinnamic acid (CHCA, ≥99 %), 2,5-dihydroxybenzoic acid (DHB, ≥99%), sinapinic acid (SA, ≥99%), D/L-dithiothreitol (DTT, >99 %), taurine (≥98 %), iodoacetamide (≥98 %), 2-mercaptoethanol (≥98 %), ammonium bicarbonate (>99 %) were purchased from Sigma-Aldrich (Budapest, Hungary). D-glucose monohydrate (puriss), D-sorbitol (puriss) urea, sodium hydroxide (analytical grade), magnesium sulfate (analytical grade), ammonium hydroxide (25 %, analytical grade), toluene (>99 %) and tetrahydrofuran (>99.8 %) were from Reanal Finechemical Co. (Budapest, Hungary). Formic acid (98-100%) was bought from Scharlau Chemie S.A. (Barcelona, Spain). Peptide calibration standard (consisting of

bradykinin, angiotensin II, angiotensin I, substance P, renin substrate, ACTH clip (1-17), ACTH clip (18-39) and somatostatin) and protein calibration standard (consisting of trypsinogen, protein A, BSA, BSA-dimer) were obtained from Bruker Daltonics (Bremen, Germany). Trypsin (sequencing grade, modified) was provided by Promega Corporation (Madison WI, USA). Bidistilled water was prepared in our laboratory.

3.2.2 Instrumentation

An AUTOLAB12 electrochemical workstation controlled with GPES software (version 4.9.009 for Windows, Eco Chemie, Utrecht, Netherlands) served as an amperometric measurement instrument. A homemade flow injection analysis (FIA) manifold [87] was used for amperometric glucose analysis of eluted samples. A wall-jet-type detector cell containing working, counter, and reference electrodes was applied in the manifold (Figure 8). A platinum wire of 1 mm diameter served as counter electrode, as did a silver wire for semireference. A copper microdisk working electrode of 30 µm diameter and 0.1 M sodium hydroxide carrier solution was employed in the FIA glucose measurements.

For analyzing glucose samples obtained with sorbitol elution from the boronate affinity tips, amperometric glucose biosensor was used. The reason why a selective biosensor needed to be employed is that sorbitol also reacts to copper electrodes in basic media; therefore, its oxidation current would have interfered in the case of FIA measurements. The glucose electrode was prepared in our laboratory by immobilizing glucose oxidase enzyme on a platinum disk surface (diameter) of 1 mm [88]. The measurements with the biosensor were carried out in intensively stirred phosphate buffer (pH 7.4). Buffer (5 ml) was pipetted into a small beaker used as measurement cell, small doses of calibrating standards or samples were added, and the amperometric current at 0.65 V (vs. Ag/AgCl reference) was taken for calibration or concentration evaluation.

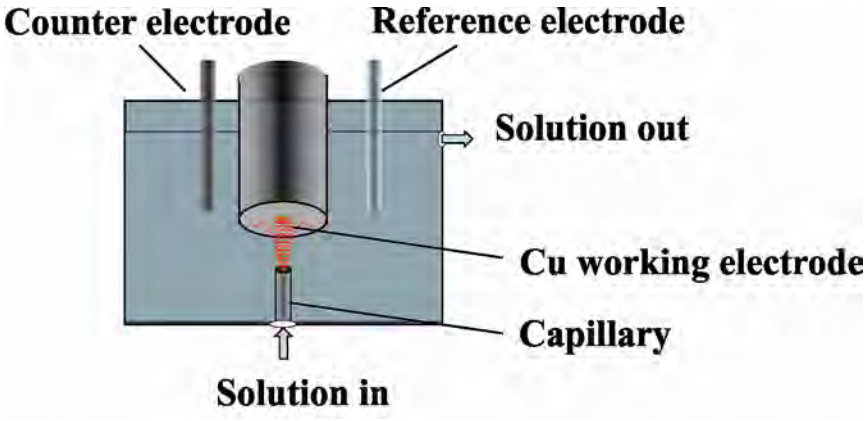

Figure 8: The walljet type detector cell arrangement [88]

For the presentation of the MALDI and HPLC instruments see section 3.1.1.

The µ-LC device consisted of an Ultimate µ-HPLC pump with column oven, a Switchos µ-column-switching device with loading pump and two 10-port valves, and a FAMOS µ-autosampler (LC Packings, Amsterdam, Netherlands). Hyphenation to the mass spectrometer was carried out by a nanoflow electrospray ionization source from Proxeon (Odense, Denmark) with Pico Tips from New Objective (FS360-20-10, Woburn, MA, USA). Mass spectrometric data were obtained on the linear ion trap LTQ mass spectrometer from Thermo Fisher Scientific (Waltham, MA, USA). A database search was carried out with BioworksBrowser 3.3.1 SP1 (Thermo Fisher Scientific) and Sequest against the Swiss–Prot database.

3.2.3 *In-vitro* glycation of RNase A and HSA

Glycation and the purification after glycation of HSA and RNase A were implemented the same way as described in section 3.1.3. above [81]. Solutions of RNase A were incubated for 14 days, whereas solutions of HSA were incubated for 12 and 28 days. Incubations were carried out under aseptic conditions at 37 °C.

In-vitro glycated HSA can be glycated *in-vitro* range from minimal levels (<10 mol modification sites per mol protein) to high levels (30-40 mol modification sites per mol protein). Highly glycated HSA is the better model to investigate the possible glycation sites of the HSA for patients suffering from type 2 diabetes mellitus [67].

3.2.4 Optimization of composition of binding buffer and circumstances of elution using amperometric method

In the **first experiment**, an ammonium chloride solution at a concentration of 250 mM was prepared and the pH values of this solution were adjusted by adding ammonia to obtain binding buffers with pH values of 7.4, 7.8, 8.2, 8.6, 9.0, and 9.4. Each solution contained 50 mM magnesium sulphate. After rehydration boronate affinity tips were equilibrated with the binding buffers mentioned above, 0.01 mol D-glucose was dissolved in 10 ml of binding buffer and the solution was aspirated through the affinity gel. This was followed by a washing step using binding buffer to eliminate the nonbound glucose. Finally, the elution of the bound D-glucose was carried out using 200 µl of formic acid solution with a pH value of 2.0. In the **next experiment**, the pH was kept at a constant level and the concentration of the ammonium chloride was changed from 50 to 300 mM. Then 0.01 mol D-glucose was again dissolved in solution and aspirated through the gel slab of the tips. Elution of the bound glucose was implemented using 200 µl of formic acid solution at pH 2.0.

From these experiments, the binding buffer in which the tip possessed the highest binding capacity toward glucose was chosen and the elution was investigated using formic acid from pH 2.0 to pH 5.0. Additional experiments for the optimization of the elution include the use of sorbitol at higher concentrations to remove D-glucose from the boronate affinity tips in the range from 0.1 to 1.6 M. It is important to mention that the presence of sorbitol had no disturbing effect on the amperometric measurement carried out with the glucose biosensor. Water from the eluates was evaporated under vacuum, and the remaining solid was taken up in 100 µl of double distilled water and analyzed by means of the amperometric method using either a wall-jet-type detector or a biosensor.

3.2.5 Isolation and purification of HSA from serum samples obtained from patients suffering from type 2 diabetes mellitus and from healthy volunteers.

Human sera taken from diabetic patients and healthy volunteers were diluted 20 times with double distilled water, and then 2 ml of this solution was centrifuged through a Centricon Ultracel YM-50 centrifugal filter tube (Millipore) at 5000g for 20 min (cutoff: 50,000 Da). This centrifugation ensured the removal of serum constituents with masses less than 50,000 Da; this step helped to prolong the lifetime of the RP-HPLC column. Proteins remaining on

the filter were further diluted with double distilled water 20 times, and the HSA was separated on a Kovasil MS-C18 non-porous column (Zeochem AG, Uetikon, Switzerland).
Eluent A consisted of 5% (v/v) ACN in water and 0.1% TFA, and eluent B consisted of 95% (v/v) ACN and 0.1% TFA. The gradient profile was: 0–20 min, 0% B→60% B; 20–25 min, 60% B→100% B. The flow rate was 0.7 ml × min^{-1}. Chromatograms were acquired at 214 nm. Fractions collected from sera were evaporated to dryness before digestion.

3.2.6 Tryptic digestion of glycated HSA and RNase A

The tryptic digestion of 1mg HSA, 1mg RNase A (Sigma-Aldrich) was carried out similarly to the way described in section 3.1.5 above. In the case of HSA isolated from sera, approximately 300 µg of proteins was in-solution digested using the protocol described above.

3.2.7 Enrichment of glycated peptides using boronate affinity tips

Pipette tips containing 5 µl of gel of immobilized m-aminophenylboronic acid with a total volume of 200 µl (PhyTip 1000+ columns, PhyNexus, San Jose, CA, USA) were used for the enrichment of the glycated peptides. After rehydration, the tips were equilibrated with binding buffers. The digest of 100 µg of protein (for each protein) was dissolved in the binding buffer, and the solution was aspirated through the affinity gel. Then the tips were washed with 1 ml of binding buffer to remove unselectively bound peptides. This was followed by an additional washing step with double distilled water to eliminate the trace of salts presented in the buffer if the elution was carried out using formic acid. Glycated peptides were eluted with 4x 50 µl of formic acid solution at pH 2.0. Elution of the bound glycated peptides has also been accomplished using sorbitol at higher concentrations. In the case of elution with sorbitol, prior to MALDI measurement the glycated peptides needed to be desalted using different sorbents (see 3.2.8).

3.2.8 Desalting of glycated peptides eluted from tips with sorbitol

For the desalting of glycated peptides eluted from boronate affinity tips, three different solid phase extraction (SPE) sorbents were compared. Here 5 mg from fullerene-derivatized silica particles made from a silica with a pore diameter of 30 nm (C60(30) silica) and 5 mg

octadecyl silica (C18 silica) was packed in SPE cartridges (Alltech Extract–Clean SPE 1.5 ml reservoir, Alltech Associates, Deer-field, IL, USA). The activation and equilibration method were the same as described in section 3.1.6. Elution of the bound peptides was implemented with 300 µl of 80% ACN and 0.1% TFA in water. The eluate was evaporated to dryness, and the peptides were taken up in 5 µl of 0.1% TFA in double distilled water. Then 1 µl of this solution was deposited on a stainless steel target mixed with 1 µl of matrix.

The desalting of glycated peptides was also carried out using the commercially available ZipTip (Millipore). For the activation, equilibration, and elution, the same conditions were used as for the C60(30) and C18 silica materials. In the case of ZipTip, the eluate was deposited directly onto a stainless steel target in 1 µl of 80% ACN and 0.1% TFA in water and then mixed with 1 µl of matrices and analyzed.

3.2.9 Preparation of different MALDI matrices

Two different matrices were compared for the ionization of glycated peptides. **DHB** was prepared in 20% (v/v) ACN and 0.1% TFA in water at a concentration of 25 $mg \times ml^{-1}$. A **mixed matrix** consisting of DHB and CHCA was also recommended for the MALDI–TOF analysis of glycated peptides [28]. CHCA (2 mg) was dissolved in 100 µl of 70% ACN and 5% formic acid. In addition, 2 mg of DHB was dissolved in 100 µl of 70% ACN and 0.1% TFA, and these two solutions were mixed in a 1:1 ratio.

For the measurement of glycated proteins, a saturated **SA** matrix was prepared in 50% (v/v) ACN and 0.1% TFA in water.

3.2.10 Conditions of electrochemical measurements

When using a **wall-jet-type detector** cell in flow injection analysis (FIA) mode, the electrochemical measurements were made in 100 mM sodium hydroxide solutions at a flow rate of 2 $ml \times min^{-1}$. In the case of using an **enzyme sensor**, the glucose measurement was carried out in a 10 ml electrochemical cell applying a three electrode cell ensemble. Then 5 ml of isotonic PBS buffer (pH 7.4) was pipetted into the cell. During the measurement, 0.65 V of working potential was used while the electrolyte solution was stirred continually.

3.2.11 MALDI–TOF/MS conditions

For the description of the MALDI measurements of proteins and peptides see section 3.1.11 above.

3.2.12 µLC–MS conditions

A poly(p-methylstyrene-co-1,2-bis(p-vinylphenyl)ethane)-based monolityc stationary phase [89] was used for the separation of the peptides of digests. The separation was performed under reversed phase conditions with eluent A (0.1% formic acid in water) and eluent B (0.1% formic acid in 30% ACN) at a flow rate of 1 µl × min^{-1} and 40 °C. A linear gradient (0–50 min: 0% B→60% B) was used. Mass spectrometric measurements were performed in positive ESI mode. The source voltage was adjusted at 1.4 kV, the capillary temperature was kept at 220 °C, the capillary voltage was at 37 V, and the tube lens was set at 94 V. When analyzing the results with Sequest, the following parameters were adjusted:

I. carbamidomethylation on cysteine (C) as fixed modification
II. 144 and 162 (fragments of glucose) variable modifications at lysine (K) and arginine (R)
III. three possible missed cleavage sites were allowed.

4. Results and discussion

4.1 Results of the solid phase (SPE) experiments

The first part of the results and discussion involves the achievement of the solid phase extraction, recovery of the solid phases and fractionation of the glycated peptides.

4.1.1 Comparison of the phases – recovery study (quantitative evaluation)

To identify the binding capacity of C30 and C60(30) the particles were incubated with a solution of Leu-enkephalin at different concentrations under vigorous shaking at 20°C. Then particles were centrifuged and the supernatants were analyzed. The concentrations of the supernatants represent equilibrium values with the adsorbed Leu-enkephalin. A calibration curve was plotted by the measurement of standard solutions of Leu-enkephalin (R^2 = 0.9899) at 232 nm employing UV–Vis spectrophotometry. The adsorption isotherms can be depicted plotting the concentrations of supernatants (C_{equ}, expressed in µg × mL^{-1}) against the adsorbed amount (m_{ads}, expressed in µg) (Figure 7/A). Data points fit the theoretical adsorption model of Langmuir with an excellent linear regression (R^2 = 0.994 for C60(30) and C30-silica, both) when plotting C_{equ} against C_{equ}/m_{ads} (Figure 7/B) [23]. The binding capacities were calculated from the reciprocal slope of the lines [86].

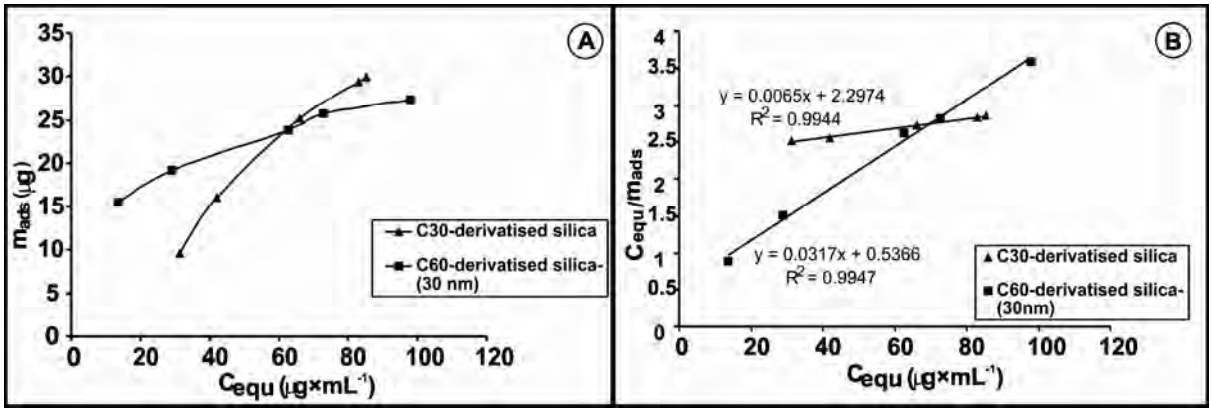

Figure 7. (A) Adsorption isotherms of Leu-enkephalin measured on C30-silica and C60(30) at 25°C. (B) The linearised forms of the isotherms. The reciprocal slope of the lines gives the binding capacity of the phases in saturation.

To characterise the **sorption behaviour** of the phases a mixture of three peptides ([Arg^8]-vasopressin, Leu-enkephalin, angiotensin I) was loaded onto the cartridge in three different concentrations (10, 30 and 50 µg). Peptides presented in the eluate and breakthrough were measured. Table 1 shows data on the recoveries and the amount of peptides lost during the whole procedure that enabled the quantitative determination of the analytes. Fullerene(C60)-silica prepared from 30 nm pore size silica material, C60(30) has proven to be the best (Table 2), in so far as no peptides could be detected from the breakthrough, by 10 µg loaded from each peptides. For vasopressin 66.2% of recovery was received indicating that 33.8% of the loaded peptide was lost through the sample preparation. The same conclusion can be drawn for each phase. For instance, in the case of fullerene(C60)-silica made up from 10 nm pore-size silica gel (C60(10)) the recovery of vasopressin was found to be 23.7%. In the breakthrough, 40.7% of 10 µg could be measured (64.4% of the total amount). C60(30) provided 94.7% recovery for angiotensin I, and 86.3% for Leu-enkephalin.

10µg	**C18**							**C30**							**C60(10)**							**C60(30)**							**C60(100)**						
	eluate			BT				eluate			BT				eluate			BT				eluate			BT				eluate			BT			
	µg	%	RSD %	µg	%	RSD %	E	µg	%	RSD %	µg	%	RSD %	E	µg	%	RSD %	µg	%	RSD %	E	µg	%	RSD %	µg	%	RSD %	E	µg	%	RSD %	µg	%	RSD %	E
[Arg^8]-vasopressin	**1.7**	17	**1**	**5.6**	56	**8**	*-27*	**4.4**	44	**8**	**2.8**	28	**2**	*-28*	**2.4**	24	**9**	**4.1**	41	**6**	*-35*	**6.6**	66	**8**	**n.d.**	-	**-**	*-34*	**5.5**	55	**8**	**1.2**	12	**2**	*-33*
Leu-enkephalin	**2.6**	26	**7**	**7.6**	76	**10**	*+2*	**7.1**	71	**6**	**3.0**	30	**2**	*+1*	**6.7**	67	**2**	**5.4**	54	**10**	*-21*	**9.5**	95	**8**	**n.d.**	-	**-**	*-5*	**8.8**	88	**7**	**3.0**	30	**5**	*+18*
angiotensin I.	**2.5**	25	**2**	**3.9**	39	**3**	*-36*	**8.1**	81	**4**	**1.5**	15	**10**	*-4*	**4.6**	46	**2**	**4.5**	45	**3**	*-9*	**8.6**	86	**7**	**n.d.**	-	**-**	*-14*	**7.9**	79	**1**	**0.6**	6	**8**	*-15*

30µg																																			
	eluate			BT				eluate			BT				eluate			BT				eluate			BT				eluate			BT			
	µg	%	RSD %	µg	%	RSD %	E	µg	%	RSD %	µg	%	RSD %	E	µg	%	RSD %	µg	%	RSD %	E	µg	%	RSD %	µg	%	RSD %	E	µg	%	RSD %	µg	%	RSD %	E
[Arg^8]-vasopressin	**7.3**	24	**2**	**9.4**	31	**3**	*-45*	**12.0**	40	**2**	**7.1**	24	**5**	*-36*	**2.9**	10	**4**	**16.5**	55	**10**	*-35*	**13.0**	43	**6**	**5.4**	18	**10**	*-39*	**7.9**	26	**9**	**9.4**	31	**8**	*-43*
Leu-enkephalin	**13.2**	44	**10**	**13.6**	45	**9**	*-11*	**21.2**	71	**1**	**10.1**	34	**10**	*+5*	**10.0**	33	**4**	**23.8**	79	**7**	*+12*	**15.6**	52	**10**	**10.2**	34	**2**	*-14*	**16.0**	53	**7**	**16.3**	54	**5**	*+7*
angiotensin I.	**17.1**	57	**10**	**6.1**	20	**4**	*-23*	**24.6**	82	**10**	**2.9**	10	**6**	*-8*	**5.4**	18	**1**	**24.2**	81	**9**	*-1*	**20.1**	67	**3**	**4.0**	13	**2**	*-20*	**13.2**	44	**3**	**9.6**	32	**10**	*-24*

50µg																																			
	eluate			BT				eluate			BT				eluate			BT				eluate			BT				eluate			BT			
	µg	%	RSD %	µg	%	RSD %	E	µg	%	RSD %	µg	%	RSD %	E	µg	%	RSD %	µg	%	RSD %	E	µg	%	RSD %	µg	%	RSD %	E	µg	%	RSD %	µg	%	RSD %	E
[Arg^8]-vasopressin	**9.7**	19	**1**	**33.1**	66	**8**	*-15*	**13.5**	27	**5**	**14.4**	29	**9**	*-44*	**2.8**	6	**4**	**31.6**	63	**8**	*-31*	**16.7**	33	**10**	**17.9**	36	**10**	*-31*	**8.1**	16	**7**	**27.9**	56	**9**	*-28*
Leu-enkephalin	**18.2**	36	**1**	**24.8**	50	**3**	*-14*	**32.2**	64	**2**	**13.2**	26	**9**	*-10*	**12.2**	24	**4**	**40.3**	81	**10**	*+5*	**15.5**	31	**7**	**25.8**	52	**2**	*-17*	**18.5**	37	**3**	**23.3**	47	**1**	*-16*
angiotensin I.	**24.0**	48	**8**	**35.5**	71	**3**	*+19*	**30.7**	61	**1**	**9.4**	19	**9**	*-20*	**8.1**	16	**3**	**40.2**	80	**2**	*-4*	**26.9**	54	**5**	**14.6**	29	**10**	*-17*	**16.2**	32	**3**	**22.0**	44	**6**	*-24*

Table 1. Recovery study using different SPE materials

Each solution was three times loaded and measured on each phase. BT, Breakthrough; E (%), Error; n.d., not detected.

Phases	Pore size (nm)	Specific surface area ($m^2 \times g^{-1}$)	Pore volume ($mL \times g^{-1}$)	Surface coverage ($\mu mol \times m^{-2}$)
Kovasil 110 C18	7.1	200	0.48	3.76
Kovasil 160 C30	9.6	155	0.49	3.79
Kovasil 100 C60	0	265	0	0.88
ProntoSil 300 C60	13	114	0.3	2.91
GromSIL 1000 C60	n.m.	32	n.m	2.27

Table 2. Properties of the investigated phases

Among fullerene-derivatised silica materials the recoveries of all peptides are the lowest for C60(10), due to the obstructed pores and consequently the lack of pore volumes. It is worth noting that the recoveries for C30-coated particles and for C60(100) particles are similar, despite the fact that the surface area of C30-silica is approximately five times higher than the surface area of fullerene C60(100)-silica. The reason for that is the different selectivity of the C30 moieties and the spherical C60 attached to the silica. In contrast to C60 phases recoveries decrease only slightly on C30-silica, witch is explained by the different sorption behaviour of the two packings: the binding capacity of C30 phase surpasses the binding capacity of C60 phase (Figure 7/A). The binding capacity of C60(30) is 31.5 $mg \times g^{-1}$, which confirms a previously published result obtained for phosphopeptides (33.6 $mg \times g^{-1}$) [42]. This value is 153.9 $mg \times g^{-1}$ for C30-silica showing a five times higher binding capacity.

Table 1 shows that for all materials recoveries dramatically decrease if the cartridges are overloaded with peptides (50 µg from each). Considering the results provided by this recovery study a considerable attention must be paid to the hydrophobicity of the authentic peptides used in this study in comparison with the hydrophobic properties of the investigated SPE materials. Overall, for the most hydrophilic [Arg^8]-vasopressin among all the investigated phases the best recoveries could be achieved using C60(30) as SPE material. This supports the observation that the presence of fullerene attached to the silica support provides material with excellent hydrophobic properties, thus enabling the binding of very hydrophilic peptides. Angiotensin I, the most hydrophobic peptide could be recovered in the highest amount from the phases derivatised with long alkyl moieties (like C18 and C30), nearly independent of the loaded amount. In the case of **C60-silicas**, it is noteworthy, that at 10 µg from each peptide

loaded onto the cartridges, Leu-enkephalin had better recovery than the more hydrophobic angiotensin I. When overloading C60-silicas with 30 and 50 µg peptides, respectively, angiotensin I possessed better recoveries than Leu-enkephalin. To explain the reason behind this phenomenon it can be assumed that at 10 µg of the peptides (when the phases are not overloaded) the accessibilities of the two-time shorter Leu-enkephalin molecules to the spherical fullerene molecules are not as hindered as angiotensin I.

4.1.2 Comparison of the phases based on the sequence coverage of HSA and fibrinogen digests received after stepwise SPE fractionation

Three MALDI matrices were tested for sequence coverage of an HSA digest. For comparison of the experimentally measured and in-silico generated masses (allowing 50 ppm mass tolerance) Böddi et al. developed a software that enables the comparison of two series of masses within a mass tolerance of 50–150 ppm if the total sequence of the protein is known, it is also possible to calculate the sequence coverage of the protein from data provided by the PMF (www.fraki.lgx.hu).

Matrices prepared as described in Section 3.1.10 were mixed with 20 pmol HSA digest on a stainless steel target and analysed. Allowing 50 ppm mass tolerance 38.6% of sequence coverage was calculated, if **CHCA** was used. In case of adjusting 150 ppm error for mass tolerance the sequence coverage only irrelevantly increased (42%), indicating that the MALDI measurement was accomplished accurately.

THAP, a matrix being frequently used for the ionisation of glycopeptides [26] was also tried. For the rough crystals of THAP, high laser energy is required, which results in higher mass errors, e.g.: at 50 ppm mass tolerance the sequence coverage of HSA (20 pmol) was only 47%, however, it increased to 68% when 150 ppm tolerance was permitted.

For the digests of HSA and fibrinogen, **DHB** has proven to be the optimal matrix because of the fine, needle-like crystals that can be excited by a low energy of a laser beam. This offers good resolution and reliable measurements with regard to mass accuracy: when 50 ppm of the tolerance was allowed, 69% of the sequence coverage was achieved, by increasing the tolerance to 150 ppm, the sequence coverage was found to be 71.5%. Due to the favourable properties of DHB, this matrix was further used for the MALDI analysis of both unmodified and glycated protein digests.

Digests of HSA and fibrinogen were **fractionated on each SPE material**. Results are reported in Table 3. In the case of fractionation of 20 pmol HSA digest, C18- and C30-silicas provide better coverages than the C60-silica materials in so far as 80.5% of the amino acids of HSA was identified after separating the peptides on C18-silica particles. This was found to be 80.7% on C30-silica, respectively. C60(30) enabled the identification of 70.8% of the amino acids of HSA.

Fibrinogen is a glycoprotein with a molecular weight of about 340 kDa. The molecules are comprised by two sets of disulphide-bridged Aα-, Bβ- and c-chains and play an important role in blood clotting [90].

	HSA	**Fibrinogen**			**total coverage of fibrinogen**
		Aα	Bß	c	
digest	71.5%	56.2%	62.3%	30.5%	50.4%
C18	80.5%	51.7%	44.0%	24.3%	41.5%
C30	**80.7%**	**62.4%**	**63.6%**	**37.1%**	**55.6%**
C60 (10 nm)	64.7%	45.8%	31. 6%	27.6%	36.2%
C60 (30 nm)	**70.8%**	**59.5%**	**63.1%**	**64.9%**	**62.2%**
C60 (100 nm)	56.4%	50.6%	51.5%	24.5%	43.4%

Table 3. Sequence coverages achieved on the phases by fractionation of 20 pmol HSA and fibrinogen digest

By the fractionation of the digest on C18-silica and C60(100) materials provided very similar results concerning the total coverage of fibrinogen (41.5% vs. 43.4%), however for Bβ-chain a slightly better result was achieved on C60(100).

While for both C30-silica and C60(30), the sequence coverage results were the same for Aα- and Bβ-chains an outstanding value for c-chain (64.9%) was achieved on C60(30), which raised the total coverage up to 62.2%.

As concluded, peptides of a tryptic digest comprising mainly hydrophilic amino acids are capable of binding stronger on a C60 derivatised silica material. The length of the peptide does play an important role because those peptides consisting of more amino acid residues have better access to the alkyl moieties – and therefore they generated stronger interactions – than to the spherical C60 molecules. Due to highest percentage of the aromatic amino acids in the c-chain of fibrinogen (11.26% of the total amino acid residues) the π–π interactions between the peptides and the fullerene play more important role than in the case of Aα- and

Bβ-chains (6.37 and 7.74% of the total amino acid residues). The π–π interactions must be responsible for increasing the sequence coverage of c-chain when the peptides are eluted from C60(30). Based on the results reported in Sections 4.1.1 and 4.1.2 **C30** silica and **C60(30)** (the best two) SPE materials were used for the analyses of glycated HSA and fibrinogen tryptic digests.

4.1.3 Identification of the possible glycation sites of HSA and fibrinogen after fractionation –comparison of the results provided by SPE experiments to boronate affinity chromatography

In hyperglycaemia HSA, the most abundant protein in serum can be non-enzymatically glycated via its basic amino acid residues. Glycated HSA is an excellent marker in diabetes and it can be used as a mid-term index of glycaemic control (approximately 20 days half-life). The role of glycated HSA in the identification of different stages of diabetes is clarified. The possible glycation sites of HSA (Figure 9) have been extensively studied with a number of methods including LC-MS and LC/off-line MALDI [50, 53, 54, 55, 67].

The applied SPE/off-line MALDI methods using novel phases made a comparison of the phases possible, using methods published for glycated HSA.

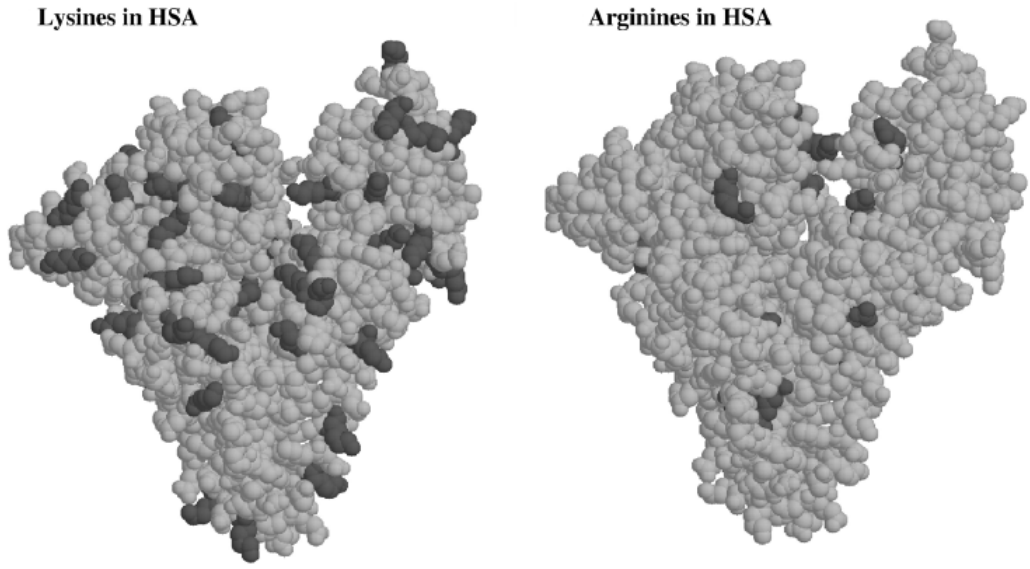

Figure 9: Lysines (K) and arginines (R) in HSA, there are the possible glycation sites of the human serum albumin [67].

Fibrinogen may significantly contribute to an increased risk of cardiovascular disease in patients with diabetes both in that they generally have elevated fibrinogen levels and that fibrinogen undergoes non-enzymatic glycation in the presence of uncontrolled blood glucose levels in the diabetic subjects. This glycation can alter the structure and function of the fibrinogen; therefore it is important to gain information about the possible glycated sites of this protein. Moreover, the analysis of fibrinogen, protein with a higher molecular weight, (glycated sites never studied before) emphasizes the selectivity differences between the phases.

Although several advanced glycated end products (AGE) have been described, in this work the identification of Amadori products (glucose molecules react with free amine groups forming glycosylamine residues through a reversible process, and later the glycosylamine can undergo an Amadori rearrangement to form a stable fructosamine residue (Figure 10)) and fructosil-lysine were the object of the investigation.

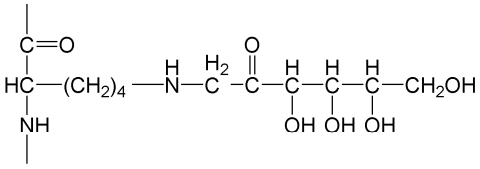

Fructosyl-lysine
(FL, ΔM=162.0528 Da)

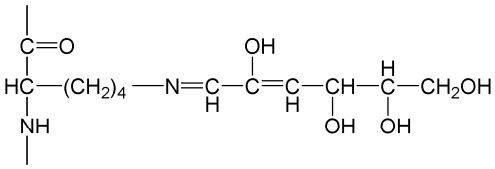

Fructosyl-lysine-1 H_2O
(FL-1 H_2O, ΔM=144.0423 Da)

Figure 10: Structure of the Amadori Compounds formed on the lysine of the protein [67]

Figure 11 shows the workflow elaborated for the investigation of the glycated residues.

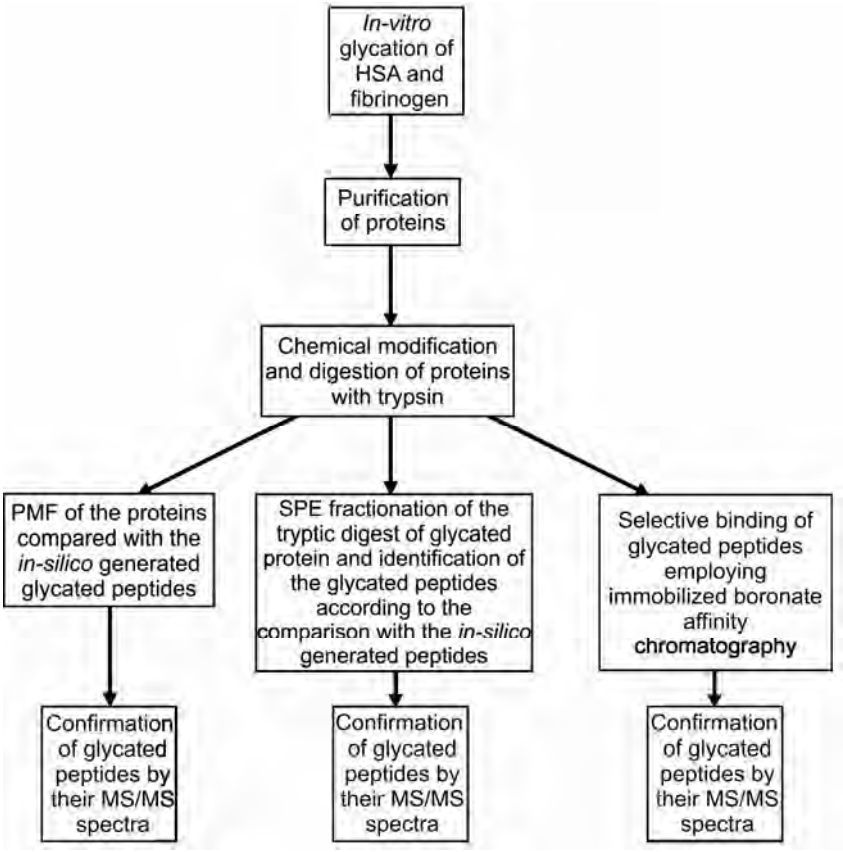

Figure 11: The elaborated workflow for the investigation of glycated peptides with SPE

Condensation of a glucose unit on an amine group causes 162.05 Da mass increase of a tryptic peptide if only one residue in the peptide is glycated. The masses of *in-silico* digestion were enhanced with 162.05 Da and compared to the measured masses of the glycated fractions with a mass tolerance of 100 ppm [26].

The **effects of non-enzymatic glycation** on the molecular weight on HSA and fibrinogen are shown in Figure 12. In the case of HSA nearly 5 kDa mass shift was measured similarly to Brancia et al. [92]. Calculating on the basis of this mass shift between non-glycated and glycated HSA, on the average 31 glucose units were found to be condensed on an HSA molecule. Boronate affinity tips were used for the selective enrichment of fibrinogen from a saline solution, to gain a better determination with MALDI despite the poor solubility and high molecular weight of this protein. The bound protein was directly eluted onto a target with formic acid. The mass received (Figure 12/C) is consistent with that described in the literature [95]. In contrast to HSA, the mass of fibrinogen is reduced during the glycation (Figure 12/D). This can be ascribed to the short half-life of the fibrinogen (4 days) [94].

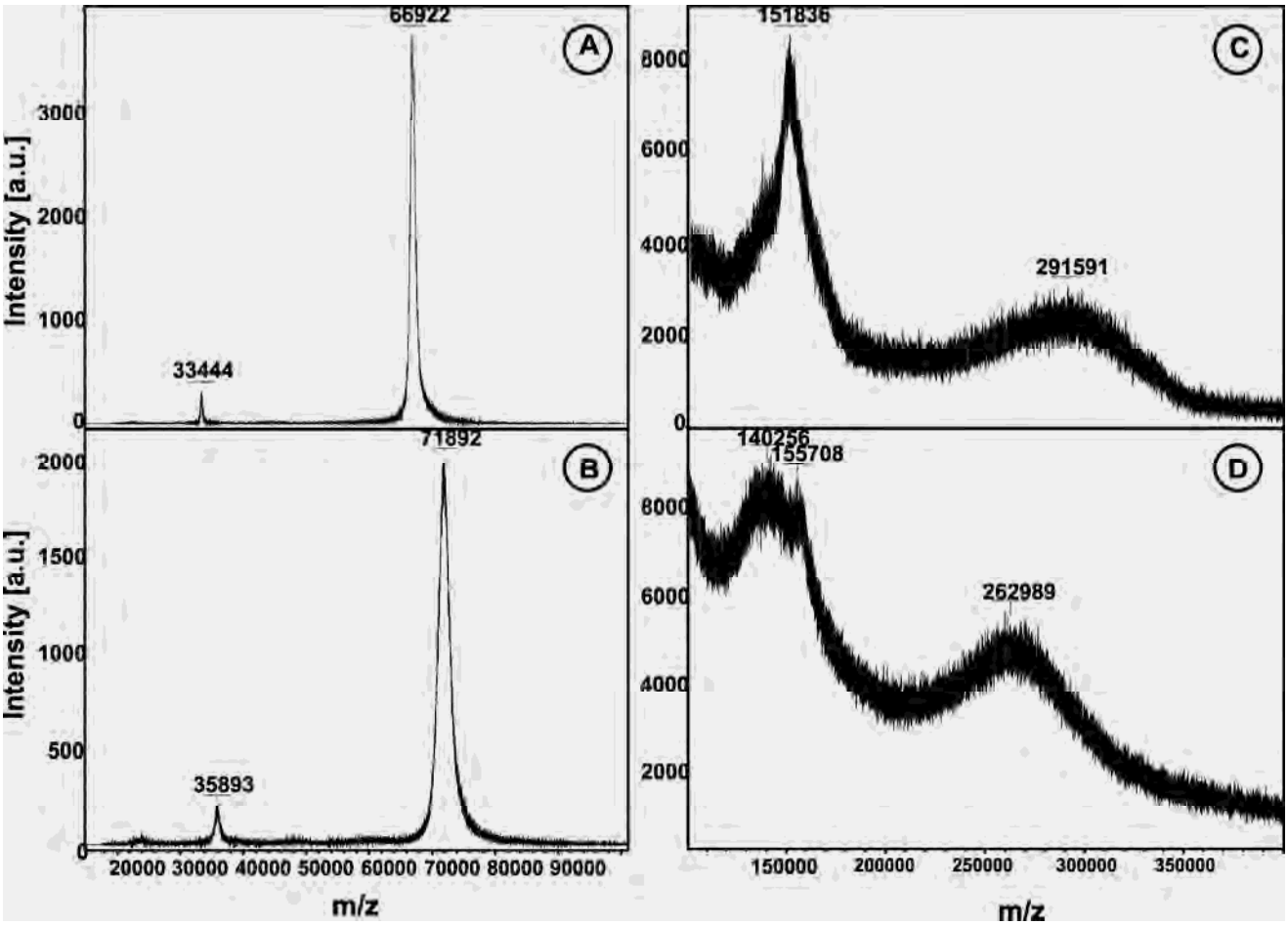

Figure 12: Comparison of unglycated (A) with glycated (B) HSA and unglycated (C) with glycated (D) fibrinogen. Each spectrum was monitored in linear mode and is a sum of 1000 shots. The applied matrix was SA.

Figures 13 and 14 demonstrate the **influence of fractionation** on the identification of glycated peptides. Figure 13/A is a part of the spectrum of the glycated HSA digest ranging between 1500 and 2000 Da. This complex mixture of peptides was loaded onto C60(30) particles and the peptides were stepwise eluted with an increasing amount of ACN. Figure 13/B is a spectrum showing peptides eluted with 20% of ACN. A peptide at 1628.85 Da appeared in the fraction at high intensity. The very intense signal that is suppressed in the unfractionated digest made it possible to acquire the appropriate PSD spectrum (Figure 13/C). The presence of the two distinctive peaks generated by neutral losses supplied further evidence for glycation at 1508.8 and 1466.7 Da. At the C-terminus of this peptide an arginine

is localised resulting in y-type ions in larger population. This peptide modified with a glucose unit at K475 has a sequence of VTKCCTESLVNR at the position of 473–484 of the HSA.

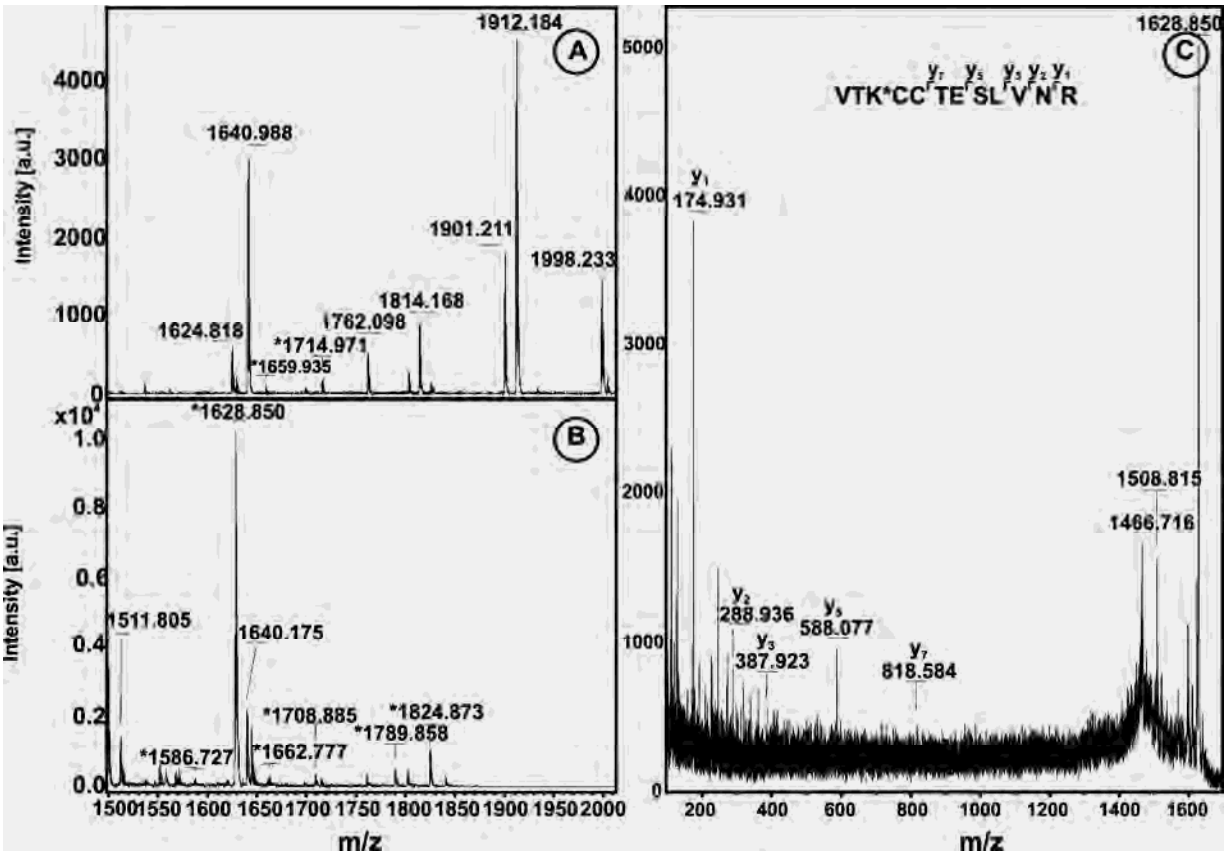

Figure 13: SPE of a glycated HSA digest on C60(30). (A) Unfractionated digest of HSA, (B) peptides released when 20% of ACN was employed as an eluent. Peptides assigned with asterisks are glycated. (C) PSD spectrum of a single glycated peptide at m/z 1628.85. For the parent ion 1000 shots were collected. The peak at m/z 1466.71 was formed by a neutral loss of dehydrated glucose (–162 Da), the other distinctive peak at m/z 1508.81 is a result of a neutral loss of a fragment of glucose (–120 Da). Spectra A and B were collected in reflectron mode. For each spectrum 1000 shots were acquired. The assigned y-ions in the low-mass range provide structural evidence for the sequence. The matrix applied was 2,5-dihydroxy benzoic acid. The presence of y-type ions refers to the arginine-terminated peptide.

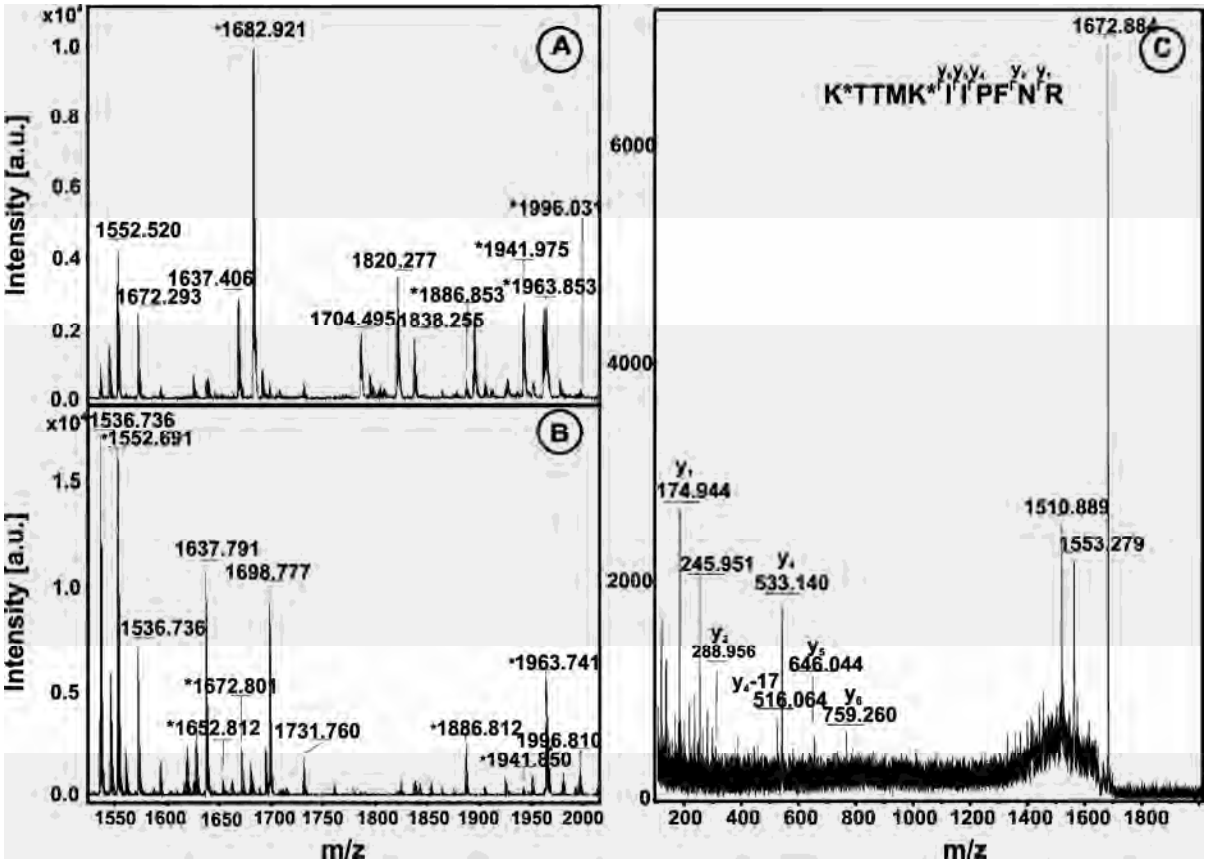

Figure 14: SPE of a glycated fibrinogen digest on C30-silica. (A) Unfractionated digest of fibrinogen, (B) peptides released when 10% of ACN was employed as an eluent. Peptides marked with asterisks are glycated. (C) PSD spectrum of a double glycated peptide of the c-chain at m/z 1672.88. For the parent ion 1000 shots were collected. The peak at m/z 1510.88 was formed by a neutral loss of dehydrated glucose (–162 Da), the other distinctive peak at m/z 1553.27 is a result of a neutral loss of a fragment of glucose (–120 Da). The presence of y-type ions in the low-mass range of the spectrum corroborates the identified sequence. Spectra A and B were collected in reflectron mode. For each spectrum 1000 shots were acquired. The applied matrix was 2,5-dihydroxy benzoic acid.

Although the spectrum of a glycated fibrinogen digest fraction from C30-silica seems to be more complex, between 1600 and 1700 Da two additional glycated peptides can be successfully detected. The peptide at 1672.8 Da is further studied by its MS/MS spectrum. The corresponding peaks – indicating the neutral losses of the dehydrated glucose (–162 Da) and its fragment (–120 Da) appear at 1510.8 and 1553.3 Da, respectively (Figure 14). According to the MS/MS spectrum of this modified peptide a double glycated peptide of the c-chain with the corresponding sequence of KTTMKIIPFNR at the position of 407–417 has

been identified. Modifications with two glucose units are at K407 and K411, respectively. The sequence of this peptide is verified by those y-type fragments in the low-mass range (Figure 14/C).

Boronate affinity chromatography is a useful tool for the enrichment of glycated and/or glycosilated proteins and peptides [69]. The glycated peptides captured using boronate affinity PhyTip 20 pmol glycated HSA digest (Figure 15/A) and from 20 pmol digest glycated fibrinogen (Figure 15/B) are shown. As shown in Figure 15/A, the most prominent, assigned peaks belong to 11 single glycated and 3 double glycated peptides. However, a considerably higher number of modified peptides has been monitored (for details see Tables 4, 5, 6 and 7). For instance, the most abundant peak appearing at m/z 1760.40 is a double glycated peptide where the possible glycated sites are K199 or K205 or R209. In addition, K276, K525 and K545 are considered to be privileged glycation sites, in agreement with the fractional solvent accessible surface values calculated by molecular modelling [95]. K276 is a modified residue of a double modified peptide detected at m/z 1870.42, while K525 and K545 were monitored from a single and a double glycated peptide measured in order at m/z 1290.48 and 2464.75.

Figure 15/B shows glycated peptides captured by boronate affinity tips from 20 pmol digest of glycated fibrinogen. Although Aα-chain is the largest part of this glycoprotein and from the minor peaks several possible glycated sites have been calculated, the most intensive peaks of this spectrum can, as a rule, be assigned to the double and single glycated peptides of Bβ- and c-chains of fibrinogen. The peak appearing at m/z 1672.82 is a double glycated peptide of c-chain (KTTMKIIPFNR) having a location of [407–417] and probably modified at K407 and K411. K411 as a possible glycated site is further confirmed by the presence of a single glycated peak of c-chain at m/z 1382.72 (TTMKIIPFNR) at the location of [408–417]. Evidence for the modification of K411 is provided by the corresponding PSD spectrum. Taking into account the number and the intensity of the modified peptides of Bβ-chain and c-chain of this protein, Bβ- and c-chains seem to be most accessible for non-enzymatic glycation process.

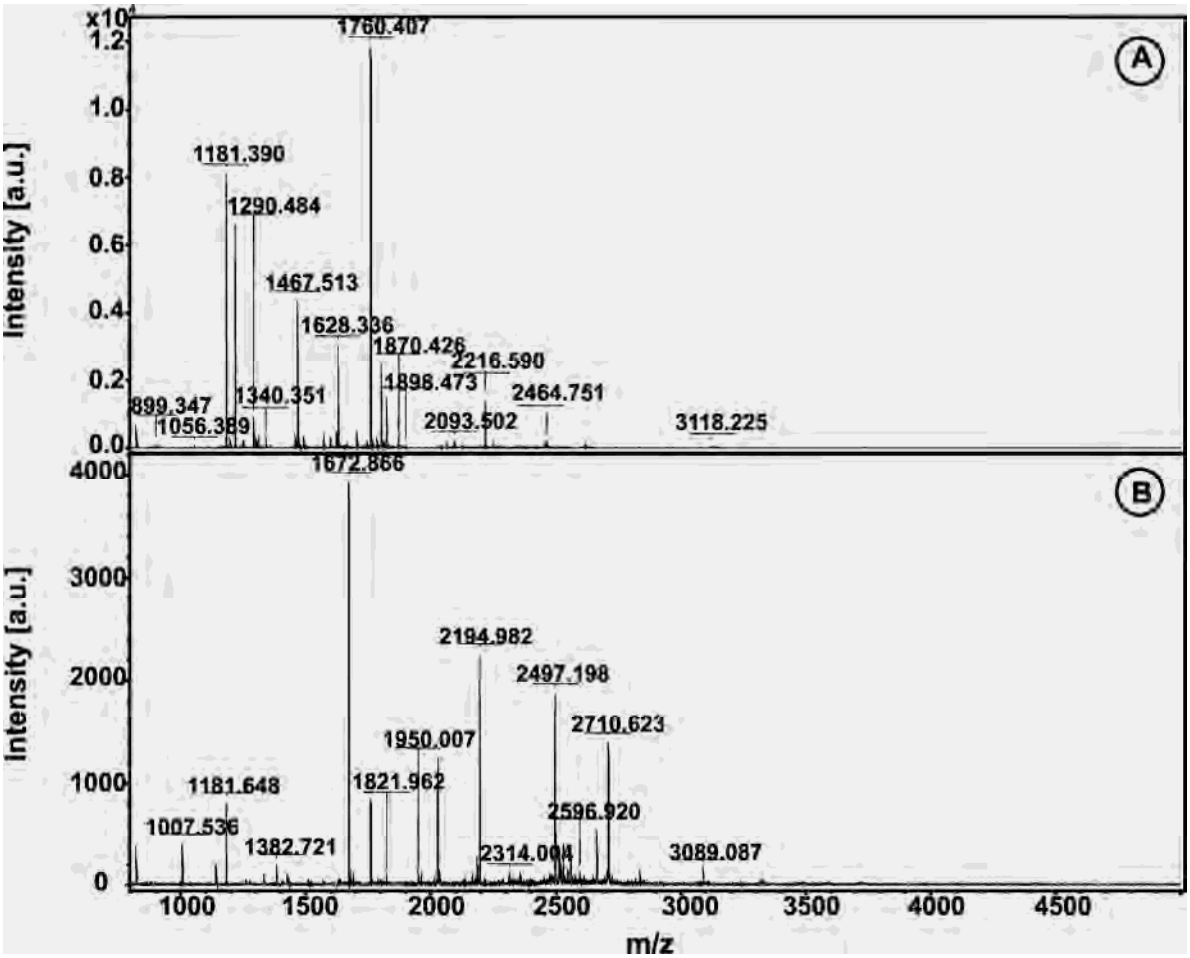

Figure 15: Boronate affinity capture of glycated peptides. (A) Glycated peptides after selective enrichment from 20 pmol glycated HSA digest. (B) Glycated peptides after selective enrichment from 20 pmol glycated fibrinogen digest. Spectra were monitored in reflectron mode. Each spectrum is a sum of 1000 shots. The matrix applied was 2,5-dihydroxy benzoic acid.

Table 4 below summarises all possible single glycated sites of HSA obtained on C30-silica and C60(30) and compared with the unfractionated digest and boronate affinity. Sixty-nine possible glycated sites (arginine and lysine) were successfully identified. Fifty-nine of these have been described in the literature [67, 81, 92, 93]. Data obtained from SPE experiments made it possible to recognise glycation that could not be detected from the digest. Peptides with two modified sites were also determined and no additional glycation were found. As long as from the digest 6 double modified peptides were only measured, 11 peptides with 2 modified residues were bound both on C30-silica and C60(30). Using

boronate affinity 14 double glycated peptides have been identified (these data are not reported in detail). Ten unknown modification sites have been identified.

		D	C30	C60	B
[1- 10]	K^{4} or R^{10}				+
[5- 12]	R^{10} or K^{12}	+			
[11- 20]	K^{12} or K^{20}	+	+	+	
[13- 20]	K^{20}			+	
[65- 81]	K^{73} or **R^{81}**			+	+
[82- 93]	**K^{93}**		+		
[82- 98]	**K^{93}** or **R^{98}**	+	+		
[94- 98]	**R^{98}**				+
[99-106]	**K^{106}**		+		
[107-114]	**R^{114}**		+	+	
[137-144]	K^{137} or R^{144}	+	+	+	+
[137-145]	K^{137} or R^{144} or R^{145}		+		
[138-144]	R^{144}			+	
[145-160]	R^{145} or K^{159} or R^{160}	+			+
[146-160]	K^{159} or R^{160}				+
[160-174]	R^{160} or K^{162} or K^{174}				+
[161-174]	K^{162} or K^{174}	+	+	+	
[175-186]	K^{181} or R^{186}	+	+	+	
[187-195]	K^{190} or K^{195}		+	+	
[187-197]	K^{190} or K^{195} or R^{197}			+	
[191-197]	K^{195} or R^{197}	+		+	+
[196-205]	K^{199} or K^{205}	+	+		
[198-205]	K^{199} or K^{205}	+	+	+	+
[198-209]	K^{199} or K^{205} or R^{209}			+	+
[200-209]	K^{205} or R^{209}	+	+	+	+
[200-212]	K^{205} or R^{209} or K^{212}				+
[206-218]	R^{209} or K^{212} or R^{218}		+	+	
[210-218]	K^{212} or R^{218}	+	+	+	+
[210-222]	K^{212} or R^{218} or R^{222}				+
[213-222]	R^{218} or R^{222}			+	
[219-225]	R^{222} or K^{225}		+	+	
[219-233]	K^{225} or K^{233}	+			+
[226-233]	K^{233}	+		+	
[226-240]	K^{233} or K^{240}	+		+	

		D	C30	C60	B
[258-274]	K^{262} or K^{274}	+	+	+	+
[263-276]	K^{274} or K^{276}	+	+	+	
[275-286]	K^{276} or K^{281} or K^{286}	+	+	+	+
[277-286]	K^{281} or K^{286}				+
[314-323]	K^{317} or K^{323}	+	+	+	
[318-336]	K^{323} or R^{336}	+			
[318-337]	R^{336} or **R^{337}**				+
[324-336]	R^{336}	+			
[338-348]	**R^{348}**		+	+	+
[349-359]	K^{351} or K^{359}	+	+	+	+
[352-359]	K^{359}		+		
[403-413]	R^{410} or K^{413}		+	+	
[403-410]	R^{410}	+	+	+	
[403-414]	R^{410} or K^{413} or K^{414}		+	+	
[411-428]	K^{413} or K^{414} or R^{428}				+
[414-428]	K^{414} or R^{428}	+	+	+	+
[415-436]	K^{432} or K^{436}				+
[429-439]	K^{432} or K^{436} or K^{439}	+			
[433-444]	K^{436} or K^{439} or K^{444}		+		
[437-444]	K^{439} or K^{444}		+		
[437-445]	K^{439} or K^{444} or R^{445}			+	
[467-484]	R^{472} or K^{475} or R^{484}	+	+		+
[473-484]	K^{475} or R^{484}				+
[501-521]	K^{519} or **R^{521}**	+			
[520-525]	**R^{521}** or K^{524} or K^{525}	+			
[525-534]	K^{525} or K^{534}	+	+	+	+
[535-541]	K^{536} or K^{538} or K^{541}	+			+
[539-557]	K^{541} or K^{545} or K^{557}				+
[558-564]	**K^{560}** or **K^{564}**	+		+	
[558-573]	**K^{560}** or **K^{564}** or K^{573}	+			
[561-574]	**K^{564}** or K^{573} or K^{574}		+	+	
[565-574]	K^{573} or K^{574}		+	+	
[574-585]	K^{574}	+	+	+	+

Table 4. Monitored glycated residues located on HSA

The positions of detected peptides are given in brackets. D, digest; C30, C30-silica, C60, C60(30); B, boronate phase. Bold type indicates the ten unknown modification sites.

Table 5 below demonstrates the **modified residues of fibrinogen**. In the sequence of *Aα-chain* 72 modifications were found but from the digest only 41 of these sites were identified. Using C30-silica 67, by means of C60(30) 63 glycated residues could be identified in SPE experiments. Boronate affinity allows identifying only 15 locations.

		D	C30	C60	B
[6- 35]	R^{35}			+	
[36- 42]	R^{38} or R^{42}		+	+	
[36- 48]	R^{38} or R^{42} or K^{48}			+	
[39- 48]	K^{48}	+	+	+	
[39- 63]	R^{42} or K^{48} or K^{63}			+	
[43- 48]	K^{48}	+	+	+	
[43- 63]	K^{48} or K^{63}	+	+	+	
[49- 63]	K^{63}		+	+	
[49- 69]	K^{63} or R^{69}		+	+	
[64- 71]	R^{69} or K^{71}	+			
[70- 84]	K^{71} or R^{84}	+	+	+	
[72- 84]	R^{84}	+	+	+	
[72- 89]	R^{84} or K^{87} or K^{89}		+		
[85- 97]	K^{87} or K^{89} or K^{97}	+	+	+	+
[88- 97]	K^{89} or K^{97}		+	+	+
[90-100]	K^{97} or K^{100}	+	+	+	
[90-114]	K^{97} or K^{100} or R^{114}		+		
[98-114]	K^{100} or R^{114}		+		
[98-123]	K^{100} or R^{114} or R^{123}			+	
[101-114]	R^{114}		+		
[101-123]	R^{114} or R^{123}			+	
[115-135]	R^{123} or R^{129} or R^{135}			+	
[124-129]	R^{129}			+	
[130-135]	R^{135}			+	
[130-137]	R^{135} or R^{137}		+		
[136-143]	R^{137} or K^{142} or R^{143}			+	
[138-143]	K^{142} or R^{143}	+	+	+	
[144-157]	K^{144} or K^{148} or K^{157}	+	+		
[145-160]	K^{148} or K^{157} or R^{160}		+		
[149-160]	K^{157} or R^{160}				+
[158-167]	K^{167}			+	
[161-167]	K^{167}		+		
[161-168]	K^{167} or R^{168}	+	+	+	
[161-176]	K^{167} or R^{168} or K^{176}			+	
[168-176]	R^{168} or K^{176}	+	+		+
[168-178]	R^{168} or K^{176} or R^{178}		+		
[169-178]	K^{176} or R^{178}		+		
[169-181]	K^{176} or R^{178} or R^{181}		+		
[177-181]	R^{178} or R^{181}			+	
[177-186]	R^{178} or R^{181} or R^{186}		+	+	
[182-190]	R^{186} or R^{190}			+	
[182-195]	R^{186} or R^{190} or K^{195}		+	+	
[187-195]	R^{190} or K^{195}			+	
[191-202]	K^{195} or K^{202}		+		
[196-202]	K^{202}		+		
[196-210]	K^{202} or K^{210}	+	+	+	
[196-216]	K^{202} or K^{210}		+		
[203-216]	K^{210} or R^{216}		+	+	
[211-218]	R^{216} or R^{218}		+	+	
[211-225]	R^{216} or R^{218} or K^{225}		+	+	+
[226-238]	K^{227} or K^{238}		+		
[226-249]	K^{227} or K^{238} or K^{243} or K^{249}	+	+		
[244-258]	K^{249} or R^{258}	+	+	+	
[244-249]	K^{249}			+	
[250-258]	R^{258}		+		
[250-287]	R^{258} or R^{263} or R^{271} or R^{287}		+		
[259-271]	R^{263} or R^{271}		+	+	
[272-287]	R^{287}			+	
[426-437]	R^{426} or K^{432} or K^{437}			+	
[427-437]	K^{432} or K^{437}		+		
[427-440]	K^{432} or K^{437} or K^{440}	+	+	+	+
[433-440]	K^{437} or K^{440}		+	+	
[433-443]	K^{437} or K^{440} or R^{443}		+	+	
[438-443]	K^{440} or R^{443}			+	
[438-446]	K^{440} or R^{443} or K^{446}		+	+	
[444-458]	K^{446} or K^{448} or R^{458}		+	+	
[447-458]	K^{448} or R^{458}		+		
[447-459]	K^{448} or R^{458} or R^{459}		+		
[460-476]	K^{463} or K^{467} or K^{476}	+	+	+	
[464-476]	K^{467} or K^{476}	+	+	+	
[468-476]	K^{476}		+	+	
[511-527]	R^{512} or K^{527}	+	+	+	
[513-527]	K^{527}		+	+	
[513-547]	K^{527} or R^{547}		+		
[548-558]	K^{558}		+		
[548-573]	K^{558} or R^{573}		+	+	
[559-575]	R^{573} or K^{575}		+		
[574-581]	K^{575} or K^{581}		+		
[574-591]	K^{575} or K^{581} or R^{591}	+	+	+	
[576-591]	K^{581} or R^{591}		+	+	
[582-591]	R^{591}			+	
[592-599]	K^{599}	+	+	+	
[592-602]	K^{599} or K^{602}				+
[600-621]	K^{602} or K^{620} or R^{621}			+	
[603-620]	K^{620}	+	+	+	
[603-621]	K^{620} or R^{621}		+		
[622-630]	K^{625} or R^{627} or R^{630}	+	+	+	
[631-644]	K^{639}	+	+	+	

Table 5. Monitored glycated residues located on the Aα-chain of fibrinogen

The positions of detected peptides are given in brackets. D, digest; C30, C30-silica, C60, C60(30); B, boronate phase.

Table 6 below shows the modifications identified from single modified peptides on the *Bβ-chain*. Of all the modified sites (59), 25 were found by analysing the digest, while this number increased with fractionations on C30-silica (53 sites) and C60(30) (47 sites). Boronate phase only recognises 20 residues.

		D	C30	C60	B
[4- 11]	K^{11}		+		
[4- 16]	K^{11} or K^{13} or K^{16}			+	
[12- 29]	K^{13} or K^{16} or K^{29}		+		
[45- 51]	R^{47} or K^{51}		+	+	
[52- 72]	K^{52} or R^{53} or R^{60} or R^{72}		+		
[53- 77]	R^{53} or R^{60} or R^{72} or R^{74}	+			
[54- 72]	R^{60} or R^{72}		+		
[54- 77]	R^{60} or R^{72} or R^{74} or K^{77}		+		
[73- 83]	R^{74} or K^{77} or K^{83}		+	+	+
[73- 84]	R^{74} or K^{77} or K^{83} or K^{84}				+
[78- 84]	K^{83} or K^{84}			+	
[84- 88]	K^{84} or R^{87} or K^{88}			+	+
[125-152]	K^{152}		+		
[153-158]	K^{157} or R^{158}	+	+	+	+
[158-163]	R^{158} or K^{160} or K^{163}	+	+	+	
[161-178]	K^{163} or K^{178}		+	+	
[164-178]	K^{178}		+		
[164-199]	K^{178} or R^{196} or R^{199}		+		
[197-206]	R^{199} or R^{206}		+		
[197-208]	R^{199} or R^{206} or K^{208}		+	+	
[200-208]	R^{206} or K^{208}	+	+	+	
[200-206]	R^{206}		+		
[207-224]	K^{208} or K^{211} or R^{224}		+		
[209-224]	K^{211} or R^{224}		+		
[225-239]	K^{239}		+		
[240-247]	R^{246} or K^{247}			+	
[247-267]	K^{247} or K^{264} or R^{267}		+	+	+
[248-267]	K^{264} or R^{267}	+	+	+	
[268-285]	R^{285}		+		
[286-294]	R^{294}		+	+	+
[286-300]	R^{294} or K^{295} or K^{300}		+	+	

		D	C30	C60	B
[295-313]	K^{295} or K^{300} or K^{313}	+	+	+	+
[296-300]	K^{300}			+	
[296-313]	K^{300} or K^{313}	+	+	+	
[314-328]	K^{328}		+		
[329-334]	R^{334}			+	
[329-348]	R^{334}		+	+	
[329-351]	R^{334} or K^{348} or K^{351}		+	+	
[335-348]	K^{348}		+	+	
[335-351]	K^{348} or K^{351}		+		
[349-367]	K^{351} or K^{353} K^{367}		+		
[352-367]	K^{353} or K^{367}		+	+	
[354-367]	K^{367}			+	
[354-376]	K^{367} or K^{374} or R^{376}			+	
[368-374]	K^{374}			+	
[368-376]	K^{374} or R^{376}	+	+	+	+
[375-395]	R^{376} or R^{395}		+		
[396-410]	R^{410}		+	+	
[411-421]	R^{421}			+	
[422-436]	K^{422} or K^{426} or R^{436}	+	+	+	
[423-436]	K^{426} or R^{436}	+	+	+	
[427-436]	R^{436}		+	+	
[427-445]	R^{436} or R^{445}	+	+	+	
[446-478]	K^{458} or K^{471} or R^{478}	+		+	
[459-471]	K^{471}		+	+	
[459-478]	K^{471} or R^{478}				
[472-479]	R^{478} or K^{479}			+	
[472-483]	R^{478} or K^{479} or K^{483}		+	+	
[479-491]	K^{479} or K^{483} or R^{485}				+
[480-491]	K^{483} or R^{485}		+	+	+
[484-491]	R^{485}	+	+	+	

Table 6: Monitored glycated residues located on the Bβ-chain of fibrinogen
The positions of detected peptides are written in brackets. D, digest; C30, C30-silica, C60, C60(30); B, boronate phase

		D	C30	C60	B
[1- 8]	R^{8}			+	
[9- 31]	R^{31}	+			
[62- 79]	K^{64} or K^{79}		+	+	
[65- 79]	K^{79}	+	+	+	
[65- 84]	K^{79} or K^{84}	+	+	+	
[89-113]	K^{101} or K^{111} or R^{113}	+	+		
[112-121]	R^{113} or K^{114} or K^{121}				+
[114-121]	K^{114} or K^{121}		+		+
[115-121]	K^{121}	+	+	+	
[122-134]	R^{134}		+	+	
[122-146]	R^{134} or K^{146}	+	+	+	
[135-151]	K^{146} or K^{151}		+		
[135-153]	K^{146} or K^{151} or K^{153}		+	+	+
[147-153]	K^{151} or K^{153}		+		
[152-166]	K^{153} or K^{166}	+	+		
[167-177]	K^{177}		+	+	
[167-188]	K^{177} or K^{185} or K^{188}		+	+	+
[178-199]	K^{185} or K^{188} or K^{196} or K^{199}				+
[189-199]	K^{196} or K^{199}			+	
[200-223]	K^{222} or R^{223}	+	+	+	
[224-231]	K^{231}			+	

		D	C30	C60	B
[224-232]	K^{231} or K^{232}	+	+	+	
[224-238]	K^{231} or K^{232} or K^{238}		+		
[232-238]	K^{232} or K^{238}	+	+	+	+
[233-258]	K^{238} or K^{258}		+	+	
[259-273]	R^{273}		+		
[259-282]	R^{273} or R^{282}		+	+	
[274-292]	K^{292}		+	+	
[274-299]	R^{282} or K^{292} or K^{299}				+
[283-299]	K^{292} or K^{299}		+	+	
[293-301]	K^{299} or R^{301}	+	+	+	
[329-347]	K^{347}	+			
[348-364]	K^{364}		+		
[365-401]	K^{382} or K^{399} or R^{401}			+	
[400-406]	R^{401} or K^{406}		+	+	
[400-407]	K^{406} or K^{407}	+	+		+
[402-406]	K^{406}			+	
[402-411]	K^{406} or K^{407} or K^{411}		+	+	
[407-417]	K^{407} or K^{411} or R^{417}				+
[408-417]	K^{411} or R^{417}	+	+	+	+
[412-417]	R^{417}		+		
[418-432]	K^{432}	+	+	+	

Table 7. Monitored glycated residues located on the c-chain of fibrinogen

The positions of detected peptides are given in brackets. D, digest; C30, C30-silica, C60, C60(30); B, boronate phase

Forty-one possible glycated sites were found for the *c-chain* of fibrinogen. Of these, 24 were recognised from the digest. Results achieved using C30-silica (33) and C60(30) (34) were similar to each other. With the boronate tip 21 glycated sites were determined (Table 7). As it was expected on the basis of previous results with phosphopeptides, Tables 5–7 above demonstrate the numerous, hydrophilic peptides glycated at arginine residues and containing less than ten amino acids bound only on C60(30). For instance, glycations on R8, R35, R123, R246 and R421 residues were only possible to be explored employing C60(30).

4.2 Results of the experiments of the boronate affinity chromatography

The method used for the enrichment of boronate affinity chromatography has never been optimized before. In these chapters the results of the optimization (binding and elution conditions) can be seen and the application of boronate affinity enrichment for patients suffering from type 2 diabetes mellitus is compared to that in healthy volunteers.

4.2.1 Evaluation of binding conditions of boronate affinity tips

Electrochemical measurements proved to be a useful approach to optimize the **ionic strength and pH of the binding buffer** as well as the most appropriate circumstances of elutions. Figure 16/A below displays the effect of the pH of binding buffer on the amount of eluted glucose. These results clearly demonstrate that the affinity tips bind the highest amount of glucose when the pH of the binding buffer varies between 7.7 and 8.2. Further enhancement of the pH of the binding buffer results in a decrease of the bound glucose. The maximal binding capacity of the tips was found to fall within the pH range of 7.8–8.2 in the curve; therefore, a value of approximately 8.2 was selected for this study. As demonstrated by Figure 16/B below, when the binding capacity of the tips was plotted against the ionic strength of the binding buffer, 150 mM ammonium chloride provided the best results. These results can be regarded as consistent with data described previously [54, 69]; however, the previously reported values were not based on quantitative evidence. Figure 16/C below shows the effect of the pH of the eluent depicted in the function of the eluted glucose when using solutions of formic acid at different pH values for the elution. This relation is exponential; the lower the **pH of the eluent**, the higher the amount of glucose eluted. The elution of bound glucose on boronate-derivatised resin can also be accomplished by means of a highly concentrated sorbitol solution. The **effects of the concentrations of sorbitol** solution are plotted against the amount of released glucose in Figure 16/D below. The curve reaches a plateau at 1.2 M; therefore, there is no need to employ sorbitol solutions for the elution at higher concentrations.

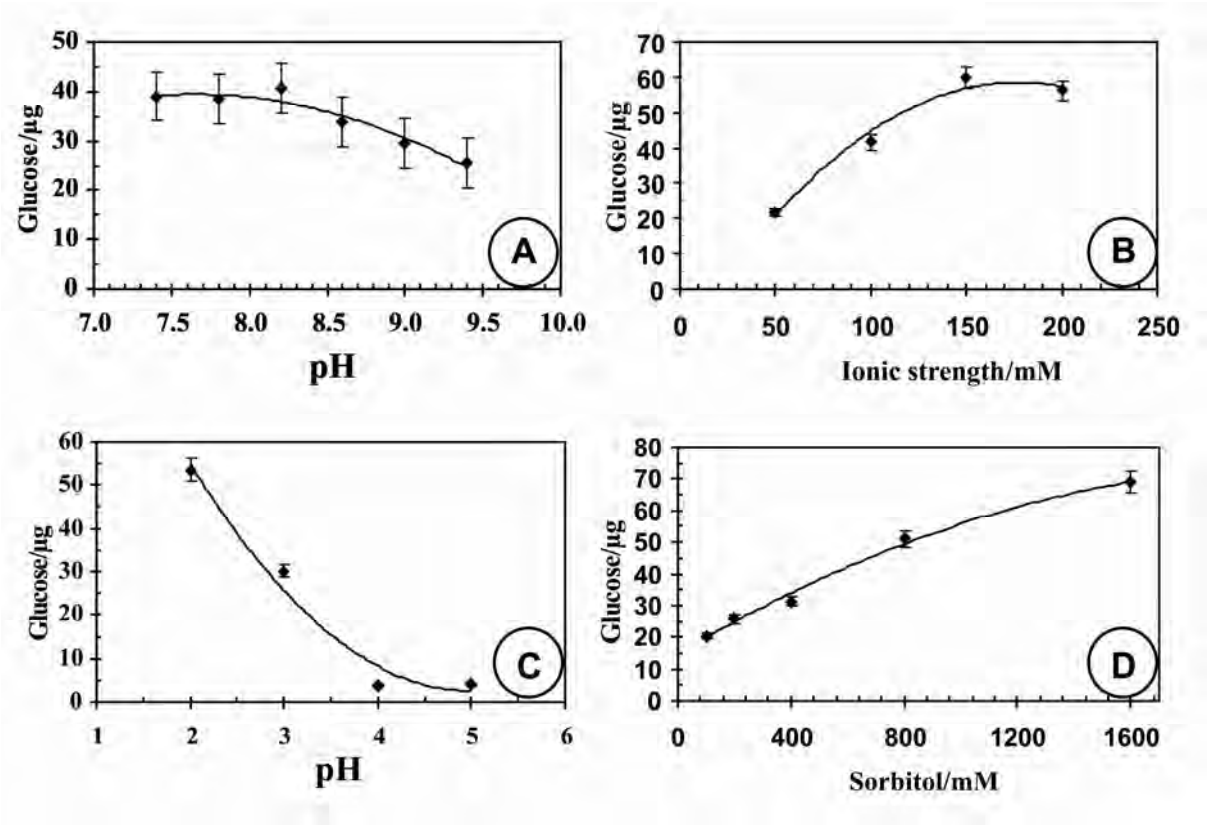

Figure 16: A.) Relationship between the bound glucose and the pH of the binding buffer B.) Amount of bound glucose plotted in the function of the ionic strength of binding buffer C.) Elution of glucose by formic acid at different pH values D.) Elution of glucose with sorbitol solution at different concentrations

4.2.2 Evaluation of performance of boronate affinity tips toward glycated peptides enriched from glycated RNase A and HSA tryptic digests

The application of the boronate affinity tips was introduced employing *in-vitro* **glycated HSA and RNase A** as model proteins. Figure 17/B shows the effect of the time of incubation with glucose on the degree of the modification of proteins. This can be calculated from the mass shift measured between the unmodified and glycated proteins. Taking into account the fact that the condensation of 1 glucose unit can cause approximately a 162 Da mass increase in comparison with the unmodified proteins (Figure 17/A), glycation of RNase A for 14 days clearly represents that, on the average, 1-2 glucose units were condensed on an RNase A molecule.

HSA was incubated with a high concentration of glucose in PBS buffer for 12 and 28 days. The reason why the shorter incubation time was also chosen is that in patients being poorly controlled and suffering from type 2 diabetes mellitus the HSA is also glycated, but the number of glucose moieties condensed on an HSA molecule is not consistent with an overglycated HSA (incubated for 28 days). In contrast to Figure 17/C below, where the mass spectrum of the non-glycated HSA is shown, Figure 17/D indicates a mass shift of 1050 Da. This means that, on the average, 6 or 7 glucose moieties are attached to an HSA molecule. Therefore, HSA glycated for 12 days can be considered as a model of HSA being glycated due to the elevated blood glucose level and isolated from patients under poor diabetic control [95]. Figure 17/E below represents a mass spectrum belonging to the overglycated HSA. The corresponding mass shift shows that approximately 31 glucose moieties are attached to an HSA molecule. This result is relevant to the results reported in previous studies [67, 95].

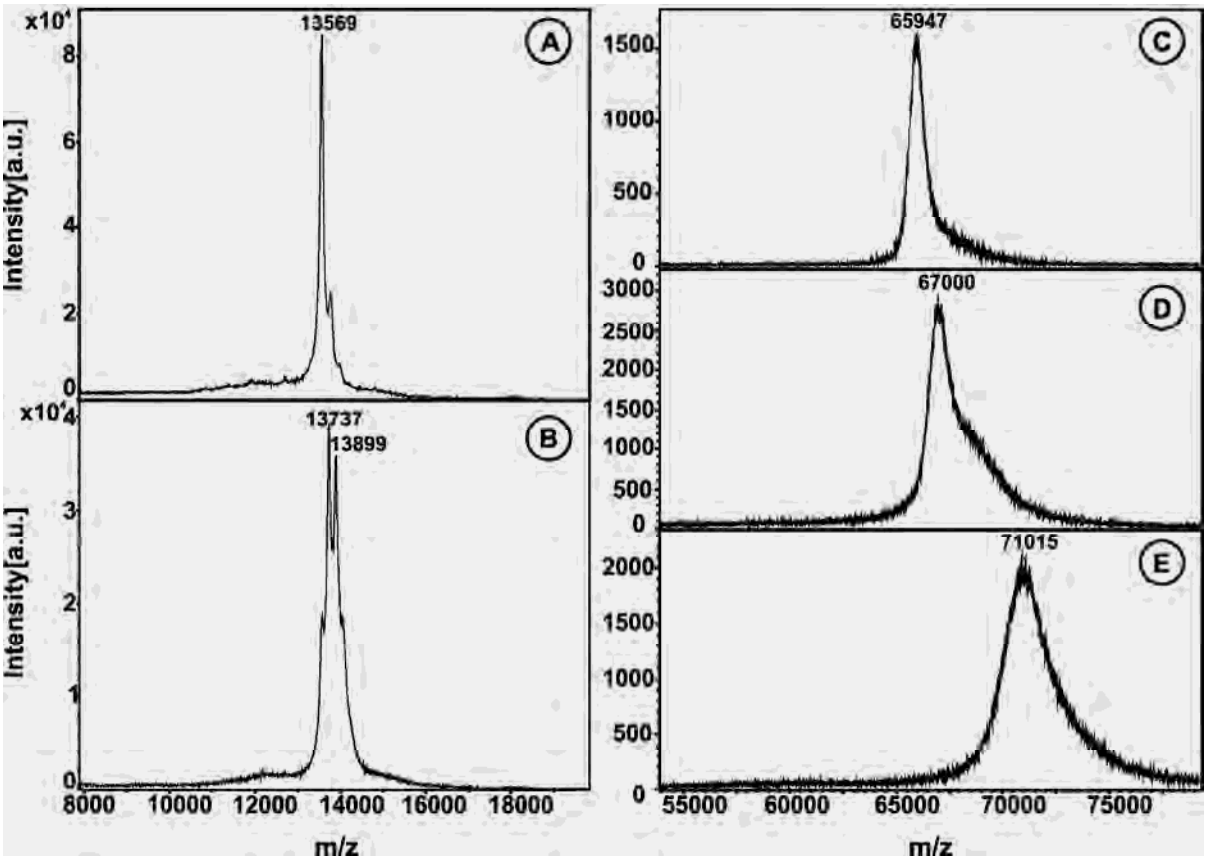

Figure 17: Effect of glycation on molecular weight of proteins. (A) Mass spectrum of unglycated RNase A. (B) Mass spectrum of RNase A glycated for 14 days. (C) Mass spectrum of unglycated HSA. (D) Mass spectrum of HSA glycated for 12 days. (E) Mass spectrum of HSA glycated for 28 days. Each spectrum was acquired in linear mode and a sum of 1000 shots. The applied matrix was SA. a.u., i.e. arbitrary units.

Evaluation of the results measured for the glycated peptides was carried out using a software developed and first employed by Böddi et al. (www.fraki.lgx.hu) [94]. The comparison of two series of masses—the *in-silico* generated and the measured—can be carried out within a mass tolerance range of 50–150 ppm. In this study, 100 ppm mass tolerance was permitted. If the measured values provided higher margins compared to *in-silico* masses, they were not included in the group of identified peptides. Further identification of glycated constituents occurred in their post-source decay spectra. Post-source decay spectra of the glycated peptides yield a specific fragmentation pattern so long as neutral losses of a dehydrated glucose ($M+H^+-162$) and a fragment of a glucose ($M+H^+-120$) serve as a basis for the identification of the modification. From these two neutral losses, the structure of $C_4H_8O_4$ can be assigned to the latter. Moreover, the series of y-ions appearing in the low mass range furnishes important information about the sequence of the peptide of interest.

Although the **mixture of two matrices (CHCA and DHB)** was proposed to be used for the analysis of peptides modified with sugars, for the glycated peptides **DHB** matrix at a concentration of 25 $mg \times ml^{-1}$ was proven to be better in terms of the number of monitored peptides and the sites of modifications localized in them. For instance, when the enrichment of a 20 pmol digest of HSA glycated for 28 days was carried out using ammonium chloride/ammonia as binding buffer and the eluate was desalted on C60(30) particles after the elution of glycated peptide, the application of DHB resulted in 41 single glycated peptides, contrary to the mixture of DHB and CHCA, where only 30 were found. This comparison was measured for each experiment conducted throughout this study, and in all cases DHB was considered as a more suitable matrix than the mixture.

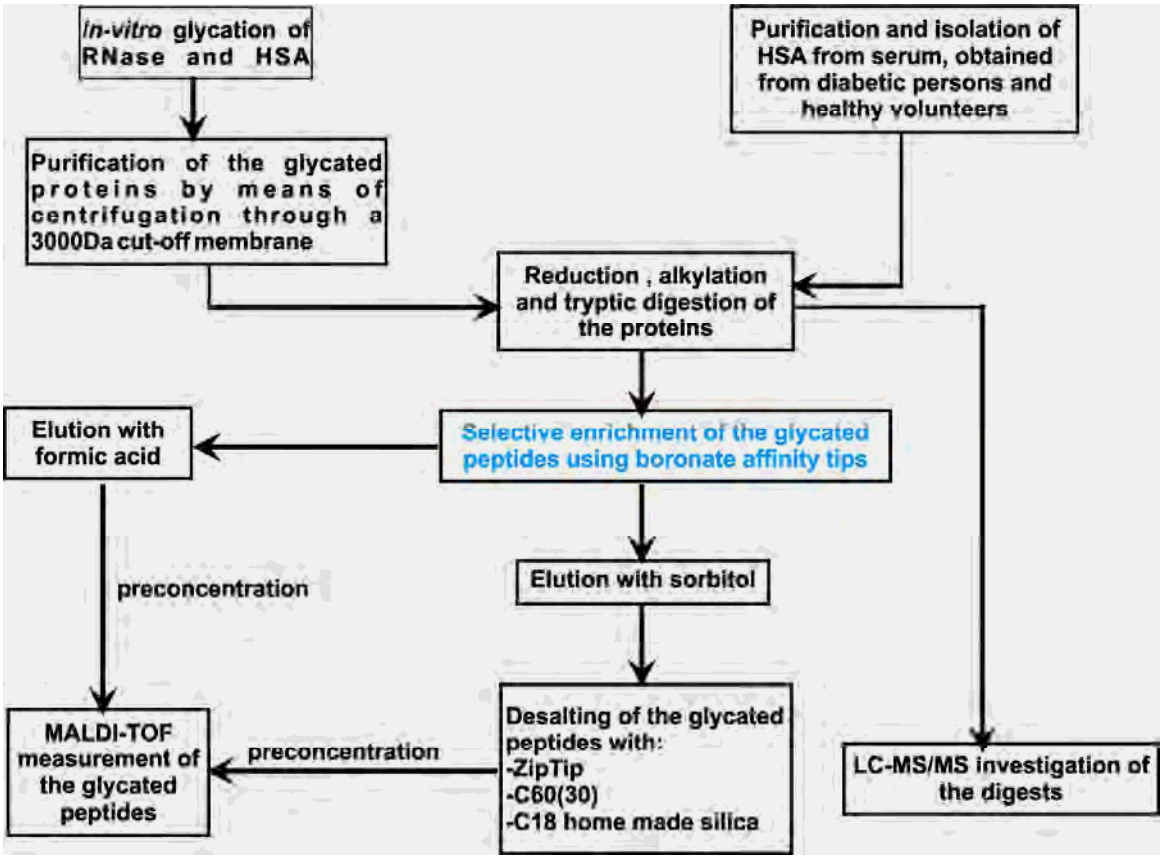

Figure 18: Workflow of different approaches throughout the application of boronate affinity enrichment for glycated peptides

Figure 18 above demonstrates the workflow accomplished throughout the application of boronate affinity tips. As can be seen, glycated authentic proteins underwent tryptic digestion. The optimized conditions, including the ionic strength and pH of the binding buffer and the ways of the different types of elutions, were applied for HSA glycated for 28 days. This is why the highest number of glycated peptides is expected in this case; therefore, the differences among the applied approaches taken are obviously better expressed. Results received from the experiments carried out with a sorbitol solution at a concentration of 1.2 M were evaluated first. Under optimized conditions, the binding of the glycated peptides was carried out using ammonium chloride/ammonia buffer and with taurine buffer using both at the same pH value (8.2) and the same concentration (150 mmol). After the elution of glycated peptides with sorbitol prior to MALDI–TOF analysis, the eluate consequently needed to be **desalted**. This was implemented using three different types of sorbents: the commercially available ZipTip, fullerene(C60)-derivatised silica material (C60(30)) [42] and the one made on the basis of silica with a 30-nm pore radius), and a homemade densely coated C18 silica [96]. The two latter types were evaluated in detail in SPE experiments carried out to separate

tryptic peptides and their glycated derivatives in the previous work. Results of that work provided a line of evidence for the excellent binding affinity of C60(30) toward constituents with enhanced hydrophilic properties such as glycated peptides [94]. The experimental circumstances, including the composition of the binding buffer, the comparison of the **elution using sorbitol and formic acid,** and the **different types of sorbents** employed for desalting the eluates after using a sorbitol solution at a concentration of 1.2 M, were evaluated on the basis of the identified single and double glycated peptides and the number of possible glycated sites on HSA glycated for 28 days. These can be plotted by means of Venn diagrams. Figure 19/A and B below depict the numbers of *single glycated peptides* captured by the boronate affinity tips employing ammonium chloride/ ammonia buffer and taurine buffer, respectively, for the enrichment of glycated constituents. In both cases, the bound glycated peptides were eluted with a highly concentrated sorbitol solution (1.2 M) and desalted on the three materials mentioned above. As shown in the number of glycated peptides bound and eluted from each sorbent, ammonium chloride/ammonia buffer proved to be more efficient than taurine buffer in that 67 single glycated peptides could be selectively captured by means of using ammonium chloride/ammonia buffer, whereas 55 peptides modified with only 1 sugar unit were possible to be monitored after the elution from all of the employed phases. The evaluation of binding buffers was also implemented for glycated peptides modified at two amino acid residues with D-glucose (double glycated peptides).

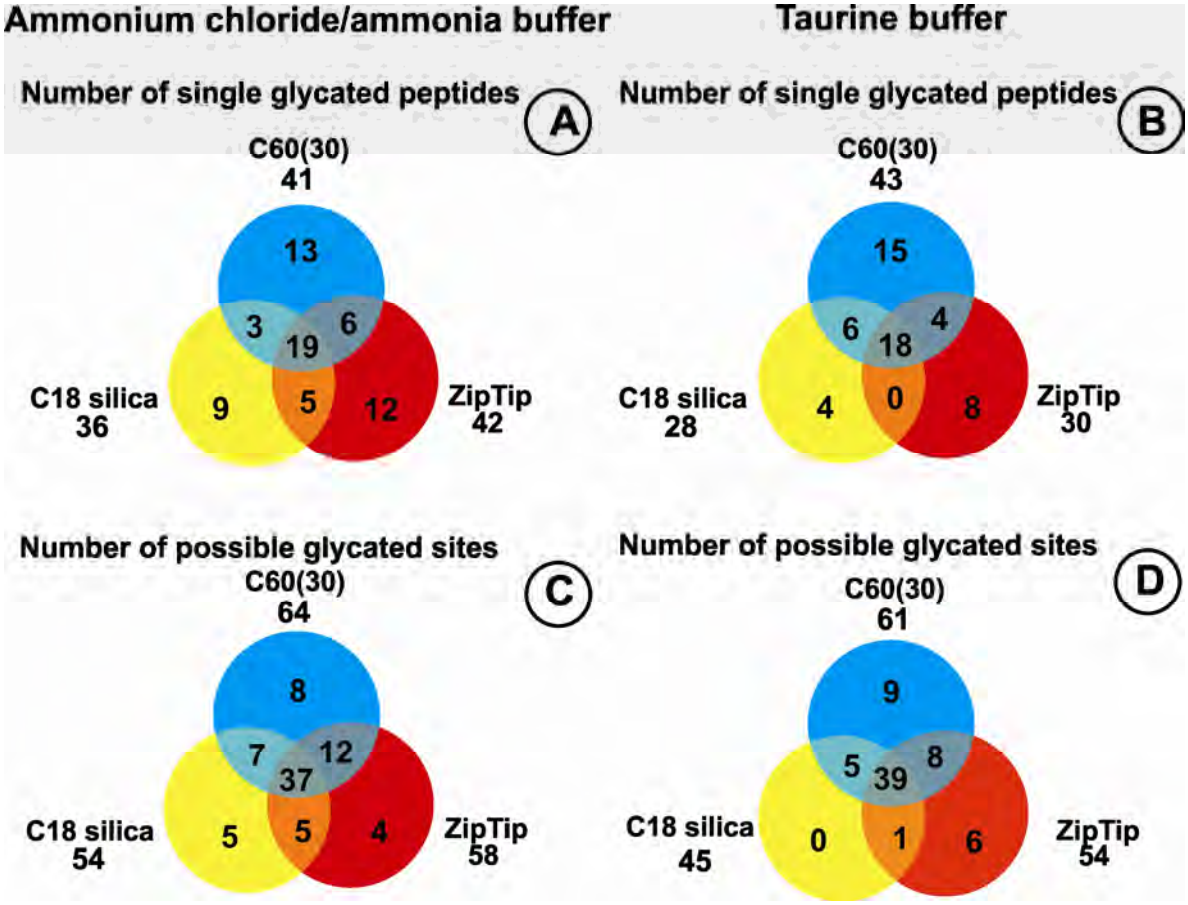

Figure 19: Comparison of different sorbents used for desalting when elution is carried out with sorbitol. (A) Venn diagram showing the numbers of detected single glycated peptides when the loading buffer was ammonium chloride/ammonia at optimized circumstances. (B) Venn diagram depicting the numbers of detected single glycated peptides in the case of using taurine buffer. (C) Venn diagram of possible glycated sites monitored from single glycated peptides bound by means of ammonium chloride/ammonia buffer. (D) Venn diagram of possible glycated sites monitored from single glycated peptides bound using taurine buffer.

The results demonstrated in Figures 20/A and B below confirm the observation made in the case of single glycated peptides. It was possible to bind 42 *double glycated peptides* selectively by applying an ammonium chloride/ammonia buffer. Considerably fewer (33) double glycated peptides were successfully monitored in the case of taurine buffer. Not only do the numbers of bound modified constituents indicate the effect of the binding buffers on the efficiency of the enrichment but also the numbers of possible modification sites located in the bound peptides must be taken into account by the evaluation. In single glycated peptides,

78 possible sites of modification were recognized using ammonium chloride/ammonia buffer (Figure 19/C below) and 68 glycated residues were identified by means of taurine buffer (Figure 19/D below). Regarding the glycated sites identified, in double modified peptides only a slight difference is observed in the number of glycated residues when comparing the two loading buffers. The use of the binding buffer consisting of ammonium chloride and ammonia allowed us to identify 63 potential glycated sites from those peptides captured by boronate affinity tips (Figure 20/C). In comparison, taurine buffer is capable of assisting with binding peptides to affinity tips, from which 60 glycated sites could have been determined (Figure 20/D below). In conclusion, the choice of an ammonium chloride/ammonia buffer with optimized pH and ionic strength enables binding more glycated peptides than the extensively used taurine buffer with the same pH and concentration.

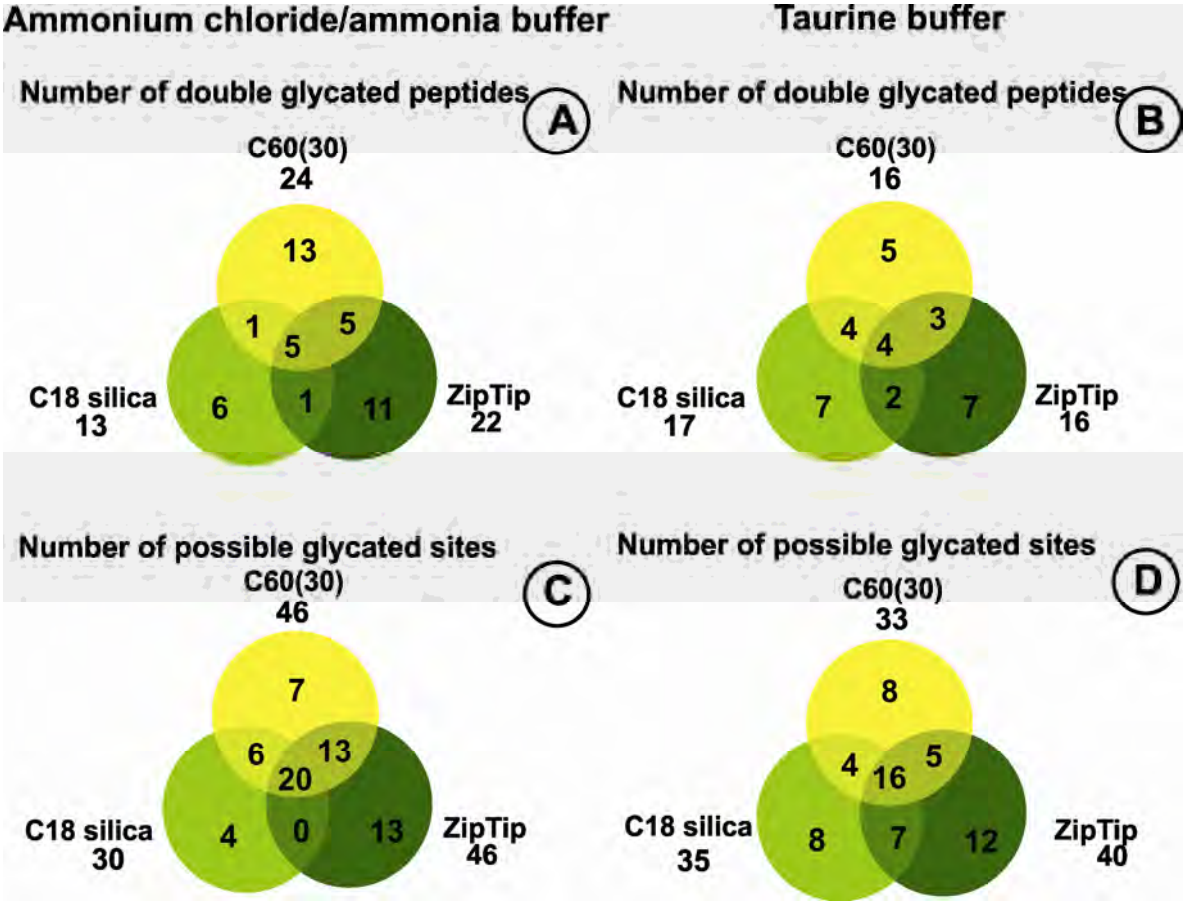

Figure 20: Comparison of different sorbents used for desalting when elution is carried out with sorbitol. (A) Venn diagram showing the numbers of detected double glycated peptides when the loading buffer was ammonium chloride/ammonia under optimized circumstances. (B) Venn diagram demonstrating the numbers of double glycated peptides detected in the case

of using taurine buffer. (C) Venn diagram of the possible glycated sites detected in double glycated peptides bound by means of ammonium chloride/ammonia buffer. (D) Venn diagram of the possible glycated sites detected in double glycated peptides bound employing taurine buffer.

It is important to emphasize that the differences in using these buffer systems are not expressed in the number of bound peptides and the identified glycated sites exclusively. For instance, after the binding of glycated peptides by applying both buffer systems, the elution of the bound constituents was accomplished with a sorbitol solution. This was followed by a **desalting** step using SPE cartridges filled with *C60(30)* silica particles. After the desalting step, 13 unique peptides of the total single glycated peptide pool adsorbed by the C60(30) particles (from 41 peptides) were possible to acquire using ammonium chloride/ammonia as binding buffer (Figure 19/A). Figure 19/B above shows unique single glycated peptides also bound exclusively by C60(30) particles when the enrichment of the glycated peptides was carried out using taurine buffer. In total, 43 of the eluted peptides could be identified when desalting them by means of employing C60(30) silica material. Of 43 single glycated peptides, 15 were identified only from the eluate of C60(30) and the remaining 28 peptides of the other sorbents could also be detected. It may be important to emphasize that these 15 unique glycated peptides must be interpreted only in the context of evaluating the three different sorbents with respect to the number of bound single glycated peptides. If the unique peptides detected in the eluates of C60(30) SPE material after the enrichment with the two above-mentioned buffer systems are compared, it can be concluded that their numbers were very similar to each other so long as 13 of them were found when enriching them with an ammonium chloride/ammonia buffer and 15 glycated peptides were found when the binding buffer was composed of taurine. Only 5 single glycated peptides with the same sequence and modifications could be analyzed from the unique peptides enriched with the two buffers and desorbed from C60(30). The majority of the unique peptides were found to be different despite the fact that they had been eluted from the same sorbent. This observation reveals that the use of different buffer systems alters the selectivity of the boronate phase insofar as the captured peptide profile and the identified potential glycated sites show great variety.

A) Single glycated peptides

Location		C60 (30)	Zip Tip	C18 silica
	unique peptides	**13**	**12**	**9**
	unique sites	**8**	**4**	**5**
[5- 20]	R^{10} or K^{12} or K^{20}	+		
[82- 98]	***K^{93}*** or ***R^{98}***		+	
[99-114]	***K^{106}*** or ***R^{114}***	+		
[115-136]	R^{117} or K^{136}		+	
[137-145]	K^{137} or R^{144} or R^{145}			+
[161-181]	K^{162} or K^{174} or K^{181}	+		
[175-181]	K^{181}		+	
[198-209]	***K^{199}*** or K^{205} or R^{209}			+
[200-212]	K^{205} or R^{209} or K^{212}			+
[206-212]	R^{209} or K^{212}	+		
[223-233]	K^{225} or K^{233}			+
[226-233]	K^{233}		+	
[241-262]	***R^{257}*** or K^{262}	+		
[275-286]	***K^{276}*** or K^{281} or K^{286}			+
[314-323]	***K^{317}*** or K^{323}			+
[318-336]	K^{323} or R^{336}		+	
[324-336]	R^{336}	+		

Location		C60 (30)	Zip Tip	C18 silica
[338-351]	***R^{348}*** or K^{351}	+		
[352-372]	K^{359} or ***K^{372}***	+		
[360-389]	***K^{372}*** or K^{378} or K^{389}	+		
[390-410]	***K^{402}*** or R^{410}		+	
[403-414]	R^{410} or K^{413} or K^{414}	+		
[411-428]	K^{413} or K^{414} or R^{428}		+	
[415-432]	R^{428} or K^{432}		+	
[429-439]	K^{432} or ***K^{436}*** or ***K^{439}***	+		
[446-466]	***K^{466}***	+		
[476-484]	R^{484}			+
[501-524]	K^{519} or R^{521} or **K^{524}**		+	
[520-525]	***K^{524}*** or K^{525}		+	
[526-541]	K^{534} or K^{536} or K^{538} or K^{541}		+	
[535-545]	K^{536} or K^{538} or K^{541} or K^{545}	+		
[539-557]	K^{541} or R^{545} or K^{557}		+	
[546-564]	K^{557} or K^{560} or ***K^{564}***			+
[565-585]	***K^{573}*** or K^{574}			+

B) Double glycated peptides

Location		C60 (30)	Zip Tip	C18 silica
	unique peptides	**13**	**11**	**6**
	unique sites	**7**	**13**	**4**
[94-114]	***R^{98}*** or K^{106} or R^{114}			+
[99-136]	K^{106} or R^{114} or R^{117} or K^{136}	+		
[138-145]	***R^{144}*** and ***R^{145}***		+	
[161-181]	***K^{162}*** or K^{174} or K^{181}		+	
[163-181]	K^{174} and K^{181}	+		
[182-190]	***R^{186}*** and K^{190}		+	
[187-195]	K^{190} and K^{195}	+		
[213-225]	***R^{218}*** or R^{222} or K^{225}	+		
[234-262]	K^{240} or ***R^{257}*** or ***K^{262}***		+	
[258-276]	***K^{262}*** or K^{274} or K^{276}		+	
[263-286]	K^{274} or K^{276} or K^{281} or K^{286}	+		
[275-286]	K^{276} or K^{281} or K^{286}	+		+
[277-286]	K^{281} and K^{286}			+

Location		C60 (30)	Zip Tip	C18 silica
[318-337]	***K^{323}*** or R^{336} or R^{337}		+	
[360-389]	***K^{372}*** or ***K^{378}*** or ***K^{389}***		+	
[373-402]	***K^{378}*** or ***K^{389}*** or ***K^{402}***		+	
[411-428]	***K^{413}*** or ***K^{414}*** or ***R^{428}***			+
[429-436]	K^{432} and K^{436}		+	
[429-439]	K^{432} or K^{436} or K^{439}	+		
[433-444]	K^{436} or K^{439} or K^{444}	+		
[437-444]	K^{439} and K^{444}			+
[467-475]	***R^{472}*** and ***K^{475}***		+	
[476-500]	***R^{484}*** or ***R^{485}*** or ***K^{500}***	+		
[485-521]	***R^{485}*** or ***K^{500}*** or ***K^{519}*** or ***R^{521}***	+		
[501-524]	K^{519} or R^{521} or K^{524}	+		
[520-525]	K^{524} and K^{525}		+	
[522-534]	K^{524} or K^{525} or K^{534}			+
[542-560]	R^{545} or K^{557} or ***K^{560}***	+		
[546-560]	K^{557} and ***K^{560}***	+		

Table 8: Detected single and double unique glycated peptides in the case of using ammonium chloride/ammonia binding buffer. Peptides were released from tips using sorbitol and desalted on C60(30), ZipTip, and homemade C18 silica. Italic bold type indicates unique glycation sites.

Tables 8 and 9 above provide detailed information about the unique glycated peptides and the locations of the recognized possible glycated sites of these peptides. Using ammonium chloride/ammonia buffer for the enrichment of glycated constituents with boronate affinity tips, as described earlier in this study, 41 single and 24 double glycated peptides were bound by C60(30) silica particles. In addition, 13 single and 13 double glycated unique peptides were explored in the eluted peptide pool. Single glycated peptides involve 8 possible glycated sites, namely K106, R114, R257, R348, K372, K436, K439, and K466, whereas 7 unique sites modified with D-glucose, namely R218, R484, R485, K500, K519, R521, and K560 were identified from double glycated peptides (Figures 19 and 20 above and Table 8 above).

These results were compared with those received after the enrichment of glycated peptides using taurine buffer. Among those peptides released from the affinity tips and desalted from the sorbitol solution on C60(30) particles, 15 single and 5 double glycated unique peptides were analyzed. Single glycated peptides made possible the identification of 9 unique glycated sites. Surprisingly, of the 5 double glycated unique peptides, 8 possible unique modified sites were recognized, as shown in Figures 19 and 20 above and Table 9 below. In single glycated unique peptides K190, K372, K413, K444, R445, K466, K536, K538, and K541, unique glycated sites were localized. In double glycated unique peptides, residues at R81, K93, R218, K372, K378, K389, R445, and K466 were likely to undergo non-enzymatic glycation.

ZipTip is a commercially available product, probably the most frequently and efficiently used tool for desalting the solutions of proteins and peptides prior to mass spectrometric measurements. In previous studies, the superiority of C60(30) to other commercial products such as Oasis and Sep-Pak and some octadecyl and triaconthyl modified silica material with high surface coverage has been reported in terms of SPE experiments of different biomolecules, including peptides, proteins, phosphorylated peptides, and glycated peptides [42]. Through the present work, an idea of trying to first use ZipTip for desalting glycated peptides emerged. When binding peptides to affinity tips with ammonium chloride/ammonia buffer, the desalting procedure carried out with ZipTip allowed the identification of 12 single glycated unique peptides modified at the residues of K93, R98, K402, and K524. Thus, in terms of the number of unique glycated sites localized in single unique glycated peptides, ZipTip does not seem to be as efficient as C60(30); however, it must be noted that 42 single glycated peptides were desalted by means of ZipTip, and 58

possible glycated sites were monitored. In addition, the analysis of 11 double glycated unique peptides comprising 13 glycated unique sites was made possible by ZipTip. These peptides were modified at the residues of R144, R145, K162, R186, R257, K262, K323, K372, K378, K389, K402, R472, and K475.

A) Single glycated peptides

Location		C60 (30)	Zip Tip	C18 silica
	unique peptides	**15**	**8**	**4**
	unique sites	**9**	**6**	**0**
[115-136]	R^{117} or K^{136}	+		
[115-137][a]	R^{117} or K^{136} or K^{137}			+
[115-144]	R^{117} or K^{136} or K^{137} or R^{144}		+	
[161-181]	K^{162} or K^{174} or K^{181}	+		
[163-174]	K^{174}	+		
[163-181]	K^{174} or ^{K181}			
[175-181]	K^{181}	+		
[175-186]	K^{181} or R^{186}			
[175-190]	K^{181} or R^{186} or ***K^{190}***	+		
[200-212]	K^{205} or R^{209} or K^{212}			+
[206-212]	R^{209} or K^{212}	+		
[226-257]	K^{233} or K^{240} or R^{257}	+		
[241-262]	R^{257} or K^{262}		+	
[241-274]	R^{257} or K^{262} or K^{274}			+

Location		C60 (30)	Zip Tip	C18 silica
[258-276]	K^{262} or K^{274} or K^{276}		+	
[275-286]	K^{276} or K^{281} or K^{286}			+
[287-323]	***K^{313}*** or ***K^{317}*** or K^{323}		+	
[314-323]	***K^{317}*** or K^{323}		+	
[352-372]	K^{359} or ***K^{372}***	+		
[390-402]	K^{402}			
[390-410]	***K^{402}*** or R^{410}		+	
[403-414]	R^{410} or ***K^{413}*** or K^{414}	+		
[411-428]	***K^{413}*** or K^{414} or R^{428}	+		
[415-432]	R^{428} or ***K^{432}***		+	
[440-445]	***K^{444}*** or ***R^{445}***	+		
[446-466]	***K^{466}***	+		
[485-519]	***R^{485}*** or ***K^{500}*** or K^{519}		+	
[526-541]	K^{534} or ***K^{536}*** or ***K^{538}*** or ***K^{541}***	+		
[539-557]	***K^{541}*** or R^{545} or K^{557}	+		
[542-560]	R^{545} or K^{557} or K^{560}	+		

B) Double glycated peptides

Location		C60 (30)	Zip Tip	C18 silica
	unique peptides	**5**	**7**	**7**
	unique sites	**8**	**12**	**8**
[5- 12]	***R^{10}*** and ***K^{12}***			+
[74- 98]	***R^{81}*** or ***K^{93}*** or R^{98}	+		
[94-114]	R^{98} or ***K^{106}*** or ***R^{114}***		+	
[99-136]	***K^{106}*** or ***R^{114}*** or R^{117} or K^{136}		+	
[115-136]	R^{117} and K^{136}	+		
[145-160]	***R^{145}*** or ***K^{159}*** or ***R^{160}***		+	
[161-181]	***K^{162}*** or K^{174} or K^{181}			+
[163-181]	K^{174} and K^{181}		+	
[213-222]	***R^{218}*** and R^{222}	+		

		C60 (30)	Zip Tip	C18 silica
[223-240]	K^{225} or K^{233} or K^{240}			+
[263-286]	***K^{274}*** or ***K^{276}*** or K^{281} or K^{286}			+
[360-389]	***K^{372}*** or ***K^{378}*** or ***K^{389}***	+		
[414-428]	***K^{414}*** and ***R^{428}***		+	
[437-444]	***K^{439}*** and ***K^{444}***		+	
[445-466]	***R^{445}*** and ***K^{466}***	+		
[526-538]	***K^{534}*** or ***K^{536}*** or ***K^{538}*** or K^{541}		+	
[539-557]	K^{541} or R^{545} or K^{557}			+
[561-573]	***K^{564}*** and ***K^{573}***			+
[561-574]	***K^{564}*** or ***K^{573}*** or ***K^{574}***			+

Table 9: Detected single and double unique glycated peptides in the case of using taurine binding buffer. Peptides were released from tips using sorbitol and desalted on C60(30), ZipTip, and homemade C18 silica. Italic bold type indicates unique glycation sites. [a] Peptide in the sequence brackets [115–137] could be detected from the digest of nonglycated HSA (standard).

Concerning **taurine binding buffer**, for single glycated peptides, ZipTip provided a worse result than C60(30) so long as only 30 peptides were bound; of these, 8 were found to be unique. Taking into account the glycated residues detected in peptides bound on ZipTip, 54 possible glycated sites were found, in contrast to C60(30), where this number was slightly higher (61). Six unique glycated sites at the positions of K402, K432, K313, K317, K500, and R485 could be observed. Regarding the number of double glycated peptides, ZipTip proved to be as efficient as C60(30) insofar as both sorbents were capable of binding 16 peptides. For ZipTip, 7 unique double glycated peptides with 12 unique sites at K106, R114, R145, K159, R160, K414, R428, K439, K444, K534, K536, and K538 were detected.

Finally, the desalting of the glycated peptides was also tried with **octadecyl silica** with high surface coverage. In the case of ammonium chloride/ammonia buffer 36 single glycated peptides were successfully bound, 9 of which were unique peptides, modified at K199, K317, K276, K564, and K573 as well. Using this buffer, only 13 double glycated peptides could be desalted. The poor performance of this material toward hydrophilic glycated peptides is also expressed in the number of unique peptides found, that is, only 6 with 4 possible unique glycated sites at R98, K413, K414 and R428. When using taurine buffer, the results of the desalting on C18 particles were even worse. In total, 28 single glycated peptides of the 4 unique peptides analyzed were bound; none of them comprised any unique glycated sites. In total, 17 double glycated peptides could be identified; of these, 7 proved to be unique with 8 possible sites of glycation at R10, K12, K162, K274, K276, K564, K573, and K574.

Elution of the bound constituents is frequently implemented in acidic media. As reported earlier [69], a **formic acid** solution of pH 2.0 proved to be the best in terms of the amount of eluted D-glucose evidenced by amperometric measurements. Elution with this solution was compared to elution implemented with sorbitol (desalted by C60(30)) regarding the number of eluted single and double glycated peptides and the possible identified glycated sites as well. These two ways of elution were compared with the digest of HSA incubated with D-glucose for 28 days to assess the efficiency of the enrichment. Surprisingly, the elution with formic acid yielded the worst results in terms of the number of identified glycated peptides and the possible sites of glycations.

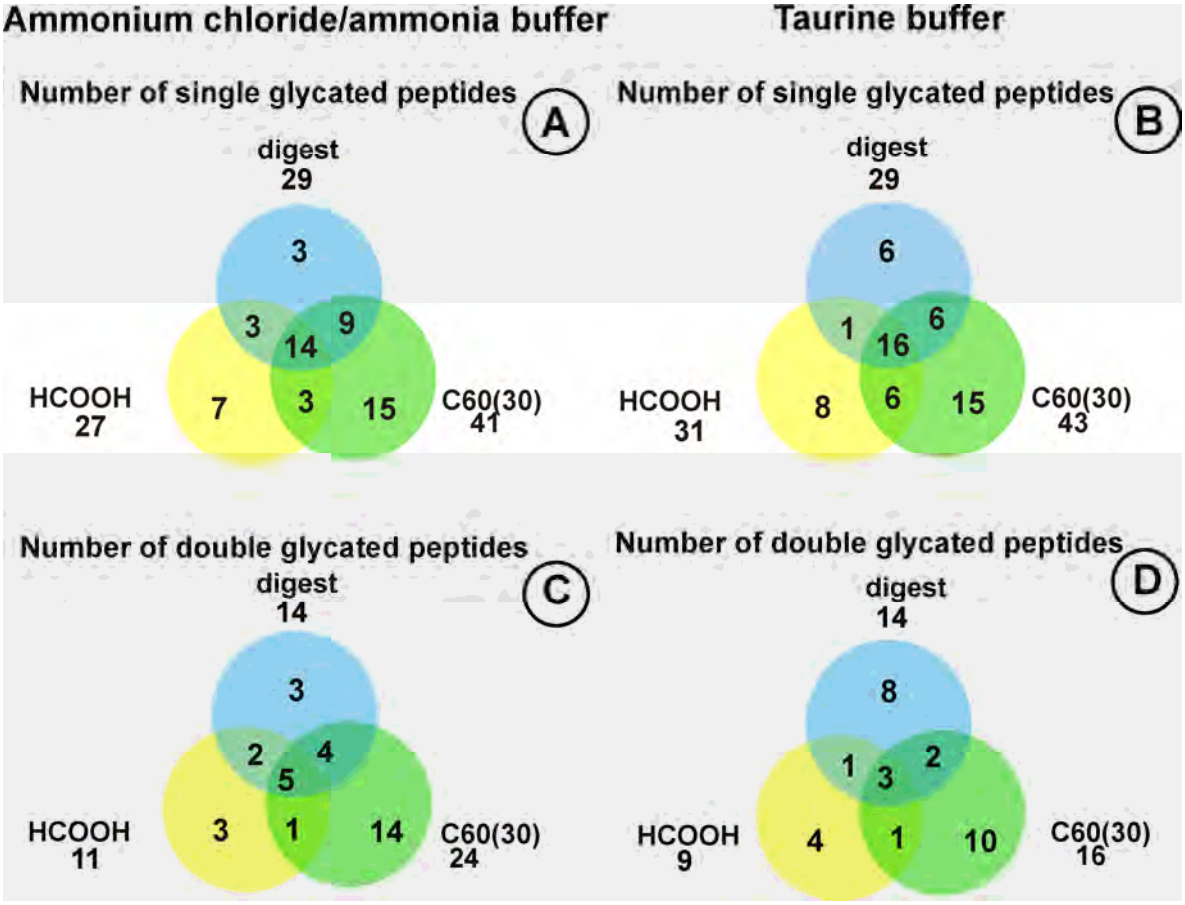

Figure 21: Comparison of elutions of glycated peptides from affinity tips with digest of HSA glycated for 28 days with the numbers of detected glycated peptides indicated. (A) Venn diagram showing the numbers of single glycated peptides when using ammonium chloride/ammonia binding buffer. (B) Venn diagram of the single glycated peptides released from the tips in the case of employing taurine binding buffer. (C) Venn diagram of the double glycated peptides detected when using ammonium chloride/ammonia buffer. (D) Venn diagram depicting double glycated peptides comparing the elutions with the digest when the binding buffer was taurine.

Figure 21/A above shows that in 100 pmol of the digest of overglycated HSA *without enrichment*, 29 single glycated peptides were recognized and 3 were found to be unique peptides with 5 unique glycated sites. When binding glycated peptides with *ammonium chloride/ ammonia buffer*, the elution of single glycated peptides with *formic acid* resulted in the release of 27 single glycated peptides from the boronate affinity tips; of these, 7 were unique peptides with 4 possible sites of modification. As mentioned earlier, the *elution with*

sorbitol yielded the detection of 41 single glycated peptides; nevertheless, the eluate was subjected to SPE on C60(30) particles prior to MALDI–TOF analysis. However, in this context of the comparison, 15 unique peptides comprising 12 unique residues were explored. Using the same buffer, the same trend could be observed for double glycated peptides given that 14 of them were identified from the digest (only 3 of them were unique with 3 unique sites). As also demonstrated in Figure 21/B above, formic acid made possible the release of only 11 peptides. Of these double glycated peptides, 3 were found to be unique, including 5 unique sites of glycation. Elution with sorbitol again showed the best results after desalting. This was expressed by 24 identified peptides; of these, 14 were observed to be unique constituents containing 16 unique glycated sites.

Figure 21/C and D above show those cases where glycated peptides were bound to the affinity tips in the presence of **taurine buffer**. Briefly, from the digest, 29 single glycated peptides were detected; of these, 6 were unique and each had 3 unique residues. Eluting the peptides with *formic acid* solution allowed the recognition of 31 single glycated peptides; of these, 8 were unique with 4 possible unique sites of glycation. When eluting the peptides with *sorbitol*, 43 single glycated peptides could be detected; of these, 15 were unique and incorporated 8 unique glycated sites. With respect to double glycated peptides in the case of using taurine buffer, 14 were found in the digest; of these, 8 were unique with 8 unique residues. Whereas elution with formic acid provided 9 double glycated peptides (4 of these were unique with 7 unique sites), elution accomplished with sorbitol caused the release of a considerably higher number of peptides so long as 16 of them could be measured after desalting (10 of these proved to be unique and comprised peptides of 13 unique glycated sites). As demonstrated above, with the elution of the bound glycated peptides with formic acid solution, it seems that no enrichment of the modified constituents occurred in spite of the fact that the highest amount of glucose could be measured at pH 2.0 (as discussed earlier in Section 4.2.1). Therefore, the acidic elution is not recommended by Takátsy et al..

The most efficient way to gain information about the modified glycated sites of a protein by MALDI–MS is to bind glycated peptides from the digest of the protein using, for instance, ammonium chloride/ammonia binding buffer under optimized circumstances, and then the selectively bound constituents are eluted with a concentrated solution of a proper sugar such as sorbitol. Furthermore, prior to analysis, the presence of undesirable sugar can be eliminated using an effective sorbent for desalting. As was demonstrated, C60(30) proved to be as efficient as ZipTip; no significant differences could be observed in the binding efficacy of either phase toward glycated peptides.

Although the methods described above were evaluated on the basis of the number of unique peptides and glycated sites, some of these modifications could be present in the nonglycated HSA standard because it was isolated from human serum. Therefore, if the aim of the work is also to identify those possible glycated sites modified only after the *in-vitro* glycation, the analysis of the digest of non-modified HSA is also an important requirement. These glycated peptides present in the digest of non-modified HSA probably comprise the most privileged accessible residues; therefore, their identification — especially after the non-enzymatic glycation (when their amounts in the digest are increased immensely) — is not a challenging task. If these peptides are taken into account, the sensitivity of the given method is undermined. The analysis of the digest of non-glycated HSA allowed us to identify 11 peptides by means of using ammonium chloride/ammonia as a binding buffer; this was followed by an elution with sorbitol, and the eluate was desalted using both C60(30) and ZipTip (see Table 10). As was expected, elution with formic acid made possible the identification of only 2 peptides, both of which could be analyzed from the eluates with sorbitol. It is also worth noting that 4 of these peptides contain K233, K378, K525 and K545 glycated residues and these residues are well known to be privileged and are able to be glycated easier [67, 81, 94]. From the digest of unglycated RNase A, no glycated peptides were monitored.

			C60 (30)	**ZipTip**	**HCOOH**
		glycated peptides	**8**	**8**	**2**
		possible glycated sites	**16**	**17**	**4**
[65- 81]	K^{73} or R^{81}	SLHTLFGDKLCTVATLR	+	+	
[115-137]	R^{117} or K^{136} or K^{137}	LVRPEVDVMCTAFHDNEETFLKK	+	+	
[137-144]	K^{137} or R^{144}	KYLYEIAR	+		
[210-218]	K^{212} or R^{218}	AFKAWAVAR	+	+	
[226-240]	K^{233} or K^{240}	AEFAEVSKLVTDLTK	+	+	+
[337-348]	R^{337} or R^{348}	RHPDYSVVLLLR	+		
[373-389]	K^{378} or K^{389}	VFDEFKPLVEEPQNLIK		+	
[414-428]	K^{414} or R^{428}	KVPQVSTPTLVEVSR	+		
[501-521]	K^{519} or R^{521}	EFNAETFTFHADICTLSEKER		+	
[525-534]	K^{525} or K^{534}	KQTALVELVK	+	+	+
[542-557]	K^{545} or K^{557}	EQLKAVMDDFAAFVEK		+	

Table 10: Glycated peptides identified from the digest of non-glycated HSA. Elutions of the bound constituents have been carried out using sorbitol and formic acid. The applied binding buffer was ammonium chloride/ammonia.

The **usefulness of the method** proposed by Takátsy et al. is clearly demonstrated in Figure 22 below. Figure 22/A below shows the MALDI spectrum of the digest of HSA (glycated *in-vitro* for 28 days) in the range from 2000 to 2230 Da. Besides a very intensive non-modified tryptic peptide appearing at m/z 2086.46, 2 less intensive glycated peptides can be observed at m/z 2060.68 and 2013.56. Moreover, the mass accuracy of these peptides is not reliable due to the very low signal- to-noise ratio of the first peptide. The latter does not possess very good mass resolution, which can be ascribed to the fact that peptides with similar masses can have a disturbing effect on mass resolution. Figure 22/C below shows the spectrum belonging to the digest of HSA glycated for 28 days after having been enriched by the method proposed above. Four glycated peptides can be seen in the figure. The peak appearing at m/z 2061.05 is a single glycated peptide. Additional peaks at m/z 2094.06, 2104.03, and 2217.24 are double glycated peptides, and their sequences are also shown in Figure 22/C below. When the profile of glycated peptides enriched from HSA glycated for 12 days (Figure 22/B) is compared to the results of enrichment from the digest of HSA glycated for 28 days (Figure 22/C), significant differences can be found. For example, as a result of the enrichment from the digest made from HSA glycated for 12 days, 3 double glycated peptides were monitored at m/z 2094.28, 2104.09, and 2207.45. The rather intensive single glycated peptide detected in the digest of HSA glycated for 28 days at m/z 2061.05 could not be detected from the digest of HSA glycated for 12 days. This means that this glycation site must be more hindered; therefore, it needs to be exposed longer to the high concentration of sugar. This observation is also relevant to the peptide detected at m/z 2217.25 from the digest of HSA glycated for 28 days. In contrast, the peptide detected at m/z 2207.45 from the digest of HSA glycated for 12 days clearly indicates that this peptide, comprising one of the most privileged glycation sites (K378) [26], was modified relatively rapidly and that further oxidation processes are responsible for the absence of this peptide in the spectrum.

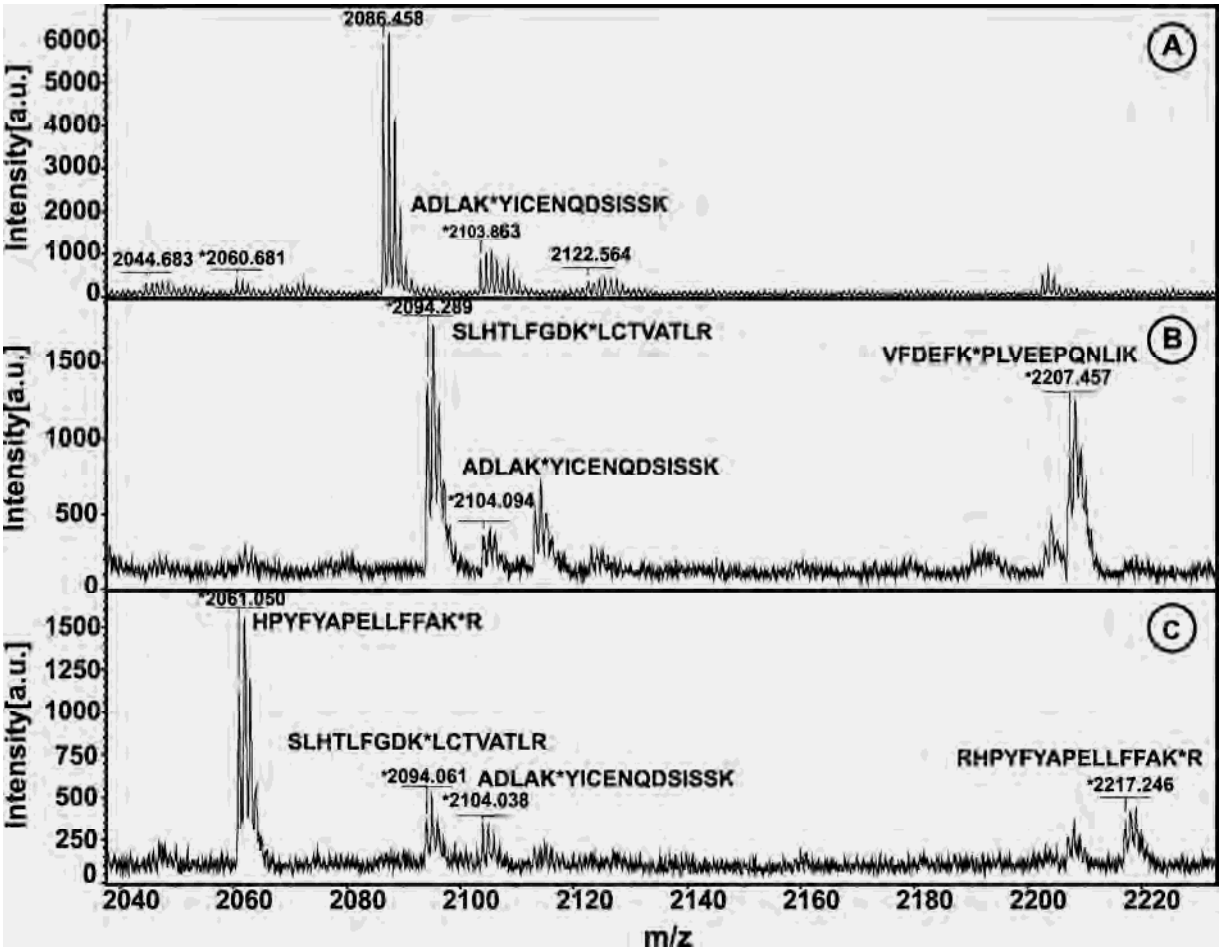

Figure 22: Enrichment of glycated peptides. (A) Mass spectrum of digest of HSA glycated for 28 days. No enrichment was used. (B) Mass spectrum of digest of HSA glycated for 12 days after selective enrichment. (C) Mass spectrum of digest of HSA glycated for 28 days after selective enrichment. In both cases, the enrichment was carried out using ammonium chloride/ammonia binding buffer and the elution of the bound peptides was carried out with sorbitol. Prior to MALDI measurement, the eluates were desalted on C60(30) particles. Each spectrum was monitored in reflectron mode and a sum of 1000 shots. The applied matrix was DHB. Asterisks (*) denote the glycated peptides. a.u., i.e arbitrary units.

Previously published studies have reported the investigation of glycated peptides employing **LC–tandem mass spectrometry** (MS/MS) techniques [10, 26]. The advantages of using these approaches in comparison with different off-line MALDI methods are that the loss of samples is largely reduced so long as the separated peptides are analyzed on-line by mass spectrometric methods. Table 11 indicates glycated peptides identified by Takátsy et al. from the digest of HSA glycated *in-vitro* for 28 days. Takátsy et al. pointed out that to the best of their knowledge, this is the first attempt to separate glycated peptides on a monolithic capillary column. The results are very similar to those reported in previous studies concerning the number of glycated peptides and the possible modified residues [81].

Location	Glycation site	
[42- 64]	K^{51} or K^{64}	
[160-174]	R^{160} or K^{162} or K^{174}	+
[226-240][a]	K^{233} or K^{240}	
[258-274]	K^{262} or K^{274}	
[263-276]	K^{274} or K^{276}	
[318-336]	K^{323} or R^{336}	
[349-359]	K^{351} or K^{359}	
[373-389][a]	K^{378} or K^{389}	
[390-402]	K^{402}	
[414-428][a]	K^{414} or R^{428}	
[473-484]	K^{475} or R^{484}	
[525-534][a]	K^{525} or K^{534}	
[539-557]	K^{541} or R^{545} or K^{557}	*
[542-557][a]	K^{545} or K^{557}	

Table 11: Glycated residues identified by LC–MS.

The plus sign (+) means that in that region of HSA both single and double glycated peptides were detected. The asterisk (*) denotes a double glycated peptide while [a] indicates that the peptide could be detected from the digest of nonglycated HSA.

Table 11 above shows that 13 of the 15 glycated peptides identified, were found to be single glycated and only 2 were modified with 2 glucose units. However, the table also shows that 5 of all the identified peptides also were present from the digest of the non-glycated HSA. This fact clearly indicates that despite using a highly efficient separation method, the efficacy of this method is overcome by the boronate affinity chromatography/off-line MALDI–TOF method introduced before. The peptides identified allowed us to localize 28 possible glycation sites. This proved to be better than previously reported data; of 15 peptides, 22 possible sites

of modification were described by Ref. [81, 97]. However, both LC–MS methods were able to recognize the privileged K233, K276, K378, K545, and K525 sites of glycation.

Table 12 below shows peptides and glycation sites of **RNase A** recognized by boronate affinity tips (using ammonium chloride/ammonia buffer). The bound peptides were eluted with sorbitol and desalted on C60(30) particles. As can be seen, by means of affinity tips, 5 single and 2 double glycated peptides comprising 12 possible glycated sites could be detected. Even though the focus of the investigation is a small protein such as RNase A where the number of glycated sites is relatively low, with the help of LC–MS, 6 glycated peptides with 8 possible modification sites were found.

Location	glycation sites	Sequence	Identified by LC-MS	Identified by boronate affinity-MALDI	
			6	**5**	
			8	**9**	
[1- 10]	K^{1} or K^{7} or R^{10}	KETAAAKFER		+	DD
[11- 31]	K^{31}	QHMDSSTSAASSSNYCNQMMK	+		
[32- 39]	R^{33} or K^{37} or R^{39}	SRNLTKDR			DD
[34- 39]	K^{37} or R^{39}	NLTKDR	+		
[38- 61]	R^{39} or K^{41} or K^{61}	DRCKPVNTFVHESLADVQAVCSQK	+		
[40- 61]	K^{41} or K^{61}	CKPVNTFVHESLADVQAVCSQK	+	+	
[62- 85]	K^{66} or R^{85}	NVACKNGQTNCYQSYSTMSITDCR	+		
[67- 91]	R^{85} or K^{91}	NGQTNCYQSYSTMSITDCRETGSSK		+	
[92-104]	K^{98} or K^{104}	YPNCAYKTTQANK		+	
[99-124]	K^{104}	TTQANKHIIVACEGNPYVPVHFDASV	+	+	

Table 12: Comparison of affinity chromatographic–off-line MALDI method with LC–MS in terms of identified glycated peptides of RNase A. DD refers to the double glycated peptides.

4.2.3 Application of boronate affinity tips for selective enrichment of Amadori products from digest of HSA collected from sera of patients suffering from type 2 diabetes mellitus and healthy volunteers

Four healthy volunteers and four patients suffering from type 2 diabetes mellitus were chosen to test the method described above for the mapping of the level of glycation of HSA. Patients were selected on the basis of the level of HbA1c and fasting plasma glucose. Because boronate affinity chromatography has been recognized to bind constituents comprising *cis*–diol, the method allows monitoring fructosyl lysine (FL, Amadori product) and its derivative

after loss of water (FL-18) (Figure 10). For healthy volunteers, besides some important clinical parameters, the fasting plasma glucose was always less than 6.1 mmol×L^{-1}. These values were by far the highest in patients 1 and 2 (12.17 and 13.02 mmol×L^{-1}, respectively). For patients 3 and 4, slightly lower values were obtained (8.53 and 7.50 mmol×L^{-1}, respectively).

Because HbA1c was used for monitoring long-term glycaemic control in patients with diabetes mellitus, this value is thought to indicate glycaemic state over the most recent 1–2 months. For all of the investigated patients, HbA1c was considered to be rather high (10.30, 11.50, 11.82, and 11.30% as measured for patients 1, 2, 3, and 4, respectively).

These two series of data served for the estimation of the glycaemic state of patients. HSA reflects the amount of blood glucose more rapidly than HbA1c; moreover, accounting for its relatively short (17 days) biological half-life, the glycation level of HSA is relevant to the condition of blood glucose over 2 weeks preceding the test.

Approximately 300 µg of the digest of HSA (HSA was collected from each patient and healthy volunteer) was enriched under optimized conditions using boronate affinity tips. Also considering the results reported earlier, the bound constituents were released from the tips by means of a 1.2 M sorbitol solution. The eluate was then desalted on C60(30) and preconcentrated. Peptides remaining after this procedure were measured by MALDI–TOF/MS.

Results reported in Table 13 show single and double glycated peptides with the corresponding possible glycation sites monitored in healthy volunteers and patients. Besides the privileged glycation sites of K12, K233, and K525 being present in each individual, many other glycated K and R residues described previously were recognized [67]. Regarding the numbers of glycated peptides and the possible identified glycated residues with the exception of patient 4 (whose fasting plasma glucose was the lowest), the clinical parameters can be associated with the glycation pattern obtained from mass spectrometric data.

Single glycated peptides

Location	Possible glycation site	H1	H2	H3	H4	P1	P2	P3	P4
[1- 12]	K^{4} or R^{10} or K^{12}	+	+	+	+			+	+
[11- 20]	K^{12} or K^{20}					+			
[52- 73]	K^{64} or K^{73}					+			
[65- 81]	K^{73} or R^{81}					+	+		
[137-144]	K^{137} or R^{144}			+	+	+	+	+	+
[191-199]	K^{195} or R^{197} or K^{199}	+				+			
[219-225]	R^{222} or K^{225}	+							
[219-233]	R^{222} or K^{225} or K^{233}						+	+	
[226-240]	K^{233} or ^{K240}	+	+	+	+	+	+	+	+
[263-274]	K^{274}			+			+		
[314-323]	K^{317} or K^{323}					+	+		
[318-336]	K^{323} or R^{336}				+		+	+	
[337-348]	R^{337} or R^{348}			+			+		+
[373-389]	K^{378} or K^{389}			+		+	+		
[390-410]	K^{402} or R^{410}						+		
[437-445]	K^{439} or K^{444} or R^{445}							+	
[525-534]	K^{525} or K^{534}	+	+	+	+	+	+	+	+
[535-541]	K^{536} or K^{538} or K^{541}							+	
[561-573]	K^{564} or K^{573}							+	

Double glycated peptides

Location	Possible glycation site	H1	H2	H3	H4	P1	P2	P3	P4
[1- 10]	K^{4} and R^{10}			+				+	
[198-209]	K^{199} or K^{205} or R^{209}	+							
[277-286]	K^{281} and K^{286}			+			+		+
[403-414]	R^{410} or K^{413} or K^{414}	+							
[440-445]	K^{444} and R^{445}							+	
[525-534]	K^{525} and K^{534}			+	+	+	+	+	+

Table 13: Single and double glycated peptides comprised by FL residues (Amadori peptides) detected in patients (P1–P4) and healthy volunteers (H1–H4).

Table 14 below summarizes the explored glycated peptides with a mass shift of 144.042. They can be either FL (Amadori product) after a loss of water or tetrahydropyrimidine bound directly to arginine residues. Both are able to bind to a boronate resin due to the presence of vicinal diol. Results also indicate that peptides appearing at m/z 1077.519 and 1783.938 are worth considering. The latter site was observed in all of the investigated digests belonging to the patients but was utterly absent from samples taken from healthy individuals. This can be clearly seen in Figure 23 below. The presence of a modification at m/z 144.042 was further corroborated by the corresponding PSD spectrum,

where the presence of a neutral loss was detected at m/z 1639.896, showing that the location of the modification can be at either K414 or R428. Similarly, the peptide at m/z 1077.519 could be detected in only three diabetic patients. This modification located at R81 is considered to be a tetrahydropyrimidine attached, as expected, to arginine.

More patients and control individuals need to be involved to make a decision as to whether these 2 peptides with the possible modifications can serve as potential biomarkers in diabetes mellitus. The method elaborated and reported here seems to be a powerful tool for the investigation of non-enzymatic glycation.

Location	Possible glycation site	H1	H2	H3	H4	P1	P2	P3	P4
[65- 73]	K^{73}					+	+		
[74- 81]	***R^{81}***						+	+	+
[137-145]	K^{137} or R^{144} or R^{145}	+		+			+		
[187-195]	K^{190} or K^{195}	+							
[191-199]	K^{195} or R^{197} or K^{199}	+							
[210-218]	K^{212} or R^{218}								
[219-225]	R^{222} or K^{225}	+		+					+
[373-389]	K^{378} or K^{389}							+	+
[414-428]	***K^{414} or R^{428}***					+	+	+	+
[437-444]	K^{439} or K^{444}						+	+	
[501-521]	K^{519} or R^{521}						+		
[520-525]	K^{524} or K^{525}	+		+	+		+	+	
[525-538]	K^{525} or K^{534} or K^{536} or K^{358}					+			
[535-545]	K^{536} or K^{538} or K^{541} or K^{545}				+			+	

Table 14: Peptides modified with glucose after a loss of water and detected in patients (P1–P4) and healthy volunteers (H1–H4).

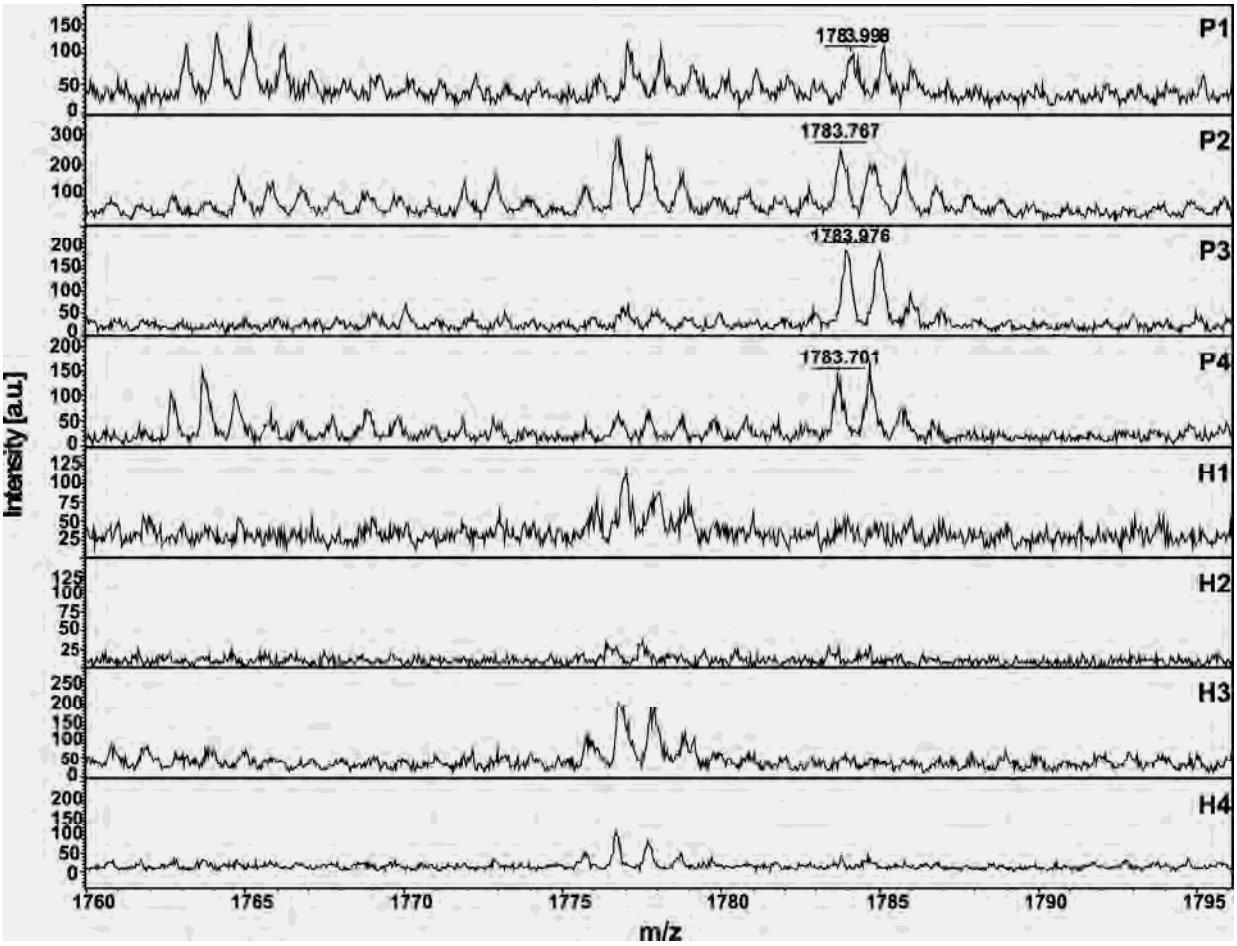

Figure 23: Comparison of mass spectra of HSA digest taken from sera of diabetic patients (P1–P4) and healthy volunteers (H1–H4) after enrichment of glycated peptides in the range of 1760–1800 Da. The presence of the peak appearing at m/z 1783.938 in patients suggests the possible distinctive role of this peptide as a biomarker. Each spectrum was monitored in reflectron mode and a sum of 1000 shots. The matrix applied was DHB. a.u., arbitrary units.

5. New results reported in the dissertation

5.1 Determination of the binding capacity of C30 and C60(30) fullerene-silica with Leu-enkephalin

After the activation and equilibration, C30-silica and C60(30) were incubated overnight with a solution of Leu-enkephalin at different concentrations. The peptide concentrations of the supernatants represent equilibrium values with the adsorbed Leu-enkephalin. The adsorption isotherms can be depicted plotting the concentrations of supernatants (C_{equ}) against the adsorbed amount. Data points fit the theoretical adsorption model of Langmuir with an excellent linear regression when plotting C_{equ} against C_{equ}/m_{ads}. The **binding capacity of C60(30)** is 31.5 mg/g, which is confirmed by a previously published result [42]. In the case of **C30-silica** the value is 153.9 mg/g showing a five times higher binding capacity.

5.2 Identification of solid phases (C18, C30, C60(10), C60(30), C60(100)) on the sequence coverage of tryptic digest of HSA and fibrinogen

DHB, CHCA and THAP were tested to identify the best MALDI matrix for mass spectrometric measurement of unfractionated tryptic digest of non-glycated HSA. **DHB** has proven to be the optimal matrix because of good resolution and reliable measurements with regard to mass accuracy. From 69% to 71% of sequence coverage was obtained by increasing the mass tolerance from 50 ppm to 150 ppm. Due to the favourable properties of DHB this matrix was further used for the MALDI analysis of both unmodified and glycated protein digests. Twenty pmol HSA digest was fractionated on each stationary phase: C18, C30, C60(10), C60(30), C60(100). The C18- and C30-silicas provided better sequence coverages (approximately 80%) than the C60-silicas. In the case of fractionation of 20 pmol fibrinogen the **C30 and C60(30)** materials yielded nearly the same results for Aα- and Bβ-chains of fibrinogen, but there was a remarkable increment for c-chain (64.9%) on C60(30) that means the total sequence coverage reached the best result 62.15%. The hydrophobicity and the length of the peptide do play an important part since those peptides have better access to the

alkyl moieties and therefore generated interactions stronger than to the spherical C60 molecules. Due to the highest percentage of the aromatic amino acids in the c-chain of fibrinogen the π-π interactions between the peptides and the fullerene play more important role than in the case of Aα- and Bβ-chains.

5.3 Determination of glycated sites of HSA and fibrinogen with C30 and C60(30)-silica

Digest of HSA glycated for 28 days were fractionated on C60(30) and C30 solid phase particles, the results were compared with unfractionated glycated HSA digest and boronate affinity. **Sixty-nine possible glycated sites** of HSA could be identified altogether, 10 of them have **never been described** in the literature before. Data provided from SPE experiments made it possible to recognise glycations that could not be detected from the unfractionated digest.

In the case of fractionation of glycated fibrinogen digest, the result cannot be compared with other data in the literature, since it has not been reported before. In the sequence of Aα-chain 72 modifications were found, using C30-silica 67, by means of C60(30) 63 glycated residues could be identified in SPE experiments. Of all the modified sites in Bβ-chain there were **59**, with fractionations on C30-silica nearly the same number **53 sites**, and on C60(30) **47 sites**. Forty-one possible glycated sites were found for the c-chain of fibrinogen. Results achieved using C30-silica (33 sites) and C60(30) (34 sites) were similar to each other. For instance, in c-chain glycation on R8, R35, R123, R246 and R421 residues were only possible to be explored employing C60(30). The **possible glycated sites of fibrinogen were described first** by Böddi et. al [85].

In the SPE experiments of glycated proteins C30-silica is a competitive candidate with regard to C60(30) concerning both the number of glycated sites and the number of bound peptides. The selectivity of these materials differs; C30-silica adsorbs larger peptides, while C60(30) possesses excellent binding capacity towards hydrophilic, arginine-rich small peptides. The findings may lie in the basis of a feasible SPE-off-line-MALDI method to be used for the investigation of polar constituents of complex biological samples.

5.4 Optimization of different approaches of elutions in the case of boronate affinity tips

Miniaturized boronate affinity chromatography was found to be the optimal method for the selective enrichment of non-ezimatically modified peptides. The proper binding condition is known (**150 mM ammonium chloride/ammonia buffer, pH 8.2**) but the appropriate circumstances of elution have never been optimized before. Data obtained from electrochemical measurements allowed us to find the optimal elution procedure of the bound glucose. It could be carried out employing either acidic conditions or a highly concentrated solution of sorbitol. Elution carried out using a **sorbitol solution** at a concentration of **1.2 M** was found to be more efficient than elution with formic acid at pH 2.0, although the more acidic solution was used; the more efficient the acidic media for the elution was. The solution of formic acid allowed us to identify 27 single glycated peptides, as long as elution with sorbitol has given 41 single glycated peptides.

5.5 Desalting of glycated peptides using different sorbents

After the elution of glycated peptides with sorbitol prior to MALDI–TOF analysis, the eluate consequently needed to be desalted. This was implemented using three different types of sorbents: the commercially available ZipTip, C60(30) and a homemade C18 silica. The eluates after using a sorbitol solution at a concentration of 1.2 M, were evaluated on the basis of the identified single and double glycated peptides and the number of possible glycated sites on HSA glycated for 28 days. These can be plotted by means of Venn diagrams (Figures 19, 20 and 21) for the best presentation of the results.

Ammonium chloride/ammonia buffer has proven to be the best binding buffer for selective enrichment of glycated peptides by boronate affinity chromatography. As the Venn diagrams show, 41 single glycated peptides were adsorbed with ammonium chloride/ammonia buffer by C60(30), of these 13 were unique with 8 possible glycated sites. While using ZipTip, 42 single glycated peptides can be found, 12 were unique with 4 unique glycation sites.

The choice of buffer and the way of elution, as well as the most appropriate sorbent used for desalting the eluate, were evaluated by means of Venn diagrams. The result were discussed on the basis of for 28 days glycated HSA digest in terms of the numbers of single and double

glycated peptides as well as the number of recognized glycation sites located on these peptides.

Regarding the numbers of single and double glycated peptides and the possible modified residues, **C60(30)** was considered as a promising sorbent with respect to its performance toward glycated constituents. Moreover, its efficacy is competitive with commercial that of **ZipTip**. The application of C18 did not meet the requirements concerning the number of glycated peptides bound during the desalting procedure.

5.6 Application of the new method for the detection of glycated peptides achieved from digested human serum albumin, collected from patients suffering from types 2 diabetes – compared to healthy volunteers

The applicability of the method was demonstrated for the digest of HSA isolated from healthy volunteers and diabetic patients. However, both the control and the diabetic groups included only four individuals, **more glycated peptides**, and consequently **more glycated sites**, were recognized for patients suffering from type 2 diabetes mellitus having been under insufficient diabetic control when being monitored FL (Amadori product).

The privileged glycation sites of K12, K233, and K525 were present in each individual. Results also indicate that peptides appearing at m/z 1077.519 and 1783.938 are worth considering, although peptide at m/z 1077.519 could be detected in only three diabetic patients. This modification, which located at R81, is considered to be an attached tetrahydropyrimidine.

When detecting FL after a loss of water (FL-18), a distinctive peptide appearing at **m/z 1783.9** was observed in each diabetic patient but was not detected in healthy control individuals. This peptide is located in the region of [414–428] of HSA and incorporates K414 and R428. This peptide and its glycated sites may serve as a **potential biomarker for diabetes**; however, further research is required to confirm this observation.

References

[1] Karas, M., Hillenkamp, F., Laser desorption ionization of proteins with molecular masses exceeding 10,000 daltons, Anal. Chem. 60 (1988) 2299-2301.

[2] James, P., Proteome Research: Mass Spectrometry, Springer-Verlag, New York, (2001) 35

[3] Bökelmann, V., Spengler, B., Kaufmann R., Dynamical parameters of ion ejection and ion formation in matrix-assisted laser desorption/ionization, Eur. Mass Spectrom., 27 (1995) 156-158.

[4] Edited by: Kinter, M., Sherman N.E., Protein sequencing and identification using tandem mass spectrometry, Wiley-Interscience Series on Mass Spectrometry, (2000) 15-62.

[5] Wiley, W.C., McLaren, I.H., Time-of-flight mass spectrometer with improved resolution, Rev. Sci. Instrument., 26 (1955) 1130-1157.

[6] Edited by: Matthiesen R., Mass spectrometry Data Analysis in Proteimics New Jersey, (2007) 7-25.

[7] Hardouin, J., Protein sequence information by matrix-assisted laser desorption in-source decay mass spectrometry, Mass Spectrom. Rev., 26 (5) (2007) 672-682.

[8] Brown, R.S., Lennon, J.J., Sequence-specific fragmentation of matrix-assisted laser-desorbed protein/peptide ions, Anal. Chem., 67 (21) (1995) 3990-3999.

[9] Pfeifer, T., Drewello, M., Schierhorn, A., Using a matrix-assisted laser desorption/ionization time-of-flight mass spectrometer for combined in-source decay/post-source decay experiments, J. Mass Spectrom., 34 (6) (1999) 644-650.

[10] Brown, R.S., Carr B.L., Lennon, J.J., Factors that influence the observed fast fragmentation of peptides in matrix-assisted laser desorption, J. Am. Soc. Mass Spectrom., 7 (1996) 225-232.

[11] Lennon, J.J., Matrix assisted laser desorption ionization time-of-flight mass spectrometry, http://www.abrf.org/ABRFNews/1997/June1997/jun97lennon.html

[12] Reiber, D.C., Grover, T.A., Brown, R.S,. Identifying proteins using matrix assisted laser desorption/ionization in-source fragmentation data combined with database searching, Anal. Chem., 70 (4) (1998) 673–683.

[13] Reiber, D.C., Brown, R.S., Weinberger, S., Kenny, J., Bailey, J., Unknown peptide sequencing using matrix-assisted laser desorption/ionization and in-source decay, Anal. Chem., 70 (6) (1998) 1214–1222.

[14] Spengler, B., Kirsch, D., Kaufmann, R., Metastable Decay of Peptides and Proteins in Matrix Assisted Laser Desorption Mass Spectrometry, Rapid Commun. Mass Spectrom., 5 (1997) 198-202.

[15] Kaufmann, R., Kirsch, D., Spengler, D., Sequenching of peptides in a time-of-flight mass spectrometer: evaluation of postsource decay following matrix-assisted laser desorption ionisation (MALDI), Int. J. Mass. Spectrom., Ion Processes 131 (1994) 355-385.

[16] Spengler, B., Kirsch, D., Kaufmann, R., Jaeger, E., Peptide sequencing by matrix-assisted laser-desorption mass spectrometry, Rapid Commun. Mass Spectrom., 6 (1992) 105-108.

[17] Kaufmann, R., Spengler, B., Lutzenkirchen, F., Mass spectrometric sequencing of linear peptides by product-ion analysis in a reflectron time-of-flight mass spectrometer using matrix-assisted laser desorption ionization, Rapid Commun. Mass Spectrom., 7 (1993) 902-910.

[18] Spengler B., Post-source decay analysis in matrix-assisted laser desorption/ionization mass spectrometry of biomolecules, J. Mass Spectrom. 32 (1997) 1019-1039.

[19] Chaurand, P., Luetzenkirchen, F., Spengler B., Peptide and protein identification by matrix-assisted laser desorption ionization (MALDI) and MALDI-post-source decay time-of-flight mass spectrometry, J. Am. Soc. Mass Spectrom., 10 (2) (1999) 91-103.

[20] Edited by: Smith B.J., Protein sequencing protocols, New Jersey (2003) 195-222.

[21] Barrett, J., Brophy, P.M., Hamilton, J.V., Analysing proteomic data, Int. J. Parasitol., 35 (5) (2005) 543-53.

[22] Guerrera, I.C., Kleiner O., Application of Mass Spectrometry in Proteomics, Bioscience Reports, 25 (2005) 71-94.

[23] Karas, M., Bahr, U., Gießmann, U., Matrix-assisted laser desorption/ionization mass spectrometry, Mass Spectrometry Reviews, 10 (5) (1991) 335–357.

[24] Wa, C., Cerny, R., Hage, D.S., Obtaining high sequence coverage in matrixassisted laser desorption time-of-flight mass spectrometry for studies of protein modification: analysis of human serum albumin as a model, Anal. Biochem., 349 (2006) 229–241.

[25] Edited by: Chapman J. R., Mass spectrometry of proteins and peptides, New Jersey (2000)

[26] Papac, D.I., Wong, A., Jones, A., Analysis of acidic oligosaccharides and glycopeptides by matrix assisted laser desorption/ionization time-of-flight mass spectrometry, J. Anal. Chem., 68 (1996) 3215 – 3223.

[27] Edited by: Thiellement, H., Zivy, M., Damerval, C., Méchin, V., Plant Proteomics: Methods and Protocols, New Jersey, (2007)

[28] Laugesen, S., Roepstroff, P., Combination of two matrices results in improved performance of MALDI MS for peptide mass mapping and protein analysis, J. Am. Soc. Mass Spectrom., 14 (2003) 992–1002.

[29] Yao, J., Scott, J.R., Young, M.K., Wilkins, C.L., Importance of matrix: analyte ratio for buffer tolerance using 2,5-Dihydroxybenzoic acid, J. Am. Soc. Mass Spectrom., 8 (1998) 805–813.

[30] Gilar, M., Bouvier, E.S., Compton, B.J., Advances in samplepreparation in electromigration chromatographic and mass spectrometric separation methods, J. Chromatogr. A, 909 (2001) 111–135.

[31] Luque-Garcia, J.L., Neubert, T.A., Sample preparation of serum/plasma profiling, J. Chromatogr. A, 1153 (2007) 259–276.

[32] Pan, C., Xu, S., Zhou, H., Fu, Y., Ye, M., Zou, H., Recent developments in methods and technology for analysis of biological samples by MALDI-TOF MS, Anal. Bioanal. Chem., 387 (2007) 193–204.

[33] Bouvier, E.S.P., Martin, D.M., Iraneta, P.C., Capparella, M., Cheng, Y.F., Phillips, D., A novel polymeric reversed-phase sorbent for solide phase extraction, LC-GC, 15 (1997) 152–157.

[34] Duan, G.L., Zheng, L.X., Chen, J., Cheng, W.B., Li, D., High-performance liquid chromatographic method for determination of leucovorin in plasma: validation and application to a pharmacokinetic study in healthy volunteers, Biomed. Chromatogr., 16 (2002) 282–286.

[35] Ding, J., Neue, U.D., A new approach to the effective preparation of plasma samples for rapid drug quantitation using on-line solid-phase extraction mass spectrometry, Rapid Commun. Mass Spectrom., 13 (1999) 2151–2159.

[36] Hennion M.C., Solid-phase extraction method development, sorbents and coupling with liquid chromatography, J. Chromatogr. A., 856 (1-2) (1999) 3-54.

[37] He, H., Sun, C., Wang, X.R., Pham-Huy, C., Chikhi-Chorfi, N., Galons, H., Thevenin, M., Claude, J. R., Warnet, J. M., Solid-phase extraction of methadone enantiomers and benzodiazepines in biological fluids by two polymeric cartridges for liquid chromatographic analysis, J. Chromatogr. B Analyt. Technol. Biomed. Life Sci., 814 (2005) 385–391.

[38] Gilar, M., Belenky, A., Wang, B.H., High Through put biopolymer desalting by solid-phase requirements of the stationary-phases, J. Chromatogr. A, 921 (2001) 3–13.

[39] Kroto, H.W., Heath, J.R., O'Brien, S.C., Curl, R.F., Smalley, R.E, C_{60}: Buckminsterfullerene, Nature, 318 (1985) 162.

[40] Pereira, M.G., Pereira-Filho, E.R., Berndt, H.. Arruda M.A.Z., Determination of cadmium and lead at low levels by using preconcentration at fullerene coupled to termospray flame furnace atomic absorption spectrometry, Spectrochimica Acta Part B: Atomic Spectroscopy, 59 (4) (2004) 515-521.

[41] Baena, J.R., Gallego, M., Valcarcel, M., Fullerenes in the analyticalsciences, Trends Anal. Chem. 21 (2002) 187-198.

[42] Vallant, R.M., Szabó, Z., Bachmann, S., Bakry, R., Ul-Haq, M.N., Rainer, M., Heigl, N., Petter, C., Huck, C.W., Bonn, G.K., Development and application of C60–fullerene bound silica for solid phase extraction of biomolecules, Anal. Chem., 79 (2007) 8144–8153.

[43] Zhang, H., Andren, P. E., Caprioli, R. M., Micro-Preparation Procedure for High - Sensitivity Matrix-Assisted Laser Desorption Ionization Mass Spectrometry, J. Mass Spectrom., 30 (1995) 1768–1771.

[44] Qi, L., Danielson, N.D., Quantitative determination of pharmaceuticals using nano-electrospray ionization mass spectrometry after reversed phase mini-solid phase extraction, J. Pharm. Biomed. Anal., 37 (2005) 225–230.

[45] Rappsilber, J., Ishihama, Y., Mann, M., Stop and go extraction tips for matrix-assisted laser desorption/ionization, nanoelectrospray, and LC/MS sample pretreatment in proteomics, Anal. Chem., 75 (2003) 663–670.

[46] Pluskal, M.G, Microscale sample preparation, Nat. Biotechnol., 18 (2000) 104–105.

[47] Danze, P.M., Tarjoman, A., Rousseaux, J., Fossati, P., Dautrevaux, M., Evidence for an increased glycation of IgG in diabetic patients, Clin. Chim. Acta, 166 (1987) 143–153.

[48] Rohovec, J., Maschmeyer, T., Aime, S., Peters, J.A., The structure of the sugar residue in glycated serum albumin and its molecular recognition by phenylboronate, Chem. Eur. J., 9 (2003) 2193–2199.

[49] Weith H.L., Wiebers J.L., Gilham P.T., Sythesis of cellulose derivatives containing the dihydroxyboryl group and a study of their capacity to form specific complexes with sugar and nucleic acid components, Biochemistry, 9 (22) (1970) 4396-4401.

[50] Liu, X.-C., Boronic acids as ligands for affinity chromatography, Chin. J. Chromatogr., 24 (2006) 73–80.

[51] Takátsy, A., Böddi, K., Nagy, L., Nagy, G., Szabó, S., Markó, L., Wittmann, I., Ohmacht, R., Ringer, T., Bonn, G.K., Gjerde, D., Szabó, Z., Enrichment of Amadori products derived from nonenzymatic glycation of proteins using microscale boronate affinity chromatography, Anal. Biochem., 393 (1) (2009) 8-22.

[52] Liu, X.C., Scouten, W.H., Boronate affinity chromatography, Methods Mol. Biol., 147 (2000) 119–128.

[53] Potter, O.G., Breadmore, M.C., Hilder, E.F., Boronate functionalised polymer monoliths for microscale affinity chromatography, Analyst, 131 (2006) 1094–1096.

[54] Middle, F.A., Bannister, A., Bellingham, A.J., Jean, P.D.G., Separation of glycated hemoglobins using immobilized phenylboronic acid, Biochem. J., 209 (1983) 771–779.

[55] Heon, J., Kim, Y., Ha, M.Y., Lee, E.K., Choo, J., Immobilization of aminophenylboronic acid on magnetic beads for the direct determination of glycoproteins by matrix assisted laser desorption ionization mass spectrometry, J. Am. Soc. Mass Spectrom., 16 (2006) 1456–1460.

[56] Gontarev, S., Shmanai, V., Frey, S.K., Kvach, M., Schweigert, F.J., Application of phenylboronic acid modified hydrogel affinity chips for high-throughput mass spectrometric analysis of glycated proteins, Rapid Commun. Mass Spectrom., 21 (2007) 1–6.

[57] Xu, Y., Wu, Z., Zhang, L., Lu, H., Yang, P., Weibley, P.A., Zhao D., High specific enrichment of glycopeptides using boronic acid-functionalized mezopoous silica, Anal. Chem., 81 (2009) 503-508.

[58] Ren L., Liu Z., Dong M., Ye M., Zou H., Synthesis and characterisation of a new boronate affinity monolithic capillary for specific capture of cis-diol containing compounds, J. Chromatogr. A, 1216 (23) (2009) 4768-4774.

[59] Preinerstorfer B., Lämmerhofer, M., Lindner W., Synthesis and application of novel phenylboronate affinity materials based on organic polymer particles for selective trapping of glycoprotein, J. Sep. Sci., 32, (10) (2009) 1673–1685.

[60] Chen M., Lu Y., Ma Q., Guo L., Feng Y.Q., Boronate affinity monolith for high selective enrichment of glycopeptides and glycoproteins, Analyst, 134 (2009) 2158-2164.

[61] Little R.R., Vesper H., Rollfing C.L., Ospina M., Safar-Pour S., Roberts W.L., Validation by a mass spectrometric reference method of use of boronate affinithy chromatography to measure glycohemoglobin int he presence of hemoglobin S and C traits, Clin. Chem., 51 (1) (2005) 264-265.

[62] McCance, D.R., Dyer, D.G., Dunn, J.A., Bailie, K.E., Thorpe, R.S. Baynes, J.W., Lyons, T.J., Maillard reaction products and their relation to complication in insulindependent diabetes mellitus, J. Clin. Invest., 91 (1993) 2470–2478.

[63] Trivelli, L.A., Ranney, H.M., Lai, H.T., Hemoglobin components in patients with diabetes mellitus, N. Engl. J. Med., 284 (1971) 353–357.

[64] Ulrich, P. Cerami, A., Protein glycation, diabetes, and aging, Recent Prog. Horm. Res., 56 (2001) 1–21.

[65] Kisugi, R., Kouzuma, T., Yamamoto, T., Akizuki, S., Miyamoto, H., Someya, Y., Yokoyama, J., Abe, I., Hiraki, N., Ohnishi, A., Structural and glycation site changes of albumin in diabetic patient with very high glycated albumin, Clin. Chim. Acta, 382 (2007) 59–64.

[66] Brancia, F.L., Bereszczak, J.Z., Lapolla, A., Fedele, D., Baccarin, L., Seraglia, R., Traldi, P., Comprehensive analysis of glycated human serum albumin tryptic peptides by off-line liquid chromatography followed by MALDI analysis on a time-of-flight/curved field reflectron tandem mass spectrometer, J. Mass Spectrom., 41 (2006) 1179–1185.

[67] Wa, C., Cerny, R.L., Clarke, W.A., Hage, D.S., Characterisation of glycation adducts on human serum albumin by matrix-assisted laser desorption/ionization timeof-flight mass spectrometry, Clin. Chim. Acta 385 (2007) 48–60.

[68] Gadgil, H.S., Bondarenko, P.V., Treuheit, M.J., Ren, D., Screening and sequencing of glycated proteins by neutral loss scan LC/MS/MS method, Anal. Chem., 79 (2007) 5991–5999.

[69] Zhang, Q., Tang, N., Brock, J.W.C., Mottaz, H.M., Ames, J.M., Baynes, J.W., Smith, R.D., Metz, T.O., Enrichment and analysis of nonenzymatically glycated peptides: boronate affinity chromatography coupled with electron-transfer dissociation mass spectrometry, J. Proteome Res., 6 (2007) 2323–2330.

[70] Maillard, L., Gautir C.R., Action des acides amines scer les sucres: formation des melanoidines per noie methodique Seances Acad. Sci., III 154 (1912) 66-68.

[71] Soskić V., Groebe K., Schrattenholz A., Nonenzymatic posttranslational protein modification in aging, Exp. Gerontol., 43 (4) (2008) 247-257.

[72] Grillo M.A., Colombatto S., Advanced glycation end-products (AGEs): involvement in aging and neurodegenerative deseases, Amino Acids, 35 (1) (2007) 29-36.

[73] Bunn H.F., Gabbay K.H., Gallop P.M., The glycosilation of hemoglobin: relevanse to diabetes mellitus, Science, 200 (4337) (1978) 21-27.

[74] Lapolla A., Fedele D., Traldi P., Glyco-oxidation in diabetes and related diseases, Clin. Chim. Acta, 357 (2) (2005) 236-250.

[75] Amadori M., Products of condesation between glucose and p-phenetidine, Atti. Accad. Naz. Lincei, 2 (1925) 337-342.

[76] Baynes, J.W., Watkins, N.G., Fisher, C.I., Hull, C.J., Patrick, S.J., Ahmed, M.U., Dunn, J.A., Thorpe, S.R., The Amadori product on protein: structure and reaction, Prog. Clin. Biol. Res., 304 (1989) 43–47.

[77] Ahmed, N., Thornalley, P.J., Quantitative screening of protein biomarkers of early glycation, advanced glycation, oxidation, and nitrosation in cellular and extracellular proteins by tandem mass spectrometry multiple reaction monitoring, Biochem. Soc. Trans., 31 (2003) 1417–1422.

[78] Takeuchi M., Kikuchi S., Sasaki N., Suzuki T., Iwaki M., Bucahe R., Yamagishi, S., Involvement of advanced glycation end-products (AGEs) in Alzheimer's disease, Curr. Alzheimer Res., 1 (2004) 39-46.

[79] Wautier, J.L., Guillausseau P.J., Advanced glycation end products, their receptors and diabetic angiopathy, Journal of the Peripheral Nervous System 7 (2) (2002) 137-138.

[80] Lapolla, A., Fedele, D., Senesi, A., Arico, N.C., Reitano, R., Seraglia, R., Astner, H., Traldi, P., Advanced glycation end-products/peptides: a preliminary investigation by LC and LC/MS, Farmaco., 57(10) (2002) 845-852.

[81] Lapolla, A., Fedele, D., Reitano, R., Arico, N.C., Seraglia, R., Traldi, P., Marotta, E., Tonani, R., Enzymatic digestion and mass spectrometry in the study of advanced glycation end products/peptides, J. Am. Soc. Mass Spectrom., 15 (2004) 496–509.

[82] Jaleel, A., Halvatsiotis, P., Williamson, B., Juhasz, P., Martin, S., Sreekumaran Nair, K., Identification of Amadori-Modified plasma proteins in type 2 diabetes and the effect of short-term intensive insulin treatment, Diabetes Care, (3) (2005) 645-652.

[83] Szabo, Z., Ohmacht, R., Huck, C.W., Stöggl, W.M., Bonn, G.K., Influence of the Pore Structure on the Properties of Silica based Reversed Phase Packings for LC, J. Sep. Sci., 28 (2005) 313–324.

[84] Li, Y.C., Jeppson, J.O., Jörntén-Karlsson, M., Larsson, E.L., Jungvid, H., Galaev, I.Y., Mattiasson, B., Application of shielding boronate affinity chromatography in the study of the glycation pattern of haemoglobin, J. Chromatogr. B, 776 (2002) 149–160.

[85] Böddi, K., Takátsy, A., Szabó, S., Markó, L. Wittmann, I., Ohmacht, R., Montskó, G., Vallant, R.M., Ringer, T., Bakry, R., Huck, C.W., Bonn, G.K., Szabó, Z., Use of fullerene, octadecyl, and triaconthyl silica for solid phase extraction of tryptic peptides obtained from unmodified and *in-vitro* glycated human serum albumin and fibrinogen, J. Sep. Sci., 32 (2009) 295–308.

[86] Finette, G.M., Mao, Q.M., Hearn, M.T., Comparative studies on the isothermal characteristics of proteins adsorbed under batch equilibrium conditions to ion-exchange, immobilised metal ion affinity and dye affinity matrices with different ionic strength and temperature conditions, J. Chromatogr. A, 763 (1997) 71–90.

[87] Nagy L., Nagy, G., Hajós, P., Copper electrode based amperometric detector cell for sugar and organic acid measurements, Sens. Actuat. B, 76 (2001) 493–498.

[88] Nagy, L., Kálmán, N., Nagy, G., Periodically interrupted amperometry: a way of improving analytical performance of membrane coated electrodes, J. Biochem. Biophys. Methods, 69 (2006) 133–141.

[89] Trojer, L., Bonn, G.K., Fabrication of organic monolithic columns for the separation of biopolymers and small molecules by modulation of the polymerization time, U.S. Patent, 11/551 181 (2006).

[90] Mosesson, M. W., Fibrinogen and fibrin structure and functions, J. Thromb. Haemost., (2005) 3 1894–1904.

[91] Li, X., Pennington, J., Stobaugh, J.F., Schöneich, C., Synthesis of sulfonamide– and sulfonyl–phenylboronic acid-modified silica phases for boronate affinity chromatography at physiological pH, Anal. Biochem., 372 (2008) 227–236.

[92] Brancia, F.L., Bereszczak, J.Z., Lapolla, A., Fedele, D., Baccarin, L., Seraglia, R., Traldi, P., Comprehensive analysis of glycated human serum albumin tryptic peptides by off-line liquide chromatography followed by MALDI analysis on a time-of-flight/curved field reflectron tandem mass spectrometer, J. Mass Spectrom., 41 (2006) 1179–1185.

[93] Gadgil, H. S., Bondarenko, P.V., Treuheit, M.J., Ren, D., Screening and sequencing of glycated proteins by neutral loss scan LC/MS/MS method, Anal. Chem., 79 (2007) 5991–5999.

[94] Pieters, M., van Zyl, D.G., Rheeder, P., Jerling, J.C., Loots, du T., van der Westhuizen, F.H., Gottsche, L.T., Weisel, J.W., Glycation of fibrinogen in uncontrolled diabetic patients

and the effects of glycaemic control on fibrinogen glycation, Thromb. Res., 120 (2007) 439–446.

[95] Thornalley, P., Argirova, M., Ahmed, N., Mann, V.M., Argirov, O., Dawnay, A., Mass spectrometric monitoring of albumin in uremia, Kidney Int., 58 (2000) 2228–2234.

[96] Szabó, Z., Ohmacht, R., Huck, C.W., Stöggl, W.M., Bonn, G.K., Influence of the pore structure on the properties of silica based reversed phase packings for LC, J. Sep. Sci., 28 (2005) 313–324.

[97] Gadgil, H.S., Bondarenko, P.V., Treuheit, M.J., Ren, D., Screening and sequencing of glycated proteins by neutral loss scan LC/MS/MS method, Anal. Chem., 79 (2007) 5991–5999.

List of publications

Publications related to this thesis:

1. **Böddi, K**., Takátsy, A., Szabó, Sz., Markó, L., Márk, L., Wittmann, I., Ohmacht, R., Montskó, G., Vallant, R.M., Ringer, T., Bakry, R., Huck, C.W., Bonn, G.K. and Szabó, Z., Use of fullerene-, octadecyl-, and triaconthyl silica for solid phase extraction of tryptic peptides obtained from unmodified and *in-vitro* glycated human serum albumin (HSA) and fibrinogen, J. Sep. Sci., 32 (2) (2009) 295-308., ***IF.: 2.745 citation: 6(3)***

2. Takátsy A., **Böddi, K.,** Nagy, L., Nagy, G., Szabó, S., Markó, L., Wittmann, I., Ohmacht, R., Ringer, T., Bonn, G.K., Gjerde, D., Szabó, Z., Enrichment of Amadori-products derived from the non-enzymatic glycation of proteins using microscale boronate affinity chromatography, Anal. Biochem., 393 (2009) 8-22., ***IF: 3.287 citation: 5(4)***

Other puplications:

3. Szabo, Z., **Boddi, K**., Mark, L., Szabo, G., Ohmacht, R: Analysis of nitrate ion in nettle (Urtica dioica L.) by ion-pair chromatographic method on a C30 stationary phase, Journal of Agricultural and Food Chemistry, 54 (12) (2006) 4082-4086., ***IF.: 2.322 citation: 3 (3)***
4. Avar, P., Pour Nikfardjam, M.S., Kunsági-Máté, S., Montskó, G., Szabó, Z**., Böddi, K**., Ohmacht, R. Márk, L. Investigation of Phenolic Components of Hungarian Wines. International Journal of Molecular Sciences, 10 (8) (2007) 1028-1038., ***IF.: 0.7500 citation: 12 (9)***
5. Montsko, G., Pour Nikfardjam, M.S., Szabo, Z.**, Boddi, K**., Lorand, T., Ohmacht, R. and Mark, L.: Determination of products derived from trans-resveratrol UV photoisomerisation by means of HPLC–APCI-MS, Journal of Photochemistry and Photobiology A: Chemistry, 196 (2008) 44-50., ***IF.: 2.362 citation:9 (9)***
6. Marko, L., Molnar, G.A., Wagner, Z., **Boeddi, K**., Koszegi, T., Szabo Z., Matus, Z., Szijarto I., Merei, A., Nagy G., Wittmann, I., Measurement of modification and

interference rate of urinary albumin detected by size-exclusion HPLC, Physiological Measurement, 30 (2009) 1137-1150., ***IF:1.4 citation: 1(1)***

7. Marko, L., Szigeti, N., Szabo, Z., **Boddi K.**, Takatsy, A., Ludany, A., Kőszegi, T., Molnar, G.A., Wittmann, I., Potential urinary biomarkers of disease activity in Crohn's disease, Scandinavian Journal of Gastroenterology, 45 (12) (2010) 1440-1448., ***IF:2.08 citation 1(1)***
8. Markó, L., Mikolás E., Molnár, G.A., Wagner, Z., Kőszegi, T., Szijártó, I. A., Mohás, M., Matus, Z., Szabó, Z., **Böddi, K**., Mérei, Á., Wittmann, I. Normo- és microalbuminuriás cukorbetegekben a HLCP-vel mért vizeletalbumin-fluoreszcencia a vesefunkciós paraméterekkel függ össze, nem a glikémiás értékkel, Diab. Hung., 17 (3) (2009) 229-238.

Abstracts:

1. Ludany, A., Koszegi, T., **Boddi, K.**, Szabo, Z., Kovacs, G.L. Human Tear Proteins as an Analytical Tool in Laboratory Medicine Euromedlab 2009 Innsbruck, Austria ***IF:1.88 citation: 0(0)***
2. Szalma, J., **Böddi, K.,** Lempel, E., Szabó, Z., Nyárády, Z., Olasz, L., Takátsy, A., Protein Identification from Submandibular Salivary Stones with MALDI TOF Mass Spectrometry, J. Craniomaxillofac. Surg., 2010 ***IF:1.36 citation: 0(0)***

Posters:

1. Szabó Z., **Böddi K**., Ohmacht R., Az "utánszilanizálás" hatása a retencióra, Elválasztástudományi Vándorgyűlés 2002. Lillafüred, Hungary
2. Szabó Z., Ohmacht R., Szabó L., **Böddi K**., Anionok ionpár.kromatográfiás elválasztása C30 fázison. Csalán (Urtica dioicasp.) nitrátion-tartalmának meghatározása ionpár-kromatográfiával Elválasztástudományi Vándorgyűlés 2004. Hévíz, Hungary
3. Szabó, Z., **Böddi, K.,** Márk, L., Szabó, L. Gy., Ohmacht, R., New HPLC Method for the Determination of Nitrate ion from Nettle (Urtica dioica L.) 6th Balaton Symposium 2005 Siófok, Hungary
4. Montskó, G., Vető, S., Márk, L., **Böddi, K.**, Dolowschiák, T., Kanizsai A., Doppler, H., Ohmacht, R., Biokompatibilis fullerén oldatok analitikai és toxicologai vizsgálata 37. Membrán-transzport Konferencia – Sümeg, 2007. május

5. **Böddi, K.,** Markó, L., Kőszegi, T., Jelinek, L., Márk, L., Montskó G., Ohmacht, R., Szabó, Z., Wittmann, I., Vizelet albumin karakterizálás tömegspektrometriás, folyadékkromatográfiás és nephelometriás módszerrel, Centenáriumi Vegyészkonferencia, 2007. Sopron, Hungary
6. Montskó, G., Avar, P., Szabó, Z., **Böddi, K**., Takátsy, A., Ohmach, R., Márk, L. Villányi borok polifenol összetételének vizsgálata HPLC-MS és LDI TOF módszerekkel Centenáriumi Vegyészkonferencia, 2007. Sopron, Hungary
7. Montskó, G., Szabó, Z., **Böddi, K**., Takátsy, A., Ohmacht, R., Wölfling, J., Mernyák, E., Márk, L. Szteránvázas hormonok kimutatása biológiai mintákból MALDI-TOF tömegspektromet-riával Centenáriumi Vegyészkonferencia, 2007. Sopron, Hungary
8. Gulyássy, P., **Böddi, K**., Markó, L., Márk, L., Wittmann, I., Ohmacht, R., Sümgi, B., Vallant R. M., Huck Ch. W., Bakry, R., Bonn, G. K., Szabó, Z. Improvement of the Sequence Coverage Applying Different Matrices, Solid Phase Extraction (SPE) and HPLC Separation of the Tryptic Digest of Human Serum Albumin (HSA) by Matrix-Assisted Laser Desorption/ionization Mass Spectrometry (MALDI)-A comprehensive study 7th Balaton Symposium 2007 Siófok, Hungary
9. Avar, P., Pour-Nikfardjam, M. S., Montskó, G., Szabó, Z., **Böddi, K**., Ohmacht, R., Márk, L. Antioxidant Analysis of Hungarian Red Wines 7th Balaton Symposium 2007 Siófok, Hungary
10. **Böddi, K**., Jámbor, É., Németh, V., Szabó, Z., Márk, L. Paleoproteomical Analysis of Mycobacterial Infected Human Remains by HPLC-MS/MS and MALDI TOF/TOF ISABS Conference n Forencic Genetics and Molecular Antropology 2007 Split, Croatia
11. Jámbor, É., **Böddi, K**., Németh, V., Tóth, G., Tóth, Cs., Szabó, Z, Márk, L., MALDI TOF Analysis of an Ancient Bone Cancer ISABS Conference n Forencic Genetics and Molecular Antropology 2007 Split, Croatia
12. **Böddi, K**., Szabó, Z., Takátsy, A., Markó, L., Wittmann, I., Ohmacht, R. Enrichment of Amadori Products Derived from the Non-enzimatic Glycation of Human Serum Albumin (HSA) using Microscale Boronate Affinity Chromatography 8th Balaton Symposium 2009 Siófok, Hungary
13. **Böddi, K**., Brochmann, A.S., Szalma, J., Lempel, E., Szabó, Z., Takátsy A., Protein Identification from Submandibular Salivary Stones with MALDI TOF Mass Spectrometry 28th Informal Meeting on Mass Spectrometry 2010 Kőszeg, Hungary

Acknowledgements

I would like to thank Professor Dr. Robert Ohmacht, my supervisor, and Professor Dr. József Deli, my PhD. Program leader for their countenance.

I am especially thankful to my co-supervisor, Dr. Zoltán Szabó, for tutoring, mentoring and funding the research. Without him the experiments of the thesis could not be accomplished properly.

I would also like to thank Dr. Anikó Takátsy for her support. She helped me writing this thesis with her valuable ideas and helpful comments

I am grateful to Professor Dr. István Wittmann, head of 2nd Department of Internal Medicine and Nephrology at Pécs University and Dr. Lajos Markó, of the same department, for the accurate selection and constitous collecting of the clinical samples.

I am thankful to Professor Günther K. Bonn and Thomas Ringer of the Institute of Analytical Chemistry and Radiochemistry, Leopold–Franzens University, Innsbruck for the LC-MS measurents.

I am grateful to Professor Géza Nagy and Lívia Nagy of the Department of General and Physical Chemistry, University of Pécs for the amperometric experiments.

I am thankful to Gábor Rébék-Nagy for the language revision of my thesis.

I am grateful to everyone who is not listed above but contributed to my research or my life.

Last, but not least, I would like to express my gratitude to my family for their infinite encouragement and support during my work.

Appendix

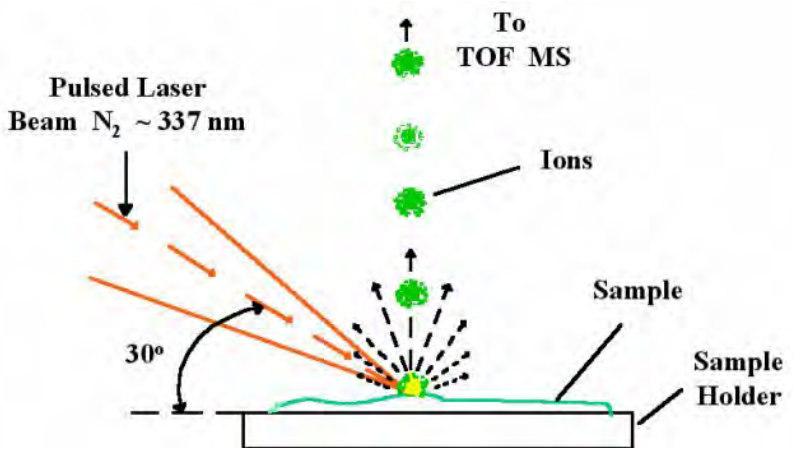

Figure A: The effect of the N_2 laser light on the co-crystallized matrix and sample molecules

http://www.psrc.usm.edu/mauritz/maldi.html

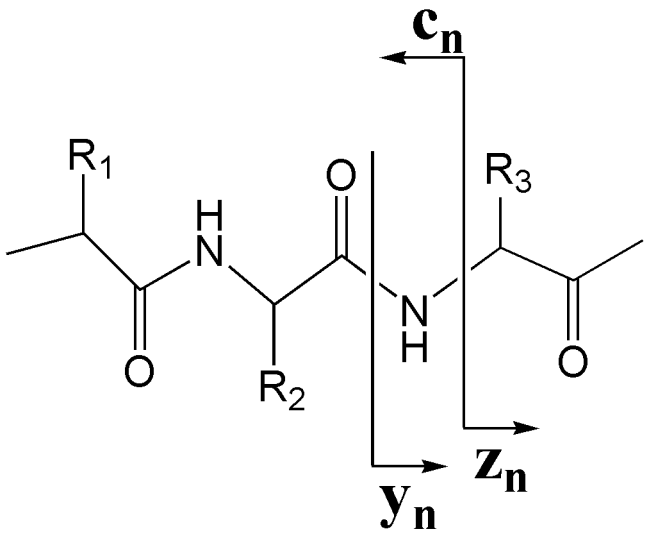

Figure B. Nomenclature of fragment ions observed in ISD [7]